BROWN UNIVERSITY

DOCTORAL THESIS

Landau Singularities in Planar Massless Theories

Author:
Igor PRLINA

Supervisor:
Dr. Marcus SPRADLIN

A thesis submitted in fulfillment of the requirements
for the degree of Doctor of Philosophy

in the

High Energy Theory Group
Department of Physics

May 16, 2019

Igor Prlina

36 Slovenska Street
Belgrade, Serbia 11080
(+1)401-347-55-94
Igor_prlina@brown.edu

EDUCATION

PhD Brown University, Providence, RI, USA, advisor: Marcus Spradlin, expected to graduate**: May 2019**

MSc Brown University, Providence, RI, USA, graduated**: May 2016**

MSc University of **Belgrade –** Faculty of Physics**, Belgrade, Serbia**, graduated: **July 2014**

BSc University of Belgrade **–** Faculty of Physics**, Belgrade, Serbia,** graduated: **July 2013**

PUBLICATIONS

Igor Prlina, Marcus Spradlin, and Stefan Stanojevic. "All-Loop Singularities of Scattering Amplitudes in Massless Planar Theories." Phys. Rev. Lett. 121 (2018) [arXiv: 1805.11617]

Igor Prlina, Marcus Spradlin, James Stankowicz and Stefan Stanojevic. "Boundaries of amplituhedra and NMHV symbol alphabets at two loops." JHEP 1804, 049 (2018) [arXiv:1712.08049]

Igor Prlina, Marcus Spradlin, James Stankowicz, Stefan Stanojevic and Anastasia Volovich. "All-helicity symbol alphabets from unwound amplituhedra." JHEP 1805, 159 (2018) [arXiv:1711.11507]

Tristan Dennen, Igor Prlina, Marcus Spradlin, Stefan Stanojevic and Anastasia Volovich. "Landau singularities from the amplituhedron." JHEP 1706, 152 (2017) [arXiv:1612.02708]

Igor Prlina and Natasa Nedeljkovic. "Time-symmetrized description of nonunitary time asymmetric quantum evolution." *Journal of Physics A: Mathematical and Theoretical* 49.3 (2015)

HONORS AND FELLOWSHIPS

Physics Merit Fellowship, 2018-2019 (awarded by the Department of Physics, Brown University)

Excellence as a Graduate Teaching Assistant award, 2015-2016

Manning Graduate Fellowship, 2014-2015 (awarded by Brown University)

Dositeja fellowship, 2013-2018

(awarded by the Ministry of Youth and Sports, Republic of Serbia for best students nationwide)

City of Belgrade fellowship , 2006 – 2012

(awarded by the City of Belgrade for talented students in Belgrade)

Fund "Prof. dr. Djordje Zivanovic" reward, 2012

(awarded by the University of Belgrade – **Faculty of Physics** and University of Belgrade - **Institute of Physics** for "outstanding success in studies of physics" to four best third year undergraduate students)

Foundation for development of scientific and artistic youth fellowship 2006-2010

TEACHING EXPERIENCE

Teaching assistant, Brown University, 2015-2017

Teaching assistant, University of Belgrade, 2013-2014

Student assistant at **Petnica Science Center,** Serbia, 2009-2014

EXTRACURRICULAR ACTIVITIES

Member of **Finance Committee** of **Graduate Student Council** of Brown University

Member and vice-president of **Students' Parliament** of Faculty of Physics of University of Belgrade

Voting student member of the **Faculty Council** of University of Belgrade Faculty of Physics

Student assistant at **Petnica Science Center**

REFERENCES

Marcus Spradlin, Department of Physics, Brown University, email marcus_spradlin@brown.edu

Anastasia Volovich, Department of Physics, Brown University, email anastasia_volovich@brown.edu

Antal Jevicki, Department of Physics, Brown University, email antal_jevicki@brown.edu

This dissertation by Igor Prlina is accepted in its present form by the Department of Physics as satisfying the dissertation requirement for the degree of Doctor of Philosophy.

Date _____ _____

Marcus Spradlin, Advisor

Recommended to the Graduate Council

Date _____ _____

JiJi Fan, Reader

Date _____ _____

Antal Jevicki, Reader

Approved by the Graduate Council

Date _____ _____

Andrew Campbell, Dean of the Graduate School

Declaration of Authorship

I, Igor PRLINA, declare that this thesis titled, "Landau Singularities in Planar Massless Theories" and the work presented in it are my own. I confirm that:

- ©Copyright 2019 by Igor Prlina.
- This work was done wholly or mainly while in candidature for a research degree at this University.
- Where any part of this thesis has previously been submitted for a degree or any other qualification at this University or any other institution, this has been clearly stated.
- Where I have consulted the published work of others, this is always clearly attributed.
- Where I have quoted from the work of others, the source is always given. With the exception of such quotations, this thesis is entirely my own work.
- I have acknowledged all main sources of help.
- Where the thesis is based on work done by myself jointly with others, I have made clear exactly what was done by others and what I have contributed myself.

Signed:

_____

Date:

_____

BROWN UNIVERSITY

Abstract

Department of Physics

Doctor of Philosophy

Landau Singularities in Planar Massless Theories

by Igor PRLINA

In this work we present our contribution to thme method of using Landau singularities for probing scattering amplitudes in planar massles quantum field theories. We start by proposing a simple geometric algorithm for determining the complete set of branch points of amplitudes in planar $\mathcal{N} = 4$ super-Yang-Mills theory directly from the amplituhedron, without resorting to any particular representation in terms of local Feynman integrals. This represents a step towards translating integrands directly into integrals. In particular, the algorithm provides information about the symbol alphabets of general amplitudes. First we illustrate the algorithm applied to the one- and two-loop MHV amplitudes. Then we demonstrate how to use the recent reformulation of amplituhedra in terms of 'sign flips' in order to streamline the application of this algorithm to amplitudes of any helicity. In this way we recover the known branch points of all one-loop amplitudes, and we find an 'emergent positivity' on boundaries of amplituhedra. Lastly, we look beyond planar $\mathcal{N} = 4$ super-Yang-Mills theory, and analyze Landau singularities of general massless planar theories. In massless quantum field theories the Landau equations are invariant under graph operations familiar from the theory of electrical circuits. Using a theorem on the Y-Δ reducibility of planar circuits we prove that the set of first-type Landau singularities of an n-particle scattering amplitude in any massless planar theory, in any spacetime dimension D, at any finite loop order in perturbation theory, is a subset of those of a certain n-particle $\lfloor (n-2)^2/4 \rfloor$-loop "ziggurat" graph. We determine this singularity locus explicitly for $D = 4$ and $n = 6$ and find that it corresponds precisely to the vanishing of the symbol letters familiar from the hexagon bootstrap in SYM theory. Further implications for SYM theory are discussed.

Acknowledgements

I primarily want to thank my collaborators, Tristan Dennen, James Stankowicz, Stefan Stanojevic, Marcus Spradlin and Anastasia Volovich. I am also grateful to Nima Arkani-Hamed for helpful discussions as well as to my fellow graduate students in HET/Ph for useful conversations.

Contents

List of Figures

List of Tables

The work before you is a culmination of decades of high-quality education I was blessed with. I dedicate this thesis to all my teachers who have selflessly worked on developping me intelectually. From my elemenary school teacher, to my thesis advisor, I am indebted to them all. My greatest debt is to my parents, for teaching me both my first and most important lessons in life.

Chapter 1

Introduction

Ever since its conception, the Feynman diagram approach has been the standard paradigm for perturbative calculations in quantum field theory. While the method can, in principle, be used at any order in perturbation theory, the calculations get more and more demanding at each new loop order. Alternately one can seek hidden symmetries and new underlying principles which motivate new calculational approaches where the most basic features of Feynman diagrams, such as unitarity and locality, are emergent instead of manifest. Recent years have seen tremendous success in "reverse engineering" such new symmetries and principles from properties of scattering amplitudes. This approach has been particularly fruitful in simple quantum field theories such as the planar maximally supersymmetric $\mathcal{N} = 4$ super-Yang-Mills (SYM) theory [1].

In particular, it has been realized that the unitarity and locality of the integrands [2] of loop-level amplitudes in SYM theory can be seen to emerge from a very simple geometric principle of positivity [3]. Moreover, it has been proposed that all information about arbitrary integrands in this theory is encapsulated in objects called amplituhedra [4, 5] that have received considerable recent attention; see for example [6, 7, 8, 9, 10, 11, 12, 13]. Unfortunately, there remains a huge gap between our understanding of integrands and our understanding of the corresponding integrated amplitudes. Despite great advances in recent years we of course don't have a magic wand that can be waved at a general integrand to "do the integrals". Indeed, modern approaches to computing multi-loop amplitudes in SYM theory, such as the amplitude bootstrap [14, 15] even eschew knowledge of the integrand completely. It would be enormously valuable to close

this gap between our understanding of integrands and amplitudes.

Physical principles impose strong constraints on the scattering amplitudes of elementary particles. For example, when working at finite order in perturbation theory, unitarity and locality appear to constrain amplitudes to be holomorphic functions with poles and branch points at precisely specified locations in the space of complexified kinematic data describing the configuration of particles. Indeed, it has been a long-standing goal to understand how to use the tightly prescribed analytic structure of scattering amplitudes to determine them directly, without relying on traditional (and, often computationally complex) Feynman diagram techniques.

The connection between the physical and mathematical structure of scattering amplitudes has been especially well studied in planar $\mathcal{N} = 4$ super-Yang–Mills [1] SYM[1] theory in four spacetime dimensions, where the analytic structure of amplitudes is especially tame. One of the overall aims of this work, its predecessors [16, 17], and its descendant(s), is to ask a question that might be hopeless in another, less beautiful quantum field theory: can we understand the branch cut structure of general scattering amplitudes in SYM theory?

The motivation for asking this question is two-fold. The first is the expectation that the rich mathematical structure that underlies the integrands of SYM theory (the rational $4L$-forms that arise from summing L-loop Feynman diagrams, prior to integrating over loop momenta) is reflected in the corresponding scattering amplitudes. For example, it has been observed that both integrands [3] and amplitudes [18, 15, 19] are deeply connected to the mathematics of cluster algebras.

Second, on a more practical level, knowledge of the branch cut structure of amplitudes is the key ingredient in the amplitude bootstrap program, which represents the current state of the art for high loop order amplitude calculations in SYM theory. In particular the hexagon bootstrap (see for example [14]), which has succeeded in computing all six-particle amplitudes through five loops [20], is predicated on the hypothesis that at any loop order, these amplitudes can have branch points only on 9 specific loci in the

[1] We use "SYM" to mean the planar limit, unless otherwise specified.

space of external data. Similarly the heptagon bootstrap [21], which has revealed the symbols of the seven-particle four-loop MHV and three-loop NMHV amplitudes [22], assumes 42 particular branch points. One result we hope follows from understanding the branch cut structure of general amplitudes in SYM theory is a proof of this counting to all loop order for six- and seven-particle amplitudes.

As a step in that direction, and motivated by [23], a systematic exploration of how integrands encode the singularities of integrated amplitudes,in particular their branch points, has been performed in [16]. Scattering amplitudes in quantum field theory generally have very complicated discontinuity structure. The discontinuities across branch cuts are given by sums of unitarity cuts [24, 25, 26, 27, 28, 29]. These discontinuities may appear on the physical sheet or after analytic continuation to other sheets; these higher discontinuities are captured by multiple unitarity cuts (see for example [30, 31]). A long-standing goal of the S-matrix program, in both its original and modern incarnations, has been to construct expressions for the scattering amplitudes of a quantum field theory based solely only on a few physical principles and a thorough knowledge of their analytic structure. In [16] the branch cut structure of one- and two-loop MHV amplitudes in SYM theory starting from certain representations of their integrands in terms of local Feynman integrals [32] has been studied. In [16] all of their known branch points have been found, but many other, spurious branch points that are artifacts of the particular representations used, were also encountered. Indeed, the analysis of [16] was completely insensitive to numerator factors in the integrand, but the numerators are really where all of the action is—in any standard quantum field theory the denominator of a loop integrand is a product of local propagators; the numerator is where all of the magic lies.

One of the goals in this work is to improve greatly on the analysis of [16]. We do this by presenting a method for asking the amplituhedron to directly provide a list of the physical branch points of a given amplitude.

It is a general property of quantum field theory (see for example [27, 33]) that the locations of singularities of an amplitude can be determined from knowledge of the

poles of its integrand by solving the Landau equations [26]. Constructing explicit representations for integrands can be a challenging problem in general, but in SYM theory this can be side-stepped by using various on-shell methods [28, 34, 35, 36] to efficiently determine the locations of integrand poles. This problem is beautifully geometrized by amplituhedra [4], which are spaces encoding representations of integrands in such a way that the boundaries of an amplituhedron correspond precisely to the poles of the corresponding integrand. Therefore, as pointed out in [17], the Landau equations can be interpreted as defining a map that associates to any boundary of an amplituhedron the locus in the space of external data where the corresponding amplitude has a singularity.

Only MHV amplitudes were considered in [17]. In this paper we also show how to extend the analysis to amplitudes of arbitrary helicity. This is greatly aided by a recent combinatorial reformulation of amplituhedra in terms of "sign flips" [37]. As a specific application of our algorithm we classify the branch points of all one-loop amplitudes in SYM theory. Although the singularity structure of these amplitudes is of course well-understood (see for example [38, 39, 40, 41, 42, 43, 44, 45, 46]), this exercise serves a useful purpose in preparing a powerful toolbox for the sequel [47] to this paper where we will see that boundaries of one-loop amplituhedra are the basic building blocks at all loop order. In particular we find a surprising 'emergent positivity' on boundaries of one-loop amplituhedra that allows boundaries to be efficiently mapped between different helicity sectors, and recycled to higher loop levels.

While we have found an efficient method to obtain non-spurious singularities in planar $\mathcal{N} = 4$ super-Yang-Mills (SYM) theory, we have also analyzed the potential singularity structure of an arbitrary planar massless theory. For over half a century much has been learned from the study of singularities of scattering amplitudes in quantum field theory, an important class of which are encoded in the Landau equations [26]. This work combines two simple statements to arrive at a general result about such singularities. The first is based on the analogy between Feynman diagrams and electrical circuits, which also has been long appreciated and exploited; see for example [48, 49, 50] and chapter 18 of [51]. Here we use the fact that in *massless* field theories, the sets

of solutions to the Landau equations are invariant under the elementary graph operations familiar from circuit theory, including in particular the Y-Δ transformation which replaces a triangle subgraph with a tri-valent vertex, or vice versa. The second is a theorem of Gitler [52], who proved that any *planar* graph (of the type relevant to the analysis of Landau equations, specified below) can be Y-Δ reduced to a class we call *ziggurats*.

We conclude that the n-particle $\lfloor (n-2)^2/4 \rfloor$-loop ziggurat graph encodes all possible first-type Landau singularities of any n-particle amplitude at any finite loop order in any massless planar theory. Although this result applies much more generally, our original motivation arose from related work [16, 17, 53, 47] on planar $\mathcal{N} = 4$ supersymmetric Yang-Mills (SYM) theory, for which our result has several interesting implications.

This work is organized as follows. In 2 we apply the Amplituhedron to directly obtain non-spurious singularities of MHV amplitudes, and we explicitely conduct the procedure at one and two loops [17]. In 3 we generalize the procedure to non MHV amplitudes and present the procedure at the one loop example [53]. Finally, in 4 we describe a method for finding all-loop singularities in general planar massless theories [54].

Chapter 2

Landau Singularities from the Amplituhedron

2.1 Introduction

2.1.1 Momentum Twistors

We begin by reviewing the basics of momentum twistor notation [55], which we use throughout our calculations. Momentum twistors are based on the correspondence between null rays in (complexified, compactified) Minkowski space and points in twistor space ($\mathbb{P}^3$), or equivalently, between complex lines in $\mathbb{P}^3$ and points in Minkowski space. We use Z_a, Z_b, etc. to denote points in $\mathbb{P}^3$, which may be represented using four-component homogeneous coordinates $Z_a^I = (Z_a^1, Z_a^2, Z_a^3, Z_a^4)$ subject to the identification $Z_a^I \sim tZ_a^I$ for any non-zero complex number t. We use $(a\,b)$ as shorthand for the bitwistor $\epsilon_{IJKL}Z_a^K Z_b^L$. Geometrically, we can think of $(a\,b)$ as the (oriented) line containing the points Z_a and Z_b. Similarly we use $(a\,b\,c)$ as shorthand for $\epsilon_{IJKL}Z_a^J Z_b^K Z_c^L$, which represents the (oriented) plane containing Z_a, Z_b and Z_c. Analogously, $(a\,b\,c)\cap(d\,e\,f)$ stands for $\epsilon^{IJKL}(a\,b\,c)_K(d\,e\,f)_L$, which represents the line where the two indicated planes intersect. In planar SYM theory we always focus on color-ordered partial amplitudes so an n-point amplitude is characterized by a set of n momentum twistors $Z_i^I, i \in \{1,\ldots,n\}$ with a specified cyclic ordering. Thanks to this implicit cyclic ordering we can use $\bar{i}$ as shorthand for the plane $(i{-}1\,i\,i{+}1)$, where indices are always understood to be mod n.

The natural $SL(4,\mathbb{C})$ invariant is the four-bracket denoted by

$$\langle a\,b\,c\,d\rangle \equiv \epsilon_{IJKL} Z_a^I Z_b^J Z_c^K Z_d^L \,. \tag{2.1}$$

We will often be interested in a geometric understanding of the locus where such four-brackets might vanish, which can be pictured in several ways. For example, $\langle a\,b\,c\,d\rangle = 0$ only if the two lines $(a\,b)$ and $(c\,d)$ intersect, or equivalently if the lines $(a\,c)$ and $(b\,d)$ intersect, or if the point a lies in the plane $(b\,c\,d)$, or if the point c lies on the plane $(a\,b\,d)$, etc. Computations of four-brackets involving intersections may be simplified via the formula

$$\langle (a\,b\,c)\cap(d\,e\,f)\,g\,h\rangle = \langle a\,b\,c\,g\rangle\langle d\,e\,f\,h\rangle - \langle a\,b\,c\,h\rangle\langle d\,e\,f\,g\rangle \,. \tag{2.2}$$

In case the two planes are specified with one common point, say $f = c$, it is convenient to use the shorthand notation

$$\langle (a\,b\,c)\cap(d\,e\,c)\,g\,h\rangle \equiv \langle c\,(a\,b)(d\,e)(g\,h)\rangle \tag{2.3}$$

which highlights the fact that this quantity is antisymmetric under exchange of any two of the three lines $(a\,b)$, $(d\,e)$, and $(g\,h)$.

2.1.2 Positivity and the MHV Amplituhedron

In this paper we focus exclusively on MHV amplitudes. The integrand of an L-loop MHV amplitude is a rational function of the n momentum twistors Z_i specifying the kinematics of the n external particles, as well as of L loop momenta, each of which corresponds to some line $\mathcal{L}^{(\ell)}$ in $\mathbb{P}^3$; $\ell \in \{1,\ldots,L\}$. The amplituhedron [4, 5] purports to provide a simple characterization of the integrand when the Z_i^I take values in a particular domain called the positive Grassmannian $G_+(4,n)$. In general $G_+(k,n)$ may be defined as the set of $k\times n$ matrices for which all ordered maximal minors are positive; that is, $\langle a_{i_1}\cdots a_{i_k}\rangle > 0$ whenever $i_1 < \cdots < i_k$.

Each line $\mathcal{L}^{(\ell)}$ may be characterized by specifying a pair of points $\mathcal{L}_1^{(\ell)}$, $\mathcal{L}_2^{(\ell)}$ that it passes through. We are always interested in $n \geq 4$, so the Z_i generically provide a

basis for $\mathbb{C}^4$. In the MHV amplituhedron a pair of points specifying each $\mathcal{L}^{(\ell)}$ may be expressed in the Z_i basis via an element of $G_+(2,n)$ called the D-matrix:

$$\mathcal{L}_\alpha^{(\ell)I} = \sum_{i=1}^{n} D_{\alpha i}^{(\ell)} Z_i^I, \qquad \alpha = 1,2\,. \tag{2.4}$$

For $n > 4$ the Z_i are generically overcomplete, so the map eq. (2.4) is many-to-one.

The L-loop n-point MHV amplituhedron is a $4L$-dimensional subspace of the $2L(n-2)$-dimensional space of L D-matrices. We will not need a precise characterization of that subspace, but only its grossest feature, which is that it is a subspace of the space of L mutually positive points in $G_+(2,n)$. This means that it lives in the subspace for which all ordered maximal minors of the matrices

$$\left(D^{(\ell)}\right), \quad \begin{pmatrix} D^{(\ell_1)} \\ D^{(\ell_2)} \end{pmatrix}, \quad \begin{pmatrix} D^{(\ell_1)} \\ D^{(\ell_2)} \\ D^{(\ell_3)} \end{pmatrix}, \quad \text{etc.}$$

are positive.

A key consequence of the positivity of the D-matrices is that, for positive external data $Z_i^I \in G_+(4,n)$, all loop variables $\mathcal{L}^{(\ell)}$ are oriented positively with respect to the external data and to each other: inside the amplituhedron,

$$\langle \mathcal{L}^{(\ell)}\, i\, i{+}1 \rangle > 0 \text{ for all } i \text{ and all } \ell, \text{ and} \tag{2.5}$$

$$\langle \mathcal{L}^{(\ell_1)}\, \mathcal{L}^{(\ell_2)} \rangle > 0 \text{ for all } \ell_1, \ell_2. \tag{2.6}$$

The boundaries of the amplituhedron coincide with the boundaries of the space of positive D-matrices, and occur for generic Z when one or more of these quantities approach zero.

It is worth noting that the above definition of positivity depends on the arbitrary choice of a special point Z_1, since for example $\langle \mathcal{L}\, 1\, 2 \rangle > 0$ but the cyclically related quantity $\langle \mathcal{L}\, n\, 1 \rangle$ is negative. The choice of special point is essentially irrelevant: it just means that some special cases need to be checked. In calculations we can sidestep this

subtlety by always choosing to analyze configurations involving points satisfying $1 \leq i < j < k < l \leq n$, which can be done without loss of generality. The geometric properties of figures 2.2–2.5 below are insensitive to the choice and always have full cyclic symmetry.

The integrand of an MHV amplitude is a canonical form $d\Omega$ defined by its having logarithmic singularities only on the boundary of the amplituhedron. The numerator of $d\Omega$ conspires to cancel all singularities that would occur outside this region (see [9] for some detailed examples). Our analysis will require no detailed knowledge of this form. Instead, we will appeal to "the amplituhedron" to tell us whether or not any given configuration of lines $\mathcal{L}^{(\ell)}$ overlaps the amplituhedron or its boundaries by checking whether eqs. (2.5) and (2.6) are satisfied (possibly with some $=$ instead of $>$).

2.1.3 Landau Singularities

The goal of this paper is to understand the singularities of (integrated) amplitudes. For standard Feynman integrals, which are characterized by having only local propagators in the denominator, it is well-known that the locus in kinematic space where a Feynman integral can potentially develop a singularity is determined by solving the Landau equations [26, 56, 33] which we now briefly review.

After Feynman parameterization any L-loop scattering amplitude in D spacetime dimensions may be expressed as a linear combination of integrals of the form

$$\int \prod_{r=1}^{L} d^D l_r \int_{\alpha_i \geq 0} d^\nu \alpha \; \delta\left(1 - \sum_{i=1}^{\nu} \alpha_i\right) \frac{\mathcal{N}(l_r^\mu, p_i^\mu, \ldots)}{\mathcal{D}^\nu} \tag{2.7}$$

where ν is the number of propagators in the diagram, each of which has an associated Feynman parameter α_i, $\mathcal{N}$ is some numerator factor which may depend on the L loop momenta l_r^μ as well as the external momenta p_i^μ, and finally the denominator involves

$$\mathcal{D} = \sum_{i=1}^{\nu} \alpha_i (q_i^2 - m_i^2)\,, \tag{2.8}$$

where q_i^μ is the momentum flowing along propagator i which carries mass m_i. The integral can be viewed as a multidimensional contour integral in the $LD + \nu$ integration variables (l_r^μ, α_i), where the α_i contours begin at $\alpha_i = 0$ and the l_r^μ contours are considered closed by adding a point at infinity. Although the correct contour for a physical scattering process is dictated by an appropriate $i\epsilon$ prescription in the propagators, a complete understanding of the integral, including its analytic continuation off the physical sheet, requires arbitrary contours to be considered.

An integral of the above type can develop singularities when the denominator $\mathcal{D}$ vanishes in such a way that the contour of integration cannot be deformed to avoid the singularity. This can happen in two distinct situations:

(1) The surface $\mathcal{D} = 0$ can pinch the contour simultaneously in all integration variables (l_r^μ, α_i). This is called the "leading Landau singularity", though it is important to keep in mind that it is only a potential singularity. The integral may have a branch point instead of a singularity, or it may be a completely regular point, depending on the behavior of the numerator factor $\mathcal{N}$.

(2) The denominator may vanish on the boundary when one or more of the $\alpha_i = 0$ and pinch the contour in the other integration variables. These are called subleading Landau singularities.

The Landau conditions encapsulating both possible situations are

$$\sum_{i \in \text{loop}} \alpha_i q_i^\mu = 0 \text{ for each loop, and} \tag{2.9}$$

$$\alpha_i (q_i^2 - m_i^2) = 0 \text{ for each } i. \tag{2.10}$$

For leading singularities eq. (2.10) is satisfied by $q_i^2 - m_i^2 = 0$ for each i, while subleading singularities have one or more i for which $q_i^2 - m_i^2 \neq 0$ but the corresponding $\alpha_i = 0$. We will always refer to equations of type $q_i^2 - m_i^2$ as "cut conditions" since they correspond to putting some internal propagators on-shell. It is important to emphasize that the Landau equations themselves have no knowledge of the numerator factor $\mathcal{N}$, which can alter the structure of a singularity or even cancel a singularity entirely.

Sometimes (i.e., for some diagram topologies), the Landau equations (2.9) and (2.10) may admit solutions for arbitrary external kinematics p_i^μ. This usually indicates an infrared divergence in the integral (we will not encounter ultraviolet divergences in SYM theory), which may or may not be visible by integration along the physical contour.

In other cases, solutions to the Landau equations might exist only when the p_i^μ lie on some subspace of the external kinematic space. MHV amplitudes in SYM theory are expected to have only branch point type singularities (after properly normalizing them by dividing out a tree-level Parke-Taylor [57] factor), so for these amplitudes we are particularly interested in solutions which exist only on codimension-one slices of the external kinematic space. Even when the p_i^μ live on a slice where solutions of the Landau equations exist, the solutions generally occur for values of the integration variables α_i and l_r^μ that are off the physical contour (for example, the α_i could be complex). This indicates a branch point of the integral that is not present on the physical sheet but only becomes apparent after suitable analytic continuation away from the physical contour.

Finally let us note that we have ignored a class of branch points called "second-type singularities" [58, 59, 33] which arise from pinch singularities at infinite loop momentum. As argued in [16], these should be absent in planar SYM theory when one uses a regulator that preserves dual conformal symmetry.

2.2 Eliminating Spurious Singularities of MHV Amplitudes

In principle one can write explicit formulas for any desired integrand in planar SYM theory by triangulating the interior of the amplituhedron and constructing the canonical form $d\Omega$ with logarithmic singularities on its boundary. However, general triangulations may produce arbitrarily complicated representations for $d\Omega$. In particular, these may have no semblance to standard Feynman integrals with only local propagators in the denominator (see [6] for some explicit examples). It is therefore not immediately clear that the Landau equations have any relevance to the amplituhedron. The connection will become clear in the following section; here we begin by revisiting the analysis of [16] with the amplituhedron as a guide.

In [16] we analyzed the potential Landau singularities of one- and two-loop MHV amplitudes by relying on the crutch of representations of these amplitudes in terms of one- and two-loop chiral pentagon and double-pentagon integrals [32]. The solutions to the various sets of Landau equations for these integral topologies represent *potential* singularities of the amplitudes, but this set of potential singularities is too large for two reasons. First of all, the chiral integrals are dressed with very particular numerator factors to which the Landau equations are completely insensitive. Scalar pentagon and double pentagon integrals certainly have singularities that are eliminated by the numerator factors of their chiral cousins. Second, some actual singularities of individual chiral integrals may be spurious in the full amplitude due to cancellations when all of the contributing chiral integrals are summed.

It is a priori highly non-trivial to see which singularities of individual integrals survive the summation to remain singularities of the full amplitude. However, the amplituhedron hypothesis provides a quick way to detect spurious singularities from simple considerations of positive geometry. In this section we refine our analysis of [16] to determine which *potential* singularities identified in that paper are *actual* singularities by appealing to the amplituhedron as an oracle to tell us which cuts of the amplitude have zero or non-zero support on the (boundary of the) amplituhedron.

Specifically, we propose a check that is motivated by the Cutkosky rules [27], which tell us that to compute the cut of an amplitude with respect to some set of cut conditions, one replaces the on-shell propagators in the integrand corresponding to those cut conditions by delta-functions, and integrates the resulting quantity over the loop momenta. The result of such a calculation has a chance to be non-zero only if the locus where the cut conditions are all satisfied has non-trivial overlap with the domain of integration of the loop momentum variables. In the present context, that domain is the space of mutually positive lines, i.e., the interior of the amplituhedron. This principle will lead to a fundamental asymmetry between the two types of Landau equations in our analysis. The full set of Landau equations including both eqs. (2.9) and (2.10) should be solvable only on a codimension-one locus in the space of external momenta in order

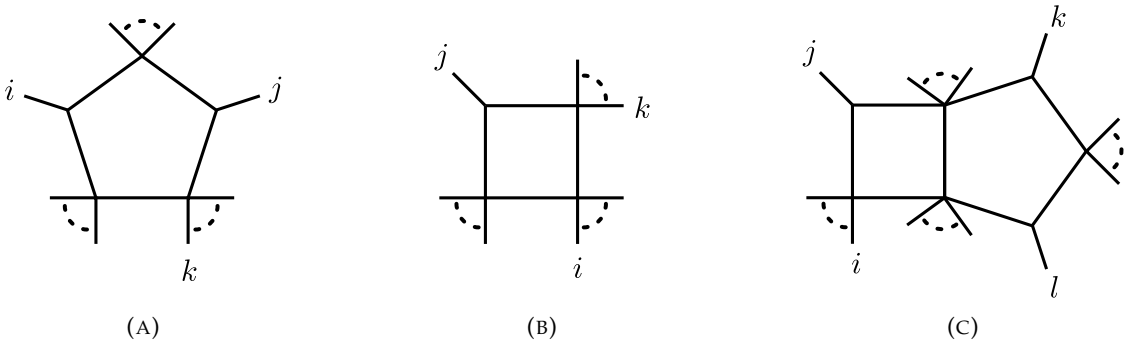

FIGURE 2.1: Three examples of cuts on which MHV amplitudes have no support; these appeared as spurious singularities in the Landau equation analysis of [16] since scalar pentagon and double pentagon integrals do have these cuts.

to obtain a valid branch point. However, guided by Cutkosky, we claim that the cut conditions (2.10) must be solvable inside the positive domain for arbitrary (positive) external kinematics; otherwise the discontinuity around the putative branch point is zero and we should discard it as spurious.

In the remainder of this section we will demonstrate this hypothesis by means of the examples shown in figure 2.1. The leading Landau singularities of each of these diagrams were found to be singularities of the scalar pentagon and double-pentagon integrals analyzed in [16], but it is clear that MHV amplitudes have no support on these cut configurations. In the next three subsections we will see how to understand their spuriousness directly from the amplituhedron. This will motivate us to seek a better, more direct algorithm to be presented in the following section.

2.2.1 The Spurious Pentagon Singularity

The first spurious singularity of MHV amplitudes arising from the integral representation used in [16] is the leading Landau singularity of the pentagon shown in figure 2.1a, which is located on the locus where

$$\langle i\,j\,k\,k{+}1\rangle\langle \bar{i}\cap\bar{j}\,k\,k{+}1\rangle = 0\,. \tag{2.11}$$

It was noted already in [27] that this solution of the Landau equations does not correspond to a branch point of the pentagon integral. It arises from cut conditions that put all five propagators of the pentagon on-shell:

$$0 = \langle \mathcal{L}\, i{-}1\, i\rangle = \langle \mathcal{L}\, i\, i{+}1\rangle = \langle \mathcal{L}\, j{-}1\, j\rangle = \langle \mathcal{L}\, j\, j{+}1\rangle = \langle \mathcal{L}\, k\, k{+}1\rangle\,, \tag{2.12}$$

where $\mathcal{L}$ is the loop momentum. The first four of these cut conditions admit two discrete solutions [32]: either $\mathcal{L} = (i\,j)$ or $\mathcal{L} = \bar{i} \cap \bar{j}$. The second of these cannot avoid lying outside the amplituhedron. We see this by representing its D-matrix as

$$D = \begin{array}{c} \begin{array}{ccc} i{-}1 & i & i{+}1 \end{array} \\ \begin{pmatrix} \langle i\,\bar{j}\rangle & -\langle i{-}1\,\bar{j}\rangle & 0 \\ 0 & \langle i{+}1\,\bar{j}\rangle & -\langle i\,\bar{j}\rangle \end{pmatrix} \end{array}, \tag{2.13}$$

where we indicate only the nonzero columns of the $2 \times n$ matrix in positions $i{-}1$, i and $i{+}1$, per the labels above the matrix. The non-zero 2×2 minors of this matrix,

$$\langle i\,\bar{j}\rangle\langle i{+}1\,\bar{j}\rangle, \qquad \langle i{-}1\,\bar{j}\rangle\langle i\,\bar{j}\rangle, \qquad -\langle i\,\bar{j}\rangle^2 \tag{2.14}$$

have indefinite signs for general positive external kinematics, so this $\mathcal{L}$ lies discretely outside the amplituhedron.

We proceed with the first solution $\mathcal{L} = (i\,j)$ which can be represented by the trivial D-matrix

$$D = \begin{array}{c} \begin{array}{cc} i & j \end{array} \\ \begin{pmatrix} 1 & 0 \\ 0 & 1 \end{pmatrix} \end{array}. \tag{2.15}$$

Although this is trivially positive, upon substituting $\mathcal{L} = (i\,j)$ into eq. (2.12) we find that the fifth cut condition can only be satisfied for special kinematics satisfying

$$\langle i\,j\,k\,k{+}1\rangle = 0\,. \tag{2.16}$$

Therefore, according to the Cutkosky-inspired rule discussed three paragraphs ago, the monodromy around this putative singularity vanishes for general kinematics and hence it is not a valid branch point at one loop. Indeed this conclusion is easily verified by looking at the explicit results of [40].

2.2.2 The Spurious Three-Mass Box Singularity

The second spurious one-loop singularity encountered in [16] is a subleading singularity of the pentagon which lives on the locus

$$\langle j\,(j{-}1\,j{+}1)(i\,i{+}1)(k\,k{+}1)\rangle = 0 \tag{2.17}$$

and arises from the cut conditions shown in figure 2.1b:

$$0 = \langle \mathcal{L}\,i\,i{+}1\rangle = \langle \mathcal{L}\,j{-}1\,j\rangle = \langle \mathcal{L}\,j\,j{+}1\rangle = \langle \mathcal{L}\,k\,k{+}1\rangle\,. \tag{2.18}$$

These are of three-mass box type and have the two solutions [4]

$$\mathcal{L} = (j\,i\,i{+}1)\cap(j\,k\,k{+}1) \text{ or } \mathcal{L} = (\bar{j}\cap(i\,i{+}1), \bar{j}\cap(k\,k{+}1)). \tag{2.19}$$

The two solutions may be represented respectively by the D-matrices

$$D = \begin{array}{c} \begin{array}{ccc} i & i{+}1 & j \end{array} \\ \begin{pmatrix} 0 & 0 & 1 \\ \langle i{+}1\,j\,k\,k{+}1\rangle & -\langle i\,j\,k\,k{+}1\rangle & 0 \end{pmatrix} \end{array} \tag{2.20}$$

and

$$D = \begin{array}{c} \begin{array}{cccc} i & i{+}1 & k & k{+}1 \end{array} \\ \begin{pmatrix} \langle i{+}1\,\bar{j}\rangle & -\langle i\,\bar{j}\rangle & 0 & 0 \\ 0 & 0 & -\langle \bar{j}\,k+1\rangle & \langle \bar{j}\,k\rangle \end{pmatrix} \end{array}. \tag{2.21}$$

Neither matrix is non-negative definite when the Z's are in the positive domain $G_+(4,n)$, so we again reach the (correct) conclusion that one-loop MHV amplitudes do not have

singularities on the locus where eq. (2.17) is satisfied (for generic i, j and k).

2.2.3 A Two-Loop Example

The two-loop scalar double-pentagon integral considered in [16] has a large number of Landau singularities that are spurious singularities of two-loop MHV amplitudes. It would be cumbersome to start with the full list and eliminate the spurious singularities one at a time using the amplituhedron. Here we will be content to consider one example in detail before abandoning this approach in favor of one more directly built on the amplituhedron.

We consider the Landau singularities shown in eq. (4.12) of [16] which live on the locus

$$\langle j\,(j{-}1\,j{+}1)(i{-}1\,i)\,(k\,l)\rangle\langle j\,(j{-}1\,j{+}1)(i{-}1\,i)\,\bar{k}\cap\bar{l}\rangle = 0\,. \tag{2.22}$$

We consider the generic case when the indices i, j, k, l are well-separated; certain degenerate cases do correspond to non-spurious singularities. This singularity is of pentagon-box type shown in figure 2.1c since it was found in [16] to arise from the eight cut conditions

$$\begin{aligned}&\langle \mathcal{L}^{(1)}\,i{-}1\,i\rangle = \langle \mathcal{L}^{(1)}\,j{-}1\,j\rangle = \langle \mathcal{L}^{(1)}\,j\,j{+}1\rangle = \langle \mathcal{L}^{(1)}\,\mathcal{L}^{(2)}\rangle = 0\,,\\ &\langle \mathcal{L}^{(2)}\,k{-}1\,k\rangle = \langle \mathcal{L}^{(2)}\,k\,k{+}1\rangle = \langle \mathcal{L}^{(2)}\,l{-}1\,l\rangle = \langle \mathcal{L}^{(2)}\,l\,l{+}1\rangle = 0\,.\end{aligned} \tag{2.23}$$

The last four equations have two solutions $\mathcal{L}^{(2)} = (k\,l)$ or $\mathcal{L}^{(2)} = \bar{k}\cap\bar{l}$, but as in the previous subsection, only the first of these has a chance to avoid being outside the amplituhedron. Taking $\mathcal{L}^{(2)} = (k\,l)$, the two solutions to the first four cut conditions are then

$$\mathcal{L}^{(1)} = (j\,i{-}1\,i)\cap(j\,k\,l) = (Z_j, Z_{i-1}\langle i\,j\,k\,l\rangle - Z_i\langle i{-}1\,j\,k\,l\rangle) \text{ or} \tag{2.24}$$

$$\mathcal{L}^{(1)} = \Big((i{-}1\,i)\cap\bar{j}, (k\,l)\cap\bar{j}\Big) = \Big(Z_{i-1}\langle i\,\bar{j}\rangle - Z_i\langle i{-}1\,\bar{j}\rangle, Z_k\langle l\bar{j}\rangle - Z_l\langle k\,\bar{j}\rangle\Big)\,. \tag{2.25}$$

The D-matrices corresponding to the first solution can be taken as

$$\begin{pmatrix} D^{(1)} \\ D^{(2)} \end{pmatrix} = \begin{array}{c} \begin{matrix} i{-}1 & i & j & k & l \end{matrix} \\ \begin{pmatrix} 0 & 0 & 1 & 0 & 0 \\ \langle i\,j\,k\,l\rangle & -\langle i{-}1\,j\,k\,l\rangle & 0 & 0 & 0 \\ 0 & 0 & 0 & 1 & 0 \\ 0 & 0 & 0 & 0 & 1 \end{pmatrix} \end{array}. \tag{2.26}$$

Evidently two of its 4×4 minors are $-\langle i\,j\,k\,l\rangle$ and $\langle i{-}1\,j\,k\,l\rangle$, which have opposite signs for generic Z in the positive domain. D-matrices corresponding to the second solution can be written as

$$\begin{pmatrix} D^{(1)} \\ D^{(2)} \end{pmatrix} = \begin{array}{c} \begin{matrix} i{-}1 & i & k & l \end{matrix} \\ \begin{pmatrix} \langle i\,\bar{j}\rangle & -\langle i{-}1\,\bar{j}\rangle & 0 & 0 \\ 0 & 0 & \langle l\bar{j}\rangle & -\langle k\,\bar{j}\rangle \\ 0 & 0 & 1 & 0 \\ 0 & 0 & 0 & 1 \end{pmatrix} \end{array}, \tag{2.27}$$

which again has minors of opposite signs.

We conclude that the locus where the cut conditions (2.23) are satisfied lies strictly outside the amplituhedron, and therefore that there is no discontinuity around the putative branch point at (2.22). Indeed, this is manifested by the known fact [60] that two-loop MHV amplitudes do not have symbol entries which vanish on this locus. Actually, while correct, we were slightly too hasty in reaching this conclusion, since we only analyzed one set of cut conditions. Although it doesn't happen in this example, in general there may exist several different collections of cut conditions associated to the same Landau singularity, and the discontinuity around that singularity would receive additive contributions from each distinct set of associated cut contributions.

2.2.4 Summary

We have shown, via a slight refinement of the analysis carried out in [16], that the spurious branch points of one- and two-loop MHV amplitudes encountered in that paper can be eliminated simply on the basis of positivity constraints in the amplituhedron. It is simple to see that the cuts considered above have no support for MHV amplitudes so it may seem like overkill to use the fancy language of the amplituhedron. However we wanted to highlight the following approach:

(1) First, consider a representation of an amplitude as a sum over a particular type of Feynman integrals. Find the Landau singularities of a generic term in the sum. These tell us the loci in Z-space where the amplitude *may* have a singularity.

(2) For each *potential* singularity obtained in (1), check whether the corresponding on-shell conditions have a non-zero intersection with the (closure of) the amplituhedron. If the answer is no, for all possible sets of cut conditions associated with a given Landau singularity, then the singularity must be spurious.

This approach is conceptually straightforward but inefficient. One manifestation of this inefficiency is that although double pentagon integrals are characterized by four free indices i, j, k, l, we will see in the next section the vast majority of the resulting potential singularities are spurious. Specifically we will see that in order for the solution to a given set of cut conditions to have support inside the (closure of the) amplituhedron, the conditions must be relaxed in such a way that they involve only three free indices. In other words, most of the $\mathcal{O}(n^4)$ singularities of individual double pentagon integrals must necessarily cancel out when they are summed, leaving only $\mathcal{O}(n^3)$ physical singularities of the full two-loop MHV amplitudes. (The fact that these amplitudes have only $\mathcal{O}(n^3)$ singularities is manifest in the result of [60].) This motivates us to seek a more "amplituhedrony" approach to finding singularities where we do not start by considering any particular representation of the amplitude, but instead start by thinking directly about positive configurations of loops $\mathcal{L}^{(\ell)}$.

2.3 An Amplituhedrony Approach

The most significant drawback of the approach taken in the previous section is that it relies on having explicit representations of an integrand in terms of local Feynman integrals. These have been constructed for all two-loop amplitudes in SYM theory [61], but at higher loop order even finding such representations becomes a huge computational challenge that we would like to be able to bypass. Also, as the loop order increases, the number of potential Landau singularities grows rapidly, and the vast majority of these potential singularities will fail the positivity analysis and hence turn out to be spurious. We would rather not have to sift through all of this chaff to find the wheat.

Let's begin by taking a step back to appreciate that the only reason we needed the crutch of local Feynman integrals in the previous section is that each Feynman diagram topology provides a set of propagators for which we can solve the associated Landau equations (2.9) and (2.10) to find potential singularities. Then, for each set of cut conditions, we can determine whether the associated Landau singularity is physical or spurious by asking the amplituhedron whether or not the set of loops $\mathcal{L}^{(\ell)}$ satisfying the cut conditions has any overlap with the amplituhedron.

In this section we propose a more "amplituhedrony" approach that does not rely on detailed knowledge of integrands. We invert the logic of the previous section: instead of using Feynman diagrams to generate sets of cut conditions that we need to check one by one, we can ask the amplituhedron itself to directly identify all potentially "valid" sets of cut conditions that are possibly relevant to the singularities of an amplitude.

To phrase the problem more abstractly: for a planar n-particle amplitude at L-loop order, there are in general $nL + L(L-1)/2$ possible local cut conditions one can write down:

$$\langle \mathcal{L}^{(\ell)}\, i\, i{+}1\rangle = 0 \text{ for all } \ell, i \text{ and } \langle \mathcal{L}^{(\ell_1)}\, \mathcal{L}^{(\ell_2)}\rangle = 0 \text{ for all } \ell_1 \neq \ell_2. \tag{2.28}$$

We simply need to characterize which subsets of these cut conditions can possibly be simultaneously satisfied for loop momenta $\mathcal{L}^{(\ell)}$ living in the closure of the amplituhedron. Each such set of cut conditions is a subset of one or more maximal subsets, and

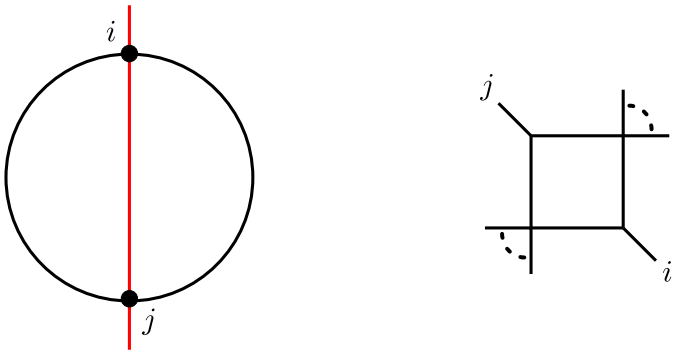

(A) (B)

FIGURE 2.2: (a) A maximum codimension boundary of the one-loop MHV amplituhedron. The circle is a schematic depiction of the n line segments $(1\,2)$, $(2\,3)$, $\ldots$, $(n\,1)$ connecting the n cyclically ordered external kinematic points $Z_i \in G_+(4,n)$ and the red line shows the loop momentum $\mathcal{L} = (i\,j)$. (b) The corresponding Landau diagram, which is a graphical depiction of the four cut conditions (2.30) that are satisfied on this boundary.

these maximal subsets are just the maximal codimension boundaries of the amplituhedron.

Fortunately, the maximal codimension boundaries of the MHV amplituhedron are particularly simple, as explained in [5]. Each loop momentum $\mathcal{L}^{(\ell)}$ must take the form $(i\,j)$ for some i and j (that can be different for different ℓ), and the condition of mutual positivity enforces an emergent planarity: if all of the lines $\mathcal{L}^{(\ell)}$ are drawn as chords on a disk between points on the boundary labeled $1, 2, \ldots, n$, then positivity forbids any two lines to cross in the interior of the disk. In what follows we follow a somewhat low-brow analysis in which we systematically consider relaxations away from the maximum codimension boundaries, but the procedure can be streamlined by better harnessing this emergent planarity, which certainly pays off at higher loop order [62].

In the next few subsections we demonstrate this "amplituhedrony" approach explicitly at one and two loops before summarizing the main idea at the end of the section.

2.3.1 One-Loop MHV Amplitudes

The maximum codimension boundaries of the one-loop MHV amplituhedron occur when

$$\mathcal{L} = (i\,j)\,, \tag{2.29}$$

as depicted in figure 2.2a. On this boundary four cut conditions of "two-mass easy" type [40] are manifestly satisfied:

$$\langle \mathcal{L}\, i{-}1\, i\rangle = \langle \mathcal{L}\, i\, i{+}1\rangle = \langle \mathcal{L}\, j{-}1\, j\rangle = \langle \mathcal{L}\, j\, j{+}1\rangle = 0\,, \tag{2.30}$$

as depicted in the Landau diagram shown in figure 2.2b. (For the moment we consider i and j to be well separated so there are no accidental degenerations.) The Landau analysis of eq. (2.30) has been performed long ago [26, 33] and reviewed in the language of momentum twistors in [16]. A leading solution to the Landau equations exists only if

$$\langle i\,\bar{j}\rangle\langle \bar{i}\,j\rangle = 0\,. \tag{2.31}$$

Subleading Landau equations are obtained by relaxing one of the four on-shell conditions. This leads to cuts of two-mass triangle type, which are uninteresting (they exist for generic kinematics, so don't correspond to branch points of the amplitude). At subsubleading order we reach cuts of bubble type. For example if we relax the second and fourth condition in eq. (2.30) then we encounter a Landau singularity which lives on the locus

$$\langle i{-}1\, i\, j{-}1\, j\rangle = 0\,. \tag{2.32}$$

Other relaxations either give no constraint on kinematics, or the same as eq. (2.32) with $i \to i{+}1$ and/or $j \to j{+}1$.

Altogether, we reach the conclusion that all physical branch points of one-loop MHV amplitudes occur on loci of the form

$$\langle a\,\bar{b}\rangle = 0 \text{ or } \langle a\, a{+}1\, b\, b{+}1\rangle = 0 \tag{2.33}$$

for various a, b. (Note that whenever we say there is a branch point at $x = 0$, we mean more specifically that there is a branch cut between $x = 0$ and $x = \infty$.) Indeed, these exhaust the branch points of the one-loop MHV amplitudes (first computed in [40]) except for branch points arising as a consequence of infrared regularization, which are captured by the BDS ansatz [63].

2.3.2 Two-Loop MHV Amplitudes: Configurations of Positive Lines

We divide the two-loop analysis into two steps. First, in this subsection, we classify valid configurations of mutually non-negative lines. This provides a list of the sets of cut conditions on which two-loop MHV amplitudes have nonvanishing support. Then in the following subsection we solve the Landau equations for each set of cut conditions, to find the actual location of the corresponding branch point.

At two loops the MHV amplituhedron has two distinct kinds of maximum codimension boundaries [5]. The first type has $\mathcal{L}^{(1)} = (i\,j)$ and $\mathcal{L}^{(2)} = (k\,l)$ for distinct cyclically ordered i, j, k, l. Since $\langle \mathcal{L}^{(1)}\ \mathcal{L}^{(2)} \rangle$ is non-vanishing (inside the positive domain $G_+(4, n)$) in this case, this boundary can be thought of as corresponding to a cut of a product of one-loop Feynman integrals, with no common propagator $\langle \mathcal{L}^{(1)}\ \mathcal{L}^{(2)} \rangle$. Therefore we will not learn anything about two-loop singularities beyond what is already apparent at one loop.

The more interesting type of maximum codimension boundary has $\mathcal{L}^{(1)} = (i\,j)$ and $\mathcal{L}^{(2)} = (i\,k)$, as depicted in figure 2.3a. Without loss of generality $i < j < k$, and for now we will moreover assume that i, j and k are well-separated to avoid any potential degenerations. (These can be relaxed at the end of the analysis, in particular to see that the degenerate case $j = k$ gives nothing interesting.) On this boundary the following nine cut conditions shown in the Landau diagram of figure 2.3b are simultaneously

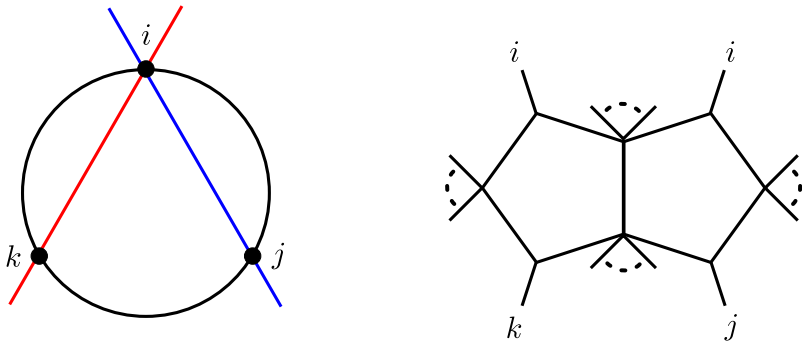

(A) (B)

FIGURE 2.3: (a) A maximum codimension boundary of the two-loop MHV amplituhedron. (b) The corresponding Landau diagram (which, it should be noted, does not have the form of a standard Feynman integral) depicting the nine cut conditions (2.34)–(2.36) that are satisfied on this boundary.

satisfied:

$$\langle \mathcal{L}^{(1)}\, i{-}1\, i\rangle = \langle \mathcal{L}^{(1)}\, i\, i{+}1\rangle = \langle \mathcal{L}^{(2)}\, i{-}1\, i\rangle = \langle \mathcal{L}^{(2)}\, i\, i{+}1\rangle = 0\,, \tag{2.34}$$

$$\langle \mathcal{L}^{(1)}\, j{-}1\, j\rangle = \langle \mathcal{L}^{(1)}\, j\, j{+}1\rangle = \langle \mathcal{L}^{(2)}\, k{-}1\, k\rangle = \langle \mathcal{L}^{(2)}\, k\, k{+}1\rangle = 0\,, \tag{2.35}$$

$$\langle \mathcal{L}^{(1)}\, \mathcal{L}^{(2)}\rangle = 0\,. \tag{2.36}$$

This is the maximal set of cuts that can be simultaneously satisfied while keeping the $\mathcal{L}^{(\ell)}$'s inside the closure of the amplituhedron for generic $Z \in G_+(4,n)$. We immediately note that since only three free indices i, j, k are involved, this set of cuts manifestly has size $\mathcal{O}(n^3)$, representing immediate savings compared to the larger $\mathcal{O}(n^4)$ set of double-pentagon cut conditions as discussed at the end of the previous section.

We can generate other, smaller sets of cut conditions by relaxing some of the nine shown in eqs. (2.34)–(2.36). This corresponds to looking at subleading singularities, in the language of the Landau equations. However, it is not interesting to consider relaxations that lead to $\langle \mathcal{L}^{(1)}\, \mathcal{L}^{(2)}\rangle \neq 0$ because, as mentioned above, it essentially factorizes the problem into a product of one-loop cuts. Therefore in what follows we only consider cuts on which $\langle \mathcal{L}^{(1)}\, \mathcal{L}^{(2)}\rangle = 0$.

By relaxing various subsets of the other 8 conditions we can generate 2^8 subsets of cut conditions. In principle each subset should be analyzed separately, but there

is clearly a natural stratification of relaxations which we can exploit to approach the problem systematically. In fact, we will see that the four cut conditions in eq. (2.34) that involve the point i play a special role. Specifically, we will see that the four cut conditions in eq. (2.35) involving j and k can always be relaxed, or un-relaxed, "for free", with no impact on positivity. Therefore, we see that whether a configuration of loops may be positive or not depends only on which subset of the four cut conditions (2.34) is relaxed.

In this subsection we will classify the subsets of eq. (2.34) that lead to valid configurations of positive lines $\mathcal{L}^{(\ell)}$, and in the next subsection we will find the locations of the corresponding Landau singularities.

Relaxing none of eq. (2.34) [figure 2.3a]. At maximum codimension we begin with the obviously valid pair of mutually non-negative lines represented trivially by

$$\begin{pmatrix} D^{(1)} \\ D^{(2)} \end{pmatrix} = \begin{array}{c} \begin{matrix} i & j & k \end{matrix} \\ \begin{pmatrix} 1 & 0 & 0 \\ 0 & 1 & 0 \\ 1 & 0 & 0 \\ 0 & 0 & 1 \end{pmatrix} \end{array} . \tag{2.37}$$

Relaxing any one of eq. (2.34). The four cases are identical up to relabeling so we consider relaxing the condition $\langle \mathcal{L}^{(2)}\, i\, i{+}1 \rangle = 0$, shown in figure 2.4a. In this case the remaining seven cut conditions on the first two lines of eqs. (2.34) and (2.35) admit the one-parameter family of solutions

$$\mathcal{L}^{(1)} = (i\, j), \qquad \mathcal{L}^{(2)} = (Z_k, \alpha Z_{i-1} + (1-\alpha) Z_i)\,. \tag{2.38}$$

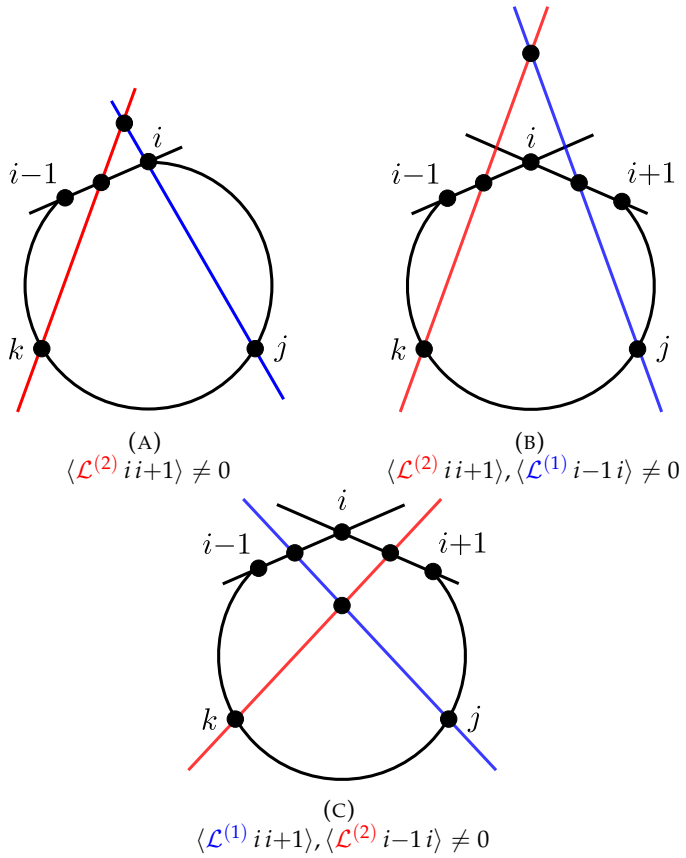

(A) $\langle \mathcal{L}^{(2)}\, i\, i{+}1\rangle \neq 0$

(B) $\langle \mathcal{L}^{(2)}\, i\, i{+}1\rangle, \langle \mathcal{L}^{(1)}\, i{-}1\, i\rangle \neq 0$

(C) $\langle \mathcal{L}^{(1)}\, i\, i{+}1\rangle, \langle \mathcal{L}^{(2)}\, i{-}1\, i\rangle \neq 0$

FIGURE 2.4: Three different invalid relaxations of the maximal codimension boundary shown in figure 2.3.

We recall that the parity conjugate solutions having $\mathcal{L}^{(1)} = \bar{i} \cap \bar{j}$ lie discretely outside the amplituhedron as seen in eq. (2.13). The corresponding D-matrices

$$\begin{pmatrix} D^{(1)} \\ D^{(2)} \end{pmatrix} = \begin{array}{c} \begin{matrix} i-1 & i & j & k \end{matrix} \\ \begin{pmatrix} 0 & 1 & 0 & 0 \\ 0 & 0 & 1 & 0 \\ \alpha & 1-\alpha & 0 & 0 \\ 0 & 0 & 0 & 1 \end{pmatrix} \end{array} \tag{2.39}$$

are mutually non-negative for $0 \leq \alpha \leq 1$. It remains to impose the final cut condition that $\mathcal{L}^{(1)}$ and $\mathcal{L}^{(2)}$ intersect:

$$\langle \mathcal{L}^{(1)} \mathcal{L}^{(2)} \rangle = \alpha \langle i{-}1\, i\, j\, k \rangle = 0\,. \tag{2.40}$$

For general positive external kinematics this will only be satisfied when $\alpha = 0$, which brings us back to the maximum codimension boundary. We conclude that the loop configurations of this type do not generate branch points.

Relaxing $\langle \mathcal{L}^{(1)}\, i{-}1\, i \rangle = 0$ and $\langle \mathcal{L}^{(2)}\, i\, i{+}1 \rangle = 0$ [figure 2.4b]. In this case the six remaining cut conditions in eqs. (2.34) and (2.35) admit the two-parameter family of solutions

$$\mathcal{L}^{(1)} = (\alpha Z_i + (1-\alpha) Z_{i+1}, Z_j), \quad \mathcal{L}^{(2)} = (\beta Z_i + (1-\beta) Z_{i-1}, Z_k)\,. \tag{2.41}$$

The corresponding D-matrices

$$\begin{pmatrix} D^{(1)} \\ D^{(2)} \end{pmatrix} = \begin{array}{c} \begin{matrix} i-1 & i & i+1 & j & k \end{matrix} \\ \begin{pmatrix} 0 & \alpha & 1-\alpha & 0 & 0 \\ 0 & 0 & 0 & 1 & 0 \\ 1-\beta & \beta & 0 & 0 & 0 \\ 0 & 0 & 0 & 0 & 1 \end{pmatrix} \end{array} \tag{2.42}$$

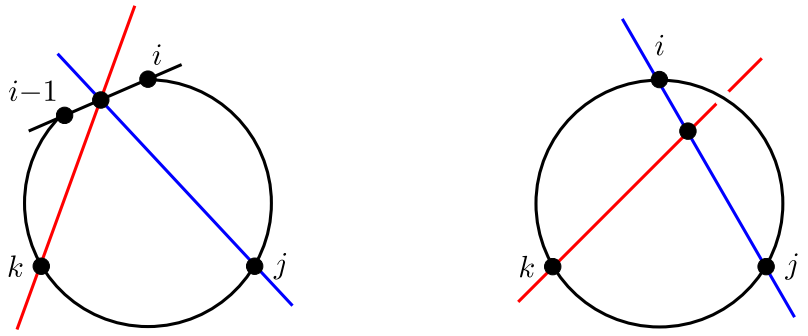

(A) $\langle \mathcal{L}^{(2)}\, i\, i{+}1\rangle, \langle \mathcal{L}^{(1)}\, i\, i{+}1\rangle \neq 0$

(B) $\langle \mathcal{L}^{(2)}\, i{-}1\, i\rangle, \langle \mathcal{L}^{(2)}\, i\, i{+}1\rangle \neq 0$

FIGURE 2.5: Two valid double relaxations of figure 2.3. The other two possibilities are obtained by taking $i \to i{+}1$ in (a) or $\mathcal{L}^{(2)} \to \mathcal{L}^{(1)}$ and $j \leftrightarrow k$ in (b).

are mutually non-negative if $0 \leq \alpha, \beta \leq 1$. Imposing that the two loops intersect gives the constraint

$$\langle \mathcal{L}^{(1)}\mathcal{L}^{(2)}\rangle = \alpha(1-\beta)\langle i{-}1\, i\, j\, k\rangle + (1-\alpha)\beta\langle i\, i{+}1\, j\, k\rangle + (1-\alpha)(1-\beta)\langle i{-}1\, i{+}1\, j\, k\rangle = 0\,, \tag{2.43}$$

which is not satisfied for general positive kinematics unless $\alpha = \beta = 1$, which again brings us back to the maximum codimension boundary.

Relaxing the two conditions $\langle \mathcal{L}^{(1)}\, i\, i{+}1\rangle = \langle \mathcal{L}^{(2)}\, i\, i{-}1\rangle = 0$, depicted in figure 2.4c, is easily seen to lead to the same conclusion.

Relaxing $\langle \mathcal{L}^{(1)}\, i\, i{+}1\rangle = 0$ and $\langle \mathcal{L}^{(2)}\, i\, i{+}1\rangle = 0$ [figure 2.5a]. In this case there is a one-parameter family of solutions satisfying all seven remaining cut conditions including $\langle \mathcal{L}^{(1)}\, \mathcal{L}^{(2)}\rangle = 0$:

$$\mathcal{L}^{(1)} = (\alpha Z_i + (1-\alpha) Z_{i+1}, Z_j), \qquad \mathcal{L}^{(2)} = (\alpha Z_i + (1-\alpha) Z_{i+1}, Z_k)\,. \tag{2.44}$$

The D-matrices can be represented as

$$\begin{pmatrix} D^{(1)} \\ D^{(2)} \end{pmatrix} = \begin{array}{c} \begin{matrix} i & i{+}1 & j & k \end{matrix} \\ \begin{pmatrix} \alpha & 1-\alpha & 0 & 0 \\ 0 & 0 & 1 & 0 \\ \alpha & 1-\alpha & 0 & 0 \\ 0 & 0 & 0 & 1 \end{pmatrix} \end{array}, \tag{2.45}$$

which is a valid mutually non-negative configuration for $0 \leq \alpha \leq 1$. We conclude that these configurations represent physical branch points of two-loop MHV amplitudes by appealing to Cutkoskian intuition, according to which we would compute the discontinuity of the amplitude around this branch point by integrating over $0 \leq \alpha \leq 1$ (in figure 2.5a this corresponds to integrating the intersection point of the two $\mathcal{L}$'s over the line segment between Z_{i-1} and Z_i).

Relaxing the two conditions $\langle \mathcal{L}^{(1)}\, i\, i{-}1 \rangle = \langle \mathcal{L}^{(2)}\, i\, i{-}1 \rangle = 0$ is clearly equivalent up to relabeling.

Relaxing $\langle \mathcal{L}^{(2)}\, i{-}1\, i \rangle = 0$ and $\langle \mathcal{L}^{(2)}\, i\, i{+}1 \rangle = 0$ [figure 2.5b]. The seven remaining cut conditions admit a one-parameter family of solutions

$$\mathcal{L}^{(1)} = (i\, j), \qquad \mathcal{L}^{(2)} = (\alpha Z_i + (1-\alpha) Z_j, Z_k)\,, \tag{2.46}$$

which can be represented by

$$\begin{pmatrix} D^{(1)} \\ D^{(2)} \end{pmatrix} = \begin{array}{c} \begin{matrix} i & j & k \end{matrix} \\ \begin{pmatrix} 1 & 0 & 0 \\ 0 & 1 & 0 \\ \alpha & 1-\alpha & 0 \\ 0 & 0 & 1 \end{pmatrix} \end{array}. \tag{2.47}$$

This is a valid configuration of mutually non-negative lines for $0 \leq \alpha \leq 1$ so we expect it to correspond to a physical branch point. Clearly the same conclusion holds if we were to completely relax $\mathcal{L}^{(1)}$ at i instead of $\mathcal{L}^{(2)}$.

Higher relaxations of eq. (2.34). So far we have considered the relaxation of any one or any two of the conditions shown in eq. (2.34). We have found that single relaxations do not yield branch points of the amplitude, and that four of the six double relaxations are valid while the two double relaxations shown in figures 2.4b and 2.4c are invalid.

What about triple relaxations? These can be checked by explicit construction of the relevant D-matrices, but it is also easy to see graphically that any triple relaxation is valid because they can all be reached by relaxing one of the valid double relaxations. For example, the triple relaxation where we relax all of eq. (2.34) except $\langle \mathcal{L}^{(1)}\, i{-}1\, i \rangle = 0$ can be realized by rotating $\mathcal{L}^{(2)}$ in figure 2.5a clockwise around the point k so that it continues to intersect $\mathcal{L}^{(1)}$. As a second example, the triple relaxation where we relax all but $\langle \mathcal{L}^{(2)}\, i{-}1\, i \rangle = 0$ can be realized by rotating $\mathcal{L}^{(1)}$ in figure 2.5a counter-clockwise around the point j so that it continues to intersect $\mathcal{L}^{(2)}$.

Finally we turn to the case when all four cut conditions in eq. (2.34) are relaxed. These relaxed cut conditions admit two branches of solutions, represented by D-matrices of the form

$$\begin{pmatrix} D^{(1)} \\ D^{(2)} \end{pmatrix} = \begin{array}{c} \begin{matrix} j & j+1 & \cdots & k-1 & k \end{matrix} \\ \begin{pmatrix} 1 & 0 & \cdots & 0 & 0 \\ \alpha_j & \alpha_{j+1} & \cdots & \alpha_{k-1} & \alpha_k \\ \alpha_j & \alpha_{j+1} & \cdots & \alpha_{k-1} & \alpha_k \\ 0 & 0 & \cdots & 0 & 1 \end{pmatrix} \end{array} \tag{2.48}$$

or a similar form with α parameters wrapping the other way around from k to j:

$$\begin{pmatrix} D^{(1)} \\ D^{(2)} \end{pmatrix} = \begin{array}{c} \begin{matrix} \cdots & j{-}1 & j & k & k{+}1 & \cdots \end{matrix} \\ \begin{pmatrix} \cdots & \alpha_{j-1} & \alpha_j & -\alpha_k & -\alpha_{k+1} & \cdots \\ \cdots & 0 & 1 & 0 & 0 & \cdots \\ \cdots & \alpha_{j-1} & \alpha_j & -\alpha_k & -\alpha_{k+1} & \cdots \\ \cdots & 0 & 0 & 1 & 0 & \cdots \end{pmatrix} \end{array} . \tag{2.49}$$

Both of these parameterize valid configuration of mutually non-negative lines as long as all of the α's are positive.

Relaxing $\mathcal{L}^{(1)}$ at j and/or $\mathcal{L}^{(2)}$ at k. All of the configurations we have considered so far keep the four propagators in eq. (2.35) on shell. However it is easy to see that none of these conditions have any bearing on positivity one way or the other. For example, there is no way to render the configuration shown in figure 2.4b positive by moving $\mathcal{L}^{(1)}$ away from the vertex j while maintaining all of the other cut conditions. On the other hand, there is no way to spoil the positivity of the configuration shown in figure 2.5b by moving $\mathcal{L}^{(2)}$ away from the vertex k while maintaining all other cut conditions.

Summary. We call a set of cut conditions "valid" if the $m \geq 0$-dimensional locus in $\mathcal{L}$-space where the conditions are simultaneously satisfied has non-trivial m-dimensional overlap with the closure of the amplituhedron. (The examples shown in figures 2.5a and 2.5b both have $m = 1$, but further relaxations would have higher-dimensional solution spaces.) As mentioned above, this criterion is motivated by Cutkoskian intuition that the discontinuity of the amplitude would be computed by an integral over the intersection of this locus with the (closure of the) amplituhedron. If this intersection is empty (or lives on a subspace that is less than m-dimensional) then such an integral would vanish, signalling that the putative singularity is actually spurious.

The nine cut conditions shown in eqs. (2.34)–(2.36) are solved by the configuration of lines shown in figure 2.3a that is a zero-dimensional boundary of the amplituhedron. We have systematically investigated relaxing various subsets of these conditions (with

the exception of eq. (2.36), to stay within the realm of genuine two-loop singularities) to determine which relaxations are "valid" in the sense just described.

Conclusion: The most general valid relaxation of the configuration shown in figure 2.3a is either an arbitrary relaxation at the points j and k, or an arbitrary relaxation of figure 2.5a (or the same with $i \mapsto i+1$), or an arbitrary relaxation of figure 2.5b (or the same with $j \leftrightarrow k$). The configurations shown in figure 2.4, and further relaxations thereof that are not relaxations of those shown in figure 2.5, are invalid.

2.3.3 Two-Loop MHV Amplitudes: Landau Singularities

In the previous subsection we asked the amplituhedron directly to tell us which possible sets of cut conditions are valid for two-loop MHV amplitudes, rather than starting from some integral representation and using the amplituhedron to laboriously sift through the many spurious singularities. We can draw Landau diagrams for each valid relaxation to serve as a graphical indicator of the cut conditions that are satisfied. The Landau diagram with nine propagators corresponding to the nine cut conditions satisfied by figure 2.3a was already displayed in figure 2.3b. The configurations shown in figures 2.5a and 2.5b satisfy the seven cut conditions corresponding to the seven propagators in figures 2.6a and 2.6b, respectively. We are now ready to determine the locations of the branch points associated to these valid cut configurations (and their relaxations) by solving the Landau equations.

The following calculations follow very closely those done in [16]. Note that throughout this section, in solving cut conditions we will always ignore branches of solutions (for example those of the type $\mathcal{L} = \bar{i} \cap \bar{j}$) which cannot satisfy positivity.

The double-box. For the double-box shown in in figure 2.6a let us use $A \in \mathbb{P}^3$ to denote the point on the line $(i-1, i)$ where the two loop lines $\mathcal{L}^{(\ell)}$ intersect. These can then be parameterized as $\mathcal{L}^{(1)} = (A, Z_j)$ and $\mathcal{L}^{(2)} = (A, Z_k)$. The quickest way to find the location of the leading Landau singularity is to impose eq. (2.9) for each of the two loops. These are both of two-mass easy type, so we find that the Landau singularity

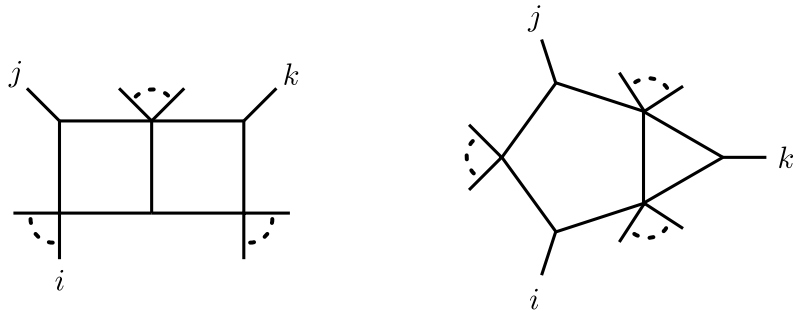

(A) (B)

FIGURE 2.6: The Landau diagrams showing the seven cut conditions satisfied by figures 2.5a and 2.5b, respectively.

lives on the locus (see [16])

$$\langle i{-}1\, i\, j\, k\rangle\langle A\, \bar{j}\rangle = \langle i{-}1\, i\, j\, k\rangle\langle A\, \bar{k}\rangle = 0\,. \tag{2.50}$$

These can be solved in two ways; either by

$$\langle i{-}1\, i\, j\, k\rangle = 0 \tag{2.51}$$

or by solving the first condition for $A = \bar{j} \cap (i{-}1\, i)$ and substituting this into the second condition to find

$$\langle i{-}1\, i\, \bar{j} \cap \bar{k}\rangle = 0\,. \tag{2.52}$$

The astute reader may recall that in (2.16) we discarded a singularity of the same type as in eq. (2.51). This example highlights that it is crucial to appreciate the essential asymmetry between the roles of the two types of Landau equations. The on-shell conditions (2.9) by themselves only provide information about *discontinuities*. We discarded eq. (2.16) because the solution has support on a set of measure zero inside the closure of the amplituhedron, signalling that there is no discontinuity around the branch cut associated to the cut conditions shown in eq. (2.11). Therefore we never needed to inquire as to the actual location where the corresponding branch point might have been. To learn about the *location* of a branch point we have to solve also the second type of Landau equations (2.10). Indeed (2.51) does correspond to a branch point that lies outside

the positive domain, but we don't discard it because the discontinuity of the amplitude around this branch point is nonzero. As mentioned above, according to the Cutkosky rules it would be computed by an integral over the line segment between Z_{i-1} and Z_i in figure 2.5a. When branch points lie outside $G_+(4,n)$, as in this case, it signals a discontinuity that does not exist on the physical sheet but on some other sheet; see the comments near the end of section 1.

Additional (sub^k-leading, for various k) Landau singularities are exposed by setting various sets of α's to zero in the Landau equations and relaxing the associated cut conditions. Although these precise configurations were not analyzed in [16], the results of that paper, together with some very useful tricks reviewed in appendix A, are easily used to reveal branch points at the loci

$$\langle j(j{-}1,j{+}1)(k,k{\pm}1)(i{-}1,i)\rangle = 0 \tag{2.53}$$

together with the same for $j \leftrightarrow k$, as well as $\langle a\, a{+}1\, b\, b{+}1\rangle = 0$ for a, b drawn from the set $\{i{-}1, j{-}1, j, k{-}1, k\}$.

The pentagon-triangle. With the help of appendix A and the results of [16] it is easily seen that the leading singularity of the pentagon-triangle shown in figure 2.6b is located on the locus where

$$\langle i\bar{j}\rangle\langle\bar{i}j\rangle = 0\,. \tag{2.54}$$

The computation of additional singularities essentially reduces to the same calculation for a three-mass pentagon, which was carried out in [16]. Altogether we find that branch

points live on the loci

$$\begin{aligned}
\langle i\,j\,k{-}1\,k\rangle &= 0\,,\\
\langle i(i{-}1\,i{+}1)(j{-}1\,j)(k{-}1\,k)\rangle &= 0\,,\\
\langle i(i{-}1\,i{+}1)(j\,j{+}1)(k{-}1\,k)\rangle &= 0\,,\\
\langle j(j{-}1\,j{+}1)(i{-}1\,i)(k{-}1\,k)\rangle &= 0\,,\\
\langle j(j{-}1\,j{+}1)(i\,i{+}1)(k{-}1\,k)\rangle &= 0\,,\\
\langle i\,i{\pm}1\,j\,k\rangle &= 0\,,\\
\langle i\,j\,j{\pm}1\,k\rangle &= 0\,,
\end{aligned} \tag{2.55}$$

together with the same collection with $(k{-}1\,k) \to (k\,k{+}1)$, as well as all $\langle a\,a{+}1\,b\,b{+}1\rangle = 0$ for a, b drawn from the set $\{i{-}1, i, j{-}1, j, k{-}1, k\}$.

The maximum codimension boundaries. We left this case for last because it is somewhat more subtle. It is known that the final entries of the symbols of MHV amplitudes always have the form $\langle a\,\bar{b}\rangle$ [60]. We expect the leading Landau singularity of the maximum codimension boundary to expose branch points at the vanishing loci of these final entries.

However, if we naively solve the Landau equations for the diagram shown in 2.3b, we run into a puzzle. The first type of Landau equations (2.9) correspond to the nine cut conditions (2.34)–(2.36), which of course are satisfied by $\mathcal{L}^{(1)} = (i\,j)$ and $\mathcal{L}^{(2)} = (i\,k)$. The second type of Landau equations (2.10) does not impose any constraints for pentagons because it is always possible to find a vanishing linear combination of the five participating four-vectors. This naive Landau analysis therefore suggests that there is no leading branch point associated to the maximum codimension boundary.

This analysis is questionable because, as already noted above, the Landau diagram associated to the maximal codimension boundary, shown in figure (2.2b), does not have the form of a valid Feynman diagram. Therefore it makes little sense to trust the associated Landau analysis. Instead let us note that the nine cut conditions (2.34)–(2.36) are

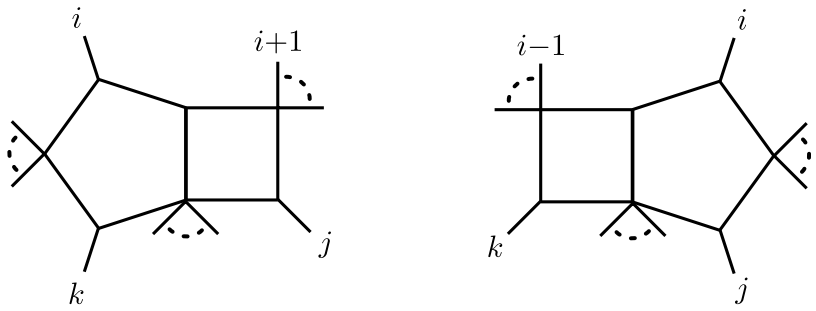

(A) (B)

FIGURE 2.7: Landau diagrams corresponding to all of the cut conditions (2.34)–(2.36) except for (a) $\langle \mathcal{L}^{(1)}\, i{-}1\, i\rangle = 0$, and (b) $\langle \mathcal{L}^{(2)}\, i\, i{+}1\rangle = 0$. These are the only two cut conditions that are redundant (each is implied by the other eight, for generic kinematics) and, when omitted, lead to Landau diagrams that have the form of a standard Feynman integral. (In both figures $\mathcal{L}^{(1)}$ is the momentum in the right loop and $\mathcal{L}^{(2)}$ is the momentum in the left loop.)

not independent; indeed they cannot be as there are only eight degrees of freedom in the loop momenta.

We are therefore motivated to identify which of the nine cut conditions (1) is redundant, in the sense that it is implied by the other eight for generic external kinematics, and (2) has the property that when omitted, the Landau diagram for the remaining eight takes the form of a valid planar Feynman diagram. None of the conditions involving j and k shown in eq. (2.35) are redundant; all of them must be imposed to stay on the maximum codimension boundary. The remaining five conditions in eqs. (2.34) and (2.36) are redundant for general kinematics, but only two of them satisfy the second property. The corresponding Landau diagrams are shown in fig. 2.7. Being valid planar Feynman diagrams, the integrand definitely receives contributions with these topologies (unlike fig. 2.2b), and will exhibit the associated Landau singularities.

It remains to compute the location of the leading Landau singularities for these diagrams. For fig. 2.7a the on-shell conditions for the pentagon set $\mathcal{L}^{(2)} = (i\, k)$ while the Kirkhoff condition for the box is

$$0 = \langle j\,(j{-}1\, j{+}1)\mathcal{L}^{(2)}(i\, i{+}1)\rangle = \langle i\, \bar{j}\rangle\langle i\, i{+}1\, j\, k\rangle\,. \tag{2.56}$$

The Landau equations associated to this topology therefore have solutions when $\langle i\, \bar{j}\rangle =$

0 or when $\langle i\, i{+}1\, j\, k\rangle = 0$. However, on the locus $\langle i\, i{+}1\, j\, k\rangle = 0$ it is no longer true that the eight on-shell conditions shown in fig. 2.7a imply the ninth condition $\langle \mathcal{L}^{(1)}\, i{-}1\, i\rangle = 0$. Therefore, this solution of the Landau equations is not relevant to the maximum codimension boundary.

We conclude that the leading Landau singularity of the maximum codimension boundary is located on the locus where $\langle i\, \bar{j}\rangle = 0$ or (from fig. 2.7b) $\langle i\, \bar{k}\rangle = 0$. These results are in agreement with our expectation about the final symbol entries of MHV amplitudes [60]. Relaxations of Figures 7a, 7b at j, k will not produce any symbol entries.

Conclusion. In conclusion, our analysis has revealed that two-loop MHV amplitudes have physical branch points on the loci of the form

$$\begin{aligned} \langle a\, \bar{b}\rangle &= 0\,, \\ \langle a\, b\, c\, c{+}1\rangle &= 0\,, \\ \langle a\, a{+}1\, \bar{b}\cap\bar{c}\rangle &= 0\,, \\ \langle a\, (a{-}1\, a{+}1)(b\, b{+}1)(c\, c{+}1)\rangle &= 0\,, \end{aligned} \tag{2.57}$$

for arbitrary indices a, b, c. Again let us note that when we say there is a branch point at $x = 0$, we mean a branch cut between $x = 0$ and $x = \infty$. Indeed, this result is in precise accord with the known symbol alphabet of two-loop MHV amplitudes in SYM theory [60].

2.4 Discussion

In this paper we have improved greatly on the analysis of [16] by asking the amplituhedron directly to tell us which branch points of an amplitude are physical. This analysis requires no detailed knowledge about how to write formulas for integrands by constructing the canonical "volume" form on the amplituhedron. We only used the amplituhedron's grossest feature, which is that it is designed to guarantee that integrands

have no poles outside the space of positive loop configurations. We have shown in several examples how to use this principle to completely classify the sets of cut conditions on which integrands can possibly have support. Let us emphasize that our proposal is a completely well-defined geometric algorithm:

- Input: a list of the maximal codimension boundaries of the amplituhedron; for MHV amplitudes these are known from [5].
- Step 1: For a given maximal codimension boundary, identify the list of all cut conditions satisfied on this boundary. For example, at the two-loop boundary shown in figure 2.3a, these would be the nine cut conditions satisfied by the Landau diagram in figure 2.3b, shown in eqs. (2.34)–(2.36). Consider all lower codimension boundaries that can be obtained by relaxing various subsets of these cut conditions, and eliminate those which do not overlap the closure of the amplituhedron, i.e. those which do not correspond to mutually non-negative configurations of lines $\mathcal{L}^{(\ell)}$.
- Step 2: For each valid set of cut conditions obtained in this manner, solve the corresponding Landau equations (2.9) and (2.10) to determine the location of the corresponding branch point of the amplitude.
- Output: a list of the loci in external kinematic space where the given amplitude has branch points.

As we have mentioned a few times in the text, this algorithm is motivated by intuition from the Cutkosky rules, according to which an amplitude's discontinuity is computed by replacing some set of propagators with delta-functions. This localizes the integral onto the intersection of the physical contour and the locus where the cut conditions are satisfied. Now is the time to confess that this intuitive motivation is not a proof of our algorithm, most notably because the positive kinematic domain lives in unphysical $(2,2)$ signature and there is no understanding of how to make sense of the physical $i\epsilon$ contour in momentum twistor space (see however [64] for work in this direction). Nevertheless, the prescription works and it warrants serious further study, in part

because it would be very useful to classify the possible branch points of more general amplitudes in SYM theory.

For amplitudes belonging to the class of generalized polylogarithm functions (which is believed to contain at least all MHV, NMHV and NNMHV amplitudes in SYM theory) the path from knowledge of branch points to amplitudes is fairly well-trodden. Such functions can be represented as iterated integrals [65] and analyzed using the technology of symbols and coproducts [66, 67]. It was emphasized in [23] that the analytic structure of an amplitude is directly imprinted on its symbol alphabet. In particular, the locus in external kinematic space where the letters of an amplitude's symbols vanish (or diverge) must exactly correspond to the locus where solutions of the Landau equations exist. The above algorithm therefore provides direct information about the zero locus of an amplitude's symbol alphabet. For example, the symbol alphabet of one-loop MHV amplitudes must vanish on the locus (2.33), and that of two-loop amplitudes must vanish on the locus (2.57). Strictly speaking this analysis does not allow one to actually determine symbol letters away from their vanishing locus, but it is encouraging that in both eqs. (2.33) and (2.57) the amplituhedron analysis naturally provides the correct symbol letters on the nose.

In general we expect that only letters of the type $\langle a\, a{+}1\, b\, b{+}1\rangle$ may appear in the first entry of the symbol of any amplitude [68]. At one loop, new letters of the type $\langle a\, \bar{b}\rangle$ begin to appear in the second entry. At two loops, additional new letters of the type $\langle a\, (a{-}1\, a{+}1)(b\, b{+}1)(c\, c{+}1)\rangle$ also begin to appear in the second entry, and new letters of the type $\langle a\, b\, c\, c{+}1\rangle$ and $\langle a\, a{+}1\, \bar{b}\cap\bar{c}\rangle$ begin to appear in the third. As discussed at the end of section 3, the final entries of MHV amplitudes are always $\langle a\, \bar{b}\rangle$ [60]. In our paper we have given almost no thought to the question of where in the symbol a given type of letter may begin to appear. However, it seems clear that our geometric algorithm can be taken much further to expose this stratification of branch points, since the relationship between boundaries of the amplituhedron and Landau singularities is the same as the relationship between discontinuities and their branch points. For example it is clear that at any loop order, the lowest codimension boundaries of the

amplituhedron that give rise to branch cuts are configurations where one of the lines $\mathcal{L}$ intersects two lines $(i\,i{+}1)$ and $(j\,j{+}1)$, with all other lines lying in generic mutually positive position. These configurations give rise to the expected first symbol entries $\langle i\,i{+}1\,j\,j{+}1\rangle$. By systematically following the degeneration of configurations of lines onto boundaries of higher and higher codimension we expect there should be a way to derive the symbol alphabet of an amplitude entry by entry.

In many examples, mere knowledge of an amplitude's symbol alphabet, together with some other physical principles, has allowed explicit formulas for the amplitude to be constructed via a bootstrap approach. This approach has been particularly powerful for 6- [69, 70, 71, 72, 73, 20], and 7-point [21] amplitudes, in which case the symbol alphabet is believed to be given, to all loop order, by the set of cluster coordinates on the kinematic configuration space [18]. It would be very interesting to use the algorithm outlined above to prove this conjecture, or to glean information about symbol alphabets for more general amplitudes, both MHV and non-MHV. One simple observation we can make in parting is to note that although maximum codimension boundaries of the L-loop MHV amplitude involve as many as $2L$ distinct points, the singularities that arise from genuinely L-loop configurations (rather than products of lower loop order) involve at most $L+1$ points. Therefore we predict that the size of the symbol alphabet of L-loop MHV amplitudes should grow with n no faster than $\mathcal{O}(n^{L+1})$.

It would be very interesting to extend our results to non-MHV amplitudes. For the N^K amplitude, singularities should still be found only on the boundary of the N^KMHV amplituhedron, so the presented approach should still be applicable, albeit more complicated. An important difference would be the existence of poles, in addition to branch points, due to the presence of rational prefactors. We are not certain our approach would naturally distinguish these two types of singularities. However, the singularities of rational prefactors can be found using other means, for example by considering the boundaries of the tree-level amplituhedron.

2.5 Elimination of Bubbles and Triangles

Here we collect a few comments on the elimination of bubble and triangle sub-diagrams in the Landau analysis. These tricks, together with the results of [16], can be used to easily obtain all of the Landau singularities reported in section 2.3.3.

2.5.1 Bubble sub-diagrams

The Landau equation for a bubble with propagators ℓ and $\ell + p$, which may be a sub-diagram of a larger diagram, are

$$\ell^2 = (\ell + p)^2 = 0\,, \tag{2.58}$$

$$\alpha_1 \ell^\mu + \alpha_2 (\ell + p)^\mu = 0\,, \tag{2.59}$$

where α_1 and α_2 are the Feynman parameters associated to the two propagators. The loop equation has solution

$$\ell^\mu = -\frac{\alpha_2}{\alpha_1 + \alpha_2} p^\mu \tag{2.60}$$

so that

$$\alpha_1 \ell^\mu = -\frac{\alpha_1 \alpha_2}{\alpha_1 + \alpha_2} p^\mu, \qquad \alpha_2 (\ell + p)^\mu = \frac{\alpha_1 \alpha_2}{\alpha_1 + \alpha_2} p^\mu, \tag{2.61}$$

while the on-shell conditions simply impose $p^2 = 0$. Therefore, we see that any Landau diagram containing this bubble sub-diagram is equivalent to the same diagram with the bubble replaced by a single on-shell line with momentum p^μ and modified Feynman parameter $\alpha' = \alpha_1 \alpha_2 / (\alpha_1 + \alpha_2)$. We do not need to keep track of the modified Feynman parameter; we simply move on to the rest of the diagram using the new Feynman parameter α'.

In conclusion, any bubble sub-diagram can be collapsed to a single edge, as far as the Landau analysis is concerned.

2.5.2 Triangle sub-diagrams

Similarly, we will now discuss the various branches associated to a triangle sub-diagram. The Landau equations for a triangle with edges carrying momenta $q_1 = \ell$, $q_2 = \ell + p_1 + p_2$ and $q_3 = \ell + p_2$, and with corresponding Feynman parameters α_1, α_2 and α_3, are

$$\ell^2 = (\ell + p_2)^2 = (\ell + p_1 + p_2)^2 = 0\,, \tag{2.62}$$

$$\alpha_1 \ell^\mu + \alpha_2 (\ell + p_1 + p_2)^\mu + \alpha_3 (\ell + p_2)^\mu = 0\,. \tag{2.63}$$

The solution to the loop equation is

$$\ell^\mu = -\frac{(\alpha_2 + \alpha_3) p_2^\mu + \alpha_2 p_1^\mu}{\alpha_1 + \alpha_2 + \alpha_3} \tag{2.64}$$

while eqs. (4.1) impose the two conditions

$$0 = p_1^2\, p_2^2\, p_3^2\,, \tag{2.65}$$

$$(\alpha_1 : \alpha_2 : \alpha_3) = \big(p_1^2(-p_1^2 + p_2^2 + p_3^2) : p_2^2(p_1^2 - p_2^2 + p_3^2) : p_3^2(p_1^2 + p_2^2 - p_3^2)\big) \tag{2.66}$$

where $p_3 = -p_1 - p_2$. Suppose we follow the branch $p_1^2 = 0$. In this case α_1 is forced to vanish, effectively reducing the triangle to a bubble with edges

$$\alpha_2 q_2^\mu = \frac{\alpha_3 p_2^2}{p_2^2 - p_3^2} p_1^\mu\,, \qquad \alpha_3 q_3^\mu = -\frac{\alpha_3 p_2^2}{p_2^2 - p_3^2} p_1^\mu\,. \tag{2.67}$$

This is equivalent (by appendix A.1) to a single on-shell line carrying momentum p_1^μ. A similar conclusion clearly holds for the branches $p_2^2 = 0$ or $p_3^2 = 0$. If any two of p_1^2, p_2^2 or p_3^2 simultaneously vanish, then the two corresponding Feynman parameters must vanish. Finally, if all three p_i^2 vanish, then the Landau equations are identically satisfied for any values of the three α_i. In conclusion, triangle sub-diagrams of a general Landau diagram can be analyzed by considering separately each of the seven branches outlined here.

Chapter 3

All-Helicity Symbol Alphabets from Unwound Amplituhedra

3.1 Review

This section provides a thorough introduction to the problem our work aims to solve. The concepts and techniques reviewed here will be illuminated in subsequent sections via several concrete examples.

3.1.1 The Kinematic Domain

Scattering amplitudes are (in general multivalued) functions of the kinematic data (the energies and momenta) describing some number of particles participating in some scattering process. Specifically, amplitudes are functions only of the kinematic information about the particles entering and exiting the process, called *external data* in order to distinguish it from information about virtual particles which may be created and destroyed during the scattering process itself. A general scattering amplitude in SYM theory is labeled by three integers: the number of particles n, the helicity sector $0 \leq \mathrm{k} \leq n-4$, and the loop order $L \geq 0$, with $L = 0$ called *tree level* and $L > 0$ called *L-loop level*. Amplitudes with $\mathrm{k} = 0$ are called maximally helicity violating (MHV) while those with $\mathrm{k} > 0$ are called (next-to-)$^{\mathrm{k}}$maximally helicity violating (N^{k}MHV).

The kinematic configuration space of SYM theory admits a particularly simple characterization: n-particle scattering amplitudes[1] are multivalued functions on $\mathrm{Conf}_n(\mathbb{P}^3)$, the space of configurations of n points in $\mathbb{P}^3$ [18]. A generic point in $\mathrm{Conf}_n(\mathbb{P}^3)$ may be represented by a collection of n homogeneous coordinates Z_a^I on $\mathbb{P}^3$ (here $I \in \{1,\ldots,4\}$ and $a \in \{1,\ldots,n\}$) called *momentum twistors* [55], with two such collections considered equivalent if the corresponding $4 \times n$ matrices $Z \equiv (Z_1 \cdots Z_n)$ differ by left-multiplication by an element of $\mathrm{GL}(4)$. We use the standard notation

$$\langle a\, b\, c\, d\rangle = \epsilon_{IJKL} Z_a^I Z_b^J Z_c^K Z_d^L \tag{3.1}$$

for the natural $\mathrm{SL}(4)$-invariant four-bracket on momentum twistors and use the shorthand $\langle \cdots \bar{a} \cdots \rangle = \langle \cdots a{-}1\, a\, a{+}1 \cdots \rangle$, with the understanding that all particle labels are always taken mod n. We write $(a\, b)$ to denote the line in $\mathbb{P}^3$ containing Z_a and Z_b, $(a\, b\, c)$ to denote the plane containing Z_a, Z_b and Z_c, and so $\bar{a}$ denotes the plane $(a{-}1\, a\, a{+}1)$. The bar notation is motivated by *parity*, which is a $\mathbb{Z}_2$ symmetry of SYM theory that maps $\mathrm{N^kMHV}$ amplitudes to $\mathrm{N}^{n-\mathrm{k}-4}\mathrm{MHV}$ amplitudes while mapping the momentum twistors according to $\{Z_a\} \mapsto \{W_a = *(a{-}1\, a\, a{+}1)\}$.

When discussing $\mathrm{N^kMHV}$ amplitudes it is conventional to consider an enlarged kinematic space where the momentum twistors are promoted to homogeneous coordinates $\mathcal{Z}_a$, bosonized momentum twistors [4] on $\mathbb{P}^{\mathrm{k}+3}$ which assemble into an $n \times (\mathrm{k}+4)$ matrix $\mathcal{Z} \equiv (\mathcal{Z}_1 \cdots \mathcal{Z}_n)$. The analog of Eq. (3.1) is then the $\mathrm{SL}(\mathrm{k}+4)$-invariant bracket which we denote by $[\cdot]$ instead of $\langle\cdot\rangle$. Given some $\mathcal{Z}$ and an element of the Grassmannian $\mathrm{Gr}(\mathrm{k}, \mathrm{k}+4)$ represented by a $\mathrm{k} \times (\mathrm{k}+4)$ matrix Y, one can obtain an element of $\mathrm{Conf}_n(\mathbb{P}^3)$ by projecting onto the complement of Y. The four-brackets of the *projected external data* obtained in this way are given by

$$\langle a\, b\, c\, d\rangle \equiv [Y\, \mathcal{Z}_a\, \mathcal{Z}_b\, \mathcal{Z}_c\, \mathcal{Z}_d]\,. \tag{3.2}$$

[1] Here and in all that follows, we mean components of superamplitudes suitably normalized by dividing out the tree-level Parke-Taylor-Nair superamplitude [57, 74]. We expect our results to apply equally well to BDS- [63] and BDS-like [75] regulated MHV and non-MHV amplitudes. The set of branch points of a non-MHV ratio function [76] should be a subset of those of the corresponding non-MHV amplitude, but our analysis cannot exclude the possibility that it may be a proper subset due to cancellations.

Tree-level amplitudes are rational functions of the brackets while loop-level amplitudes have both poles and branch cuts, and are properly defined on an infinitely-sheeted cover of $\text{Conf}_n(\mathbb{P}^3)$. For each k there exists an open set $\mathcal{D}_{n,\text{k}} \subset \text{Conf}_n(\mathbb{P}^3)$ called the *principal domain* on which amplitudes are known to be holomorphic and non-singular. Amplitudes are initially defined only on $\mathcal{D}_{n,\text{k}}$ and then extended to all of (the appropriate cover of) $\text{Conf}_n(\mathbb{P}^3)$ by analytic continuation.

A simple characterization of the principal domain for n-particle N^kMHV amplitudes was given in [37]: $\mathcal{D}_{n,\text{k}}$ may be defined as the set of points in $\text{Conf}_n(\mathbb{P}^3)$ that can be represented by a Z-matrix with the properties

1. $\langle a\, a{+}1\, b\, b{+}1\rangle > 0$ for all a and $b \notin \{a{-}1, a, a{+}1\}$[2], and
2. the sequence $\langle 1\,2\,3\,\bullet\rangle$ has precisely k sign flips,

where we use the notation $\bullet \in \{1, 2, \ldots, n\}$ so that

$$\langle 1\,2\,3\,\bullet\rangle \equiv \{0, 0, 0, \langle 1\,2\,3\,4\rangle, \langle 1\,2\,3\,5\rangle, \ldots, \langle 1\,2\,3\,n\rangle\}\,. \tag{3.3}$$

It was also shown that an alternate but equivalent condition is to say that the sequence $\langle a\, a{+}1\, b\,\bullet\rangle$ has precisely k sign flips for all a, b (omitting trivial zeros, and taking appropriate account of the twisted cyclic symmetry where necessary). The authors of [37] showed, and we review in Sec. 3.1.2, that for Y's inside an N^kMHV amplituhedron, the projected external data have the two properties above.

3.1.2 Amplituhedra ...

A matrix is said to be *positive* or *non-negative* if all of its ordered maximal minors are positive or non-negative, respectively. In particular, we say that the external data are positive if the $n \times (\text{k}+4)$ matrix $\mathcal{Z}$ described in the previous section is positive.

A point in the n-particle N^kMHV L-loop *amplituhedron* $\mathcal{A}_{n,\text{k},L}$ is a collection $(Y, \mathcal{L}^{(\ell)})$ consisting of a point $Y \in \text{Gr}(\text{k}, \text{k}+4)$ and L lines $\mathcal{L}^{(1)}, \ldots, \mathcal{L}^{(L)}$ (called the *loop momenta*)

[2] As explained in [37], the cyclic symmetry on the n particle labels is "twisted", which manifests itself here in the fact that if k is even, and if $a = n$ or $b = n$, then cycling around n back to 1 introduces an extra minus sign. The condition in these cases is therefore $(-1)^{\text{k}+1}\langle c\, c{+}1\, n\, 1\rangle > 0$ for all $c \notin \{1, n{-}1, n\}$.

in the four-dimensional complement of Y. We represent each $\mathcal{L}^{(\ell)}$ as a $2 \times (\mathrm{k}+4)$ matrix with the understanding that these are representatives of equivalence classes under the equivalence relation that identifies any linear combination of the rows of Y with zero.

For given positive external data $\mathcal{Z}$, the amplituhedron $\mathcal{A}_{n,\mathrm{k},L}(\mathcal{Z})$ was defined in [4] for $n \geq 4$ as the set of $(Y, \mathcal{L}^{(\ell)})$ that can be represented as

$$Y = C\mathcal{Z}\,, \tag{3.4}$$

$$\mathcal{L}^{(\ell)} = D^{(\ell)}\mathcal{Z}\,, \tag{3.5}$$

in terms of a $\mathrm{k} \times n$ real matrix C and L $2 \times n$ real matrices $D^{(\ell)}$ satisfying the positivity property that for any $0 \leq m \leq L$, all $(2m+\mathrm{k}) \times n$ matrices of the form

$$\begin{pmatrix} D^{(i_1)} \\ D^{(i_2)} \\ \vdots \\ D^{(i_m)} \\ C \end{pmatrix} \tag{3.6}$$

are positive. The D-matrices are understood as representatives of equivalence classes and are defined only up to translations by linear combinations of rows of the C-matrix.

One of the main results of [37] was that amplituhedra can be characterized directly by (projected) four-brackets, Eq. (3.2), without any reference to C or $D^{(\ell)}$'s, by saying that for given positive $\mathcal{Z}$, a collection $(Y, \mathcal{L}^{(\ell)})$ lies inside $\mathcal{A}_{n,\mathrm{k},L}(\mathcal{Z})$ if and only if

1. the projected external data lie in the principal domain $\mathcal{D}_{n,\mathrm{k}}$,
2. $\langle \mathcal{L}^{(\ell)}\, a\, a{+}1 \rangle > 0$ for all ℓ and a[3],
3. for each ℓ, the sequence $\langle \mathcal{L}^{(\ell)}\, 1\, \bullet \rangle$ has precisely $\mathrm{k}+2$ sign flips, and
4. $\langle \mathcal{L}^{(\ell_1)}\, \mathcal{L}^{(\ell_2)} \rangle > 0$ for all $\ell_1 \neq \ell_2$.

[3] Again, the twisted cyclic symmetry implies that the correct condition for the case $a = n$ is $(-1)^{\mathrm{k}+1}\langle \mathcal{L}^{(\ell)}\, n\, 1 \rangle > 0$.

Here the notation $\langle \mathcal{L}\, a\, b\rangle$ means $\langle A\, B\, a\, b\rangle$ if the line $\mathcal{L}$ is represented as $(A\, B)$ for two points A, B. It was also shown that items 2 and 3 above are equivalent to saying that the sequence $\langle \mathcal{L}^{(\ell)}\, a\, \bullet\rangle$ has precisely $\mathrm{k}+2$ sign flips for any ℓ and a.

3.1.3 ... and their Boundaries

The amplituhedron $\mathcal{A}_{n,\mathrm{k},L}$ is an open set with boundaries at loci where one or more of the inequalities in the above definitions become saturated. For example, there are boundaries where Y becomes such that one or more of the projected four-brackets $\langle a\, a{+}1\, b\, b{+}1\rangle$ become zero. Such projected external data lie on a boundary of the principal domain $\mathcal{D}_{n,\mathrm{k}}$. Boundaries of this type are already present in tree-level amplituhedra, which are well-understood and complementary to the focus of our work.

Instead, the boundaries relevant to our analysis occur when Y is such that the projected external data are generic, but the $\mathcal{L}^{(\ell)}$ satisfy one or more *on-shell conditions* of the form

$$\langle \mathcal{L}^{(\ell)}\, a\, a{+}1\rangle = 0 \quad \text{and/or} \quad \langle \mathcal{L}^{(\ell_1)}\, \mathcal{L}^{(\ell_2)}\rangle = 0\,. \tag{3.7}$$

We refer to boundaries of this type as *$\mathcal{L}$-boundaries*[4]. The collection of loop momenta satisfying a given set of on-shell conditions comprises a set whose connected components we call *branches*. Consider two sets of on-shell conditions S, S', with $S' \subset S$ a proper subset, and B (B') a branch of solutions to S (S'). Since $S' \subset S$, B' imposes fewer constraints on the degrees of freedom of the loop momenta than B does. In the case when $B \subset B'$, we say B' is a *relaxation* of B. We use $\overline{\mathcal{A}_{n,\mathrm{k},L}}$ to denote the closure of the amplituhedron, consisting of $\mathcal{A}_{n,\mathrm{k},L}$ together with all of its boundaries. We say that $\mathcal{A}_{n,\mathrm{k},L}$ *has a boundary of type* B if $B \cap \overline{\mathcal{A}_{n,\mathrm{k},L}} \neq \emptyset$ and $\dim(B \cap \overline{\mathcal{A}_{n,\mathrm{k},L}}) = \dim(B)$.

3.1.4 The Landau Equations

In [17] it was argued, based on well-known and general properties of scattering amplitudes in quantum field theory (see in particular [27]), that all information about the

[4] In the sequel [47] we will strengthen this definition to require that $\langle \mathcal{L}^{(1)}\, \mathcal{L}^{(2)}\rangle = 0$ at two loops.

locations of branch points of amplitudes in SYM theory can be extracted from knowledge of the $\mathcal{L}$-boundaries of amplituhedra via the Landau equations [26, 33]. In order to formulate the Landau equations we must parameterize the space of loop momenta in terms of $4L$ variables d_A. For example, we could take[5] $\mathcal{L}^{(\ell)} = D^{(\ell)}\mathcal{Z}$ with

$$D^{(1)} = \begin{pmatrix} 1 & 0 & d_1 & d_2 \\ 0 & 1 & d_3 & d_4 \end{pmatrix}, \quad D^{(2)} = \begin{pmatrix} 1 & 0 & d_5 & d_6 \\ 0 & 1 & d_7 & d_8 \end{pmatrix}, \quad \text{etc.}, \tag{3.8}$$

but any other parameterization works just as well.

Consider now an $\mathcal{L}$-boundary of some $\mathcal{A}_{n,\mathrm{k},L}$ on which the L lines $\mathcal{L}^{(\ell)}$ satisfy d on-shell constraints

$$f_J = 0 \qquad (J = 1, 2, \ldots, d)\,, \tag{3.9}$$

each of which is of the form of one of the brackets shown in Eq. (3.7). The *Landau equations* for this set of on-shell constraints comprise Eq. (3.9) together with a set of equations on d auxiliary variables α_J known as *Feynman parameters*:

$$\sum_{J=1}^{d} \alpha_J \frac{\partial f_J}{\partial d_A} = 0 \qquad (A = 1, \ldots, 4L)\,. \tag{3.10}$$

The latter set of equations are sometimes referred to as the *Kirchhoff conditions*.

We are never interested in the values of the Feynman parameters, we only want to know under what conditions nontrivial solutions to Landau equations exist. Here, "nontrivial" means that the α_J must not all vanish[6]. Altogether we have $d + 4L$ equations in $d + 4L$ variables (the d α_J's and the $4L$ d_A's). However, the Kirchhoff conditions are clearly invariant under a projective transformation that multiplies all of the α_J simultaneously by a common nonzero number, so the effective number of free parameters is

[5] By writing each $\mathcal{L}$ as a 2×4 matrix, instead of $2 \times (\mathrm{k}+4)$, we mean to imply that we are effectively working in a gauge where the last four columns of Y are zero and so the first k columns of each $\mathcal{L}$ are irrelevant and do not need to be displayed.

[6] Solutions for which some of the Feynman parameters vanish are often called "subleading" Landau singularities in the literature, in contrast to a "leading" Landau singularity for which all α's are nonzero. We will make no use of this terminology and pay no attention to the values of the α's other than ensuring they do not all vanish.

only $d + 4L - 1$. Therefore, we might expect that nontrivial solutions to the Landau equations do not generically exist, but that they may exist on codimension-one loci in $\text{Conf}_n(\mathbb{P}^3)$ — these are the loci on which the associated scattering amplitude may have a singularity according to [26, 33].

However the structure of solutions is rather richer than this naive expectation suggests because the equations are typically polynomial rather than linear, and they may not always be algebraically independent. As we will see in the examples considered in Sec. 3.5, it is common for nontrivial solutions to exist for generic projected external data[7], and it can happen that there are branches of solutions that exist only on loci of codimension higher than one. We will not keep track of solutions of either of these types since they do not correspond to branch points in the space of generic projected external data.

There are two important points about our procedure which were encountered in [17] and deserve to be emphasized. The first is a subtlety that arises from the fact that the on-shell conditions satisfied on a given boundary of some amplituhedron are not always independent. For example, the end of Sec. 3 of [17] discusses a boundary of $\mathcal{A}_{n,0,2}$ described by nine on-shell conditions with the property that the ninth is implied by the other eight. This situation arises generically for $L > 1$, and a procedure — called *resolution* — for dealing with these cases was proposed in [17]. We postpone further discussion of this point to the sequel as this paper focuses only on one-loop examples.

Second, there is a fundamental asymmetry between the two types of Landau equations, (3.9) and (3.10), in two respects. When solving the on-shell conditions we are only interested in branches of solutions that (A1) exist for generic projected external data, and that (A2) have nonempty intersection with $\overline{\mathcal{A}_{n,\text{k},L}}$ with correct dimension. In contrast, when further imposing the Kirchhoff constraints on these branches, we are interested in solutions that (B1) exist on codimension-one loci in $\text{Conf}_n(\mathbb{P}^3)$, and (B2) need not

[7] Solutions of this type were associated with infrared singularities in [16]. We do not keep track of these solutions since the infrared structure of amplitudes in massless gauge theory is understood to all loop order based on exponentiation [77, 63]. However, if some set of Landau equations has an "IR solution" at some particular $\mathcal{L}^{(\ell)}$, there may be other solutions, at different values of $\mathcal{L}^{(\ell)}$, that exist only on loci of codimension one. In such cases we do need to keep track of the latter.

remain within $\overline{\mathcal{A}_{n,\mathrm{k},L}}$. The origin of this asymmetry was discussed in [17]. In brief, it arises from Cutkoskian intuition whereby singularities of an amplitude may arise from configurations of loop momenta that are outside the physical domain of integration (by virtue of being complex; or, in the current context, being outside the closure of the amplituhedron), and are only accessible after analytic continuation to some higher sheet; whereas the monodromy of an amplitude around a singularity is computed by an integral over the physical domain with the cut propagators replaced by delta functions. The resulting monodromy will be zero, i.e. the branch point doesn't really exist, if there is no overlap between the physical domain and the locus where the cuts are satisfied, motivating (A2) above. In summary, it is important to "solve the on-shell conditions first" and then impose the Kirchhoff conditions on the appropriate branches of solutions only afterwards.

3.1.5 Summary: The Algorithm

The Landau equations may be interpreted as defining a map which associates to each boundary of the amplituhedron $\mathcal{A}_{n,\mathrm{k},L}$ a locus in $\mathrm{Conf}_n(\mathbb{P}^3)$ on which the corresponding n-point N$^{\mathrm{k}}$MHV L-loop amplitude has a singularity. The Landau equations themselves have no way to indicate whether a singularity is a pole or branch point. However, it is expected that all poles in SYM theory arise from boundaries that are present already in the tree-level amplituhedra [4]. These occur when some $\langle a\, a{+}1\, b\, b{+}1\rangle$ go to zero as discussed at the beginning of Sec. 3.1.3. The aim of our work is to understand the loci where amplitudes have branch points, so we confine our attention to the $\mathcal{L}$-boundaries defined in that section.

The algorithm for finding all branch points of the n-particle N$^{\mathrm{k}}$MHV L-loop amplitude is therefore simple in principle:

1. Enumerate all $\mathcal{L}$-boundaries of $\mathcal{A}_{n,\mathrm{k},L}$ for generic projected external data.

2. For each $\mathcal{L}$-boundary, identify the codimension-one loci (if there are any) in $\mathrm{Conf}_n(\mathbb{P}^3)$ on which the corresponding Landau equations admit nontrivial solutions.

However, it remains a difficult and important outstanding problem to fully characterize the boundaries of general amplituhedra. In the remainder of this paper we focus on the special case $L = 1$, since all $\mathcal{L}$-boundaries of $\mathcal{A}_{n,k,1}$ (which have been discussed extensively in [10]) may be enumerated directly for any given n:

1(a). Start with a list of all possible sets of on-shell conditions of the form $\langle \mathcal{L}\, a\, a{+}1\rangle = 0$.

1(b). For each such set, identify all branches of solutions that exist for generic projected external data.

1(c). For each such branch B, determine the values of k for which $\mathcal{A}_{n,k,1}$ has a boundary of type B.

It would be enormously inefficient to carry out this simple-minded algorithm beyond one loop. Fortunately, we will see in the sequel that the one-loop results of this paper can be exploited very effectively to generate $\mathcal{L}$-boundaries of $L > 1$ amplituhedra.

3.2 One-Loop Branches

In this section we carry out steps 1(a) and 1(b) listed at the end of Sec. 3.1.5. To that end we first introduce a graphical notation for representing sets of on-shell conditions via *Landau diagrams*. Landau diagrams take the form of ordinary Feynman diagrams, with external lines labeled $1, \ldots, n$ in cyclic order and one internal line (called a *propagator*) corresponding to each on-shell condition. Landau diagrams relevant to amplituhedra are always planar. Each internal face of an L-loop Landau diagram is labeled by a distinct $\ell \in \{1, \ldots, L\}$, and each external face may be labeled by the pair $(a\, a{+}1)$ of external lines bounding that face.

The set of on-shell conditions encoded in a given Landau diagram is read off as follows:

- To each propagator bounding an internal face ℓ and an external face $(a\, a{+}1)$ we associate the on-shell condition $\langle \mathcal{L}^{(\ell)}\, a\, a{+}1\rangle = 0$.

- To each propagator bounding two internal faces ℓ_1, ℓ_2 we associate the on-shell condition $\langle \mathcal{L}^{(\ell_1)}\, \mathcal{L}^{(\ell_2)} \rangle = 0$.

At one loop we only have on-shell conditions of the first type. Moreover, since $\mathcal{L}$ only has four degrees of freedom (the dimension of $\mathrm{Gr}(2,4)$ is four), solutions to a set of on-shell conditions will exist for generic projected external data only if the number of conditions is $d \leq 4$. Diagrams with $d = 1,2,3,4$ are respectively named tadpoles, bubbles, triangles and boxes. The structure of solutions to a set of on-shell conditions can change significantly depending on how many pairs of conditions involve adjacent indices. Out of abundance of caution it is therefore necessary to consider separately the eleven distinct types of Landau diagrams shown in the second column of Tab. 3.1. For $d > 1$ their names are qualified by indicating the number of nodes with valence greater than three, called *masses*. These rules suffice to uniquely name each distinct type of diagram except the two two-mass boxes shown in Tab. 3.1 which are conventionally called "easy" and "hard". This satisfies step 1(a) of the algorithm.

Proceeding now to step 1(b), we display in the third column of Tab. 3.1 all branches of solutions (as always, for generic projected external data) to the on-shell conditions associated to each Landau diagram. These expressions are easily checked by inspection or by a short calculation. More details and further discussion of the geometry of these problems can be found for example in [32]. The three-mass triangle solution involves the quantities

$$\begin{aligned} \rho(\alpha) &= -\alpha\langle i\, j{+}1\, k\, k{+}1\rangle - (1-\alpha)\langle i{+}1\, j{+}1\, k\, k{+}1\rangle\,, \\ \sigma(\alpha) &= \alpha\langle i\, j\, k\, k{+}1\rangle + (1-\alpha)\langle i{+}1\, j\, k\, k{+}1\rangle\,, \end{aligned} \tag{3.11}$$

and the four-mass box solution is sufficiently messy that we have chosen not to write it out explicitly.

Altogether there are nineteen distinct types of branches, which we have numbered (1) through (19) in Tab. 3.1 for ease of reference. The set of solutions to any set of on-shell conditions of the form $\langle \mathcal{L}\, a\, a{+}1\rangle$ must be closed under parity, since each line $(a\, a{+}1)$ maps to itself. Most sets of on-shell conditions have two branches of solutions related

to each other by parity. Only the tadpole, two-mass bubble, and three-mass triangle (branches (1), (4), and (9) respectively) have single branches of solutions that are closed under parity.

Name	Landau Diagram	Branches		k-Validity	Low-k Twistor Diagram	Singularity Locus/Loci
tadpole ($n \geq 4$)	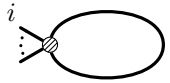	(1) $\mathcal{L}$	$= (\alpha Z_i + (1-\alpha) Z_{i+1}, A)$	$0 \leq \mathrm{k} \leq n-4$		0
one-mass bubble ($n \geq 4$)		(2) $\mathcal{L}$	$= (Z_i, A)$	$0 \leq \mathrm{k} \leq n-4$	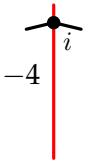	0
		(3) $\mathcal{L}$	$= \bar{i} \cap P$	$n-4 \geq \mathrm{k} \geq 0$		
two-mass bubble ($n \geq 4$)	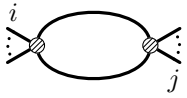	(4) $\mathcal{L}$	$= (\alpha Z_i + (1-\alpha) Z_{i+1},$ $\beta Z_j + (1-\beta) Z_{j+1})$	$0 \leq \mathrm{k} \leq n-4$		$\langle i\, i{+}1\, j\, j{+}1 \rangle$
one-mass triangle ($n \geq 4$)	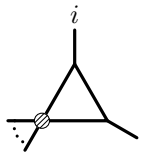	(5) $\mathcal{L}$	$= (Z_i, \alpha Z_{i+1} + (1-\alpha) Z_{i+2})$	$0 \leq \mathrm{k} \leq n-4$	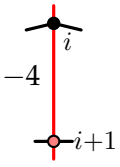	0
		(6) $\mathcal{L}$	$= (Z_{i+1}, \alpha Z_{i-1} + (1-\alpha) Z_i)$	$n-4 \geq \mathrm{k} \geq 0$		

two-mass triangle ($n \geq 5$)	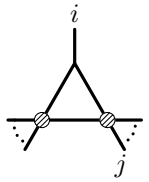	(7) $\mathcal{L}$ = $(Z_i, \alpha Z_j + (1-\alpha) Z_{j+1})$	$0 \leq k \leq n-5$	0
		(8) $\mathcal{L}$ = $\bar{i} \cap (j\, j{+}1\, A)$	$n-4 \geq k \geq 1$	
three-mass triangle ($n \geq 6$)	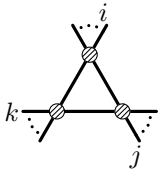	(9) $\mathcal{L}$ = $(\alpha Z_i + (1-\alpha) Z_{i+1},$ $\rho(\alpha) Z_j + \sigma(\alpha) Z_{j+1})$	$1 \leq k \leq n-5$	$f_{ij} f_{jk} f_{ki}$
one-mass box ($n \geq 5$)	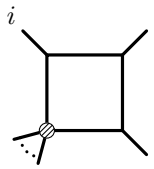	(10) $\mathcal{L}$ = $(i\, i{+}2)$	$0 \leq k \leq n-5$	$\langle i\, \overline{i{+}2} \rangle \langle \bar{i}\, i{+}2 \rangle$
		(11) $\mathcal{L}$ = $\bar{i} \cap \overline{i{+}2}$	$n-4 \geq k \geq 1$	
two-mass easy box ($n \geq 6$)	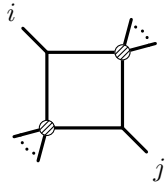	(12) $\mathcal{L}$ = $(i\, j)$	$0 \leq k \leq n-6$	$\langle i\, \bar{j} \rangle \langle \bar{i}\, j \rangle$
		(13) $\mathcal{L}$ = $\bar{i} \cap \bar{j}$	$n-4 \geq k \geq 2$	

two-mass hard box ($n \geq 6$)	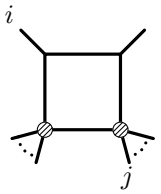	(14) $\mathcal{L} = \overline{i{+}1} \cap (i\,j\,j{+}1)$	$1 \leq k \leq n{-}5$	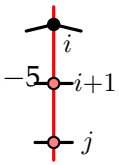	$\langle \bar{i}\, i{+}2\rangle\langle i\, i{+}1\, j\, j{+}1\rangle$
		(15) $\mathcal{L} = \bar{i} \cap (i{+}1\,j\,j{+}1)$	$n{-}5 \geq k \geq 1$		
three-mass box ($n \geq 7$)	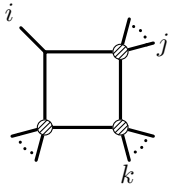	(16) $\mathcal{L} = (i\,j\,j{+}1) \cap (i\,k\,k{+}1)$	$1 \leq k \leq n{-}6$	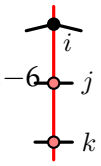	$\langle i(i{-}1\,i{+}1)(j\,j{+}1)(k\,k{+}1)\rangle$
		(17) $\mathcal{L} = (\bar{i} \cap (j\,j{+}1), \bar{i} \cap (k\,k{+}1))$	$n{-}5 \geq k \geq 2$		
four-mass box ($n \geq 8$)	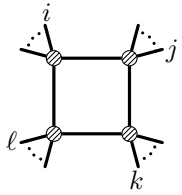	(18) $\mathcal{L} =$ (19) $\mathcal{L} =$	see Tab. 2 of [78]	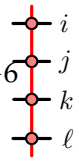	$(f_{ij}f_{k\ell} - f_{ik}f_{j\ell} + f_{i\ell}f_{jk})^2$ $-4f_{ij}f_{jk}f_{k\ell}f_{i\ell} \equiv \Delta_{ijk\ell}$
			$2 \leq k \leq n{-}6$ $n{-}6 \geq k \geq 2$		

TABLE 3.1: This table shows: the eleven Landau diagrams corresponding to sets of one-loop on-shell conditions that can be satisfied for generic projected external data; the nineteen branches of solutions to these on-shell conditions; the range of k for which $\mathrm{N^kMHV}$ amplituhedra have boundaries of each type; the twistor diagram depicting the low-k solution (or one low-k solution for the one-mass triangle and two-mass hard box); the loci in $\mathrm{Conf}_n(\mathbb{P}^3)$ where the Landau equations for each branch admit nontrivial solutions (where the quantity in the last column vanishes). At one loop it happens that the loci are the same for each branch of solutions to a given set of on-shell conditions. Here α, β are arbitrary numbers, A is an arbitrary point in $\mathbb{P}^3$, P is an arbitrary plane in $\mathbb{P}^3$, $\rho(\alpha), \sigma(\alpha)$ are defined in Eq. (3.11), $f_{ab} \equiv \langle a\, a{+}1\, b\, b{+}1\rangle$, and $\langle i(i{-}1\,i{+}1)(j\,j{+}1)(k\,k{+}1)\rangle \equiv \langle i{-}1\,i\,j\,j{+}1\rangle\langle i\,i{+}1\,k\,k{+}1\rangle - (j \leftrightarrow k)$.

3.3 One-Loop Boundaries

We now turn to the last step 1(c) from the end of Sec. 3.1.5: for each of the nineteen branches B listed in Tab. 3.1, we must determine the values of k for which $\mathcal{A}_{n,\mathrm{k},1}$ has a boundary of type B (defined in Sec. 3.1.3). The results of this analysis are listed in the fourth column of the Tab. 3.1. Our strategy for obtaining these results is two-fold.

In order to prove that an amplituhedron has a boundary of type B, it suffices to write down a pair of matrices C, D such that definitions (3.4) and (3.5) hold, C and $\binom{D}{C}$ are both non-negative, and the external data projected through $Y = C\mathcal{Z}$ are generic for generic positive $\mathcal{Z}$. We call such a pair C, D a *valid configuration* for B. In the sections below we present explicit valid configurations for each of the nineteen branches. Initially we consider for each branch only the lowest value of k for which a valid configuration exists; in Sec. 3.3.7 we explain how to grow these to larger values of k and establish the upper bounds on k shown in Tab. 3.1.

However, in order to prove that an amplituhedron does not have a boundary of type B, it does not suffice to find a configuration that is not valid; one must show that no valid configuration exists. We address this problem in the next section.

3.3.1 A Criterion for Establishing Absent Branches

Fortunately, for $\mathcal{L}$-boundaries of the type under consideration there is a simple criterion for establishing when no valid configuration can exist. The crucial ingredient is that if $(Y, \mathcal{L}) \in \overline{\mathcal{A}_{n,\mathrm{k},1}}$ and $\langle \mathcal{L}\, a\, a{+}1\rangle = 0$ for some a, then $\langle \mathcal{L}\, a\, a{+}2\rangle$ must necessarily be non-positive[8]; the proof of this assertion, which we omit here, parallels that of a closely related statement proven in Sec. 6 of [37].

Consider now a line of the form $\mathcal{L} = (\alpha Z_a + \beta Z_{a+1}, A)$ for some point A and some parameters α, β which are not both vanishing. We will show that an $\mathcal{L}$ of this form can lie in the closure of an amplituhedron only if $\mathcal{L} = (a\, a{+}1)$ or $\alpha\beta \geq 0$.

[8] Unless $a \in \{n-1, n\}$, when one must take into account the twisted cyclic symmetry. In all that follows we will for simplicity always assume that indices are outside of this range, which lets us uniformly ignore all sign factors that might arise from the twisted cyclic symmetry; these signs necessarily always conspire to ensure that all statements about amplitudes are $\mathbb{Z}_n$ cyclically invariant.

First, as just noted, since $\langle \mathcal{L}\, a\, a{+}1\rangle = 0$ we must have

$$0 \geq \langle \mathcal{L}\, a\, a{+}2\rangle = \beta \langle a{+}1\, A\, a\, a{+}2\rangle\,. \tag{3.12}$$

On the other hand, as mentioned at the end of Sec. 3.1.2, we also have $\langle \mathcal{L}\, a\, a{+}1\rangle \geq 0$ for all a. Applying this to $a+1$ gives

$$0 \leq \langle \mathcal{L}\, a{+}1\, a{+}2\rangle = \alpha \langle a\, A\, a{+}1\, a{+}2\rangle\,. \tag{3.13}$$

If $\langle a\, a{+}1\, a{+}2\, A\rangle \neq 0$, then the two inequalities (3.12) and (3.13) imply that $\alpha\beta \geq 0$.

This is the conclusion we wanted, but it remains to address what happens if $\langle a\, a{+}1\, a{+}2\, A\rangle = 0$. In this case $\mathcal{L}$ lies in the plane $(a\, a{+}1\, a{+}2)$ so we can take $\mathcal{L} = (\alpha Z_a + \beta Z_{a+1}, \gamma Z_{a+1} + \delta Z_{a+2})$. Then we have

$$\begin{aligned} 0 &\geq \langle \mathcal{L}\, a{+}1\, a{+}3\rangle = -\alpha\delta \langle a\, a{+}1\, a{+}2\, a{+}3\rangle\,, \\ 0 &\leq \langle \mathcal{L}\, a{-}1\, a\rangle = \beta\delta \langle a{-}1\, a\, a{+}1\, a{+}2\rangle\,. \end{aligned} \tag{3.14}$$

Both of the four-brackets in these inequalities are positive (for generic projected external data) since they are of the form $\langle a\, a{+}1\, b\, b{+}1\rangle$, so we conclude that either $\delta = 0$, which means that $\mathcal{L} = (a\, a{+}1)$, or else we again have $\alpha\beta \geq 0$.

In conclusion, we have developed a robust test which establishes that

$$\mathcal{L} = (\alpha Z_a + \beta Z_{a+1}, A) \in \overline{\mathcal{A}_{n,\mathrm{k},1}} \text{ only if } \mathcal{L} = (a\, a{+}1) \text{ or } \alpha\beta \geq 0\,. \tag{3.15}$$

This statement is independent of k (and Y), but when applied to particular branches, we will generally encounter cases for which $\alpha\beta$ is negative unless certain sequences of four-brackets of the projected external data have a certain number of sign flips; this signals that the branch may intersect $\overline{\mathcal{A}_{n,\mathrm{k},1}}$ only for certain values of k.

3.3.2 MHV Lower Bounds

The fact that MHV amplituhedra only have boundaries of type (1)–(7), (10) and (12) (referring to the numbers given in the "Branches" column of Tab. 3.1) follows implicitly from the results of [17] where all boundaries of one- (and two-) loop MHV amplituhedra were studied. It is nevertheless useful to still consider these cases since we will need the corresponding D-matrices below to establish that amplituhedra have boundaries of these types for all $0 \leq \mathrm{k} \leq n-4$.

In this and the following two sections we always assume, without loss of generality, that indices i, j, k, ℓ are cyclically ordered and non-adjacent ($i{+}1 < j < j{+}1 < k < k{+}1 < \ell$), and moreover that $1 < i$ and $\ell < n$. In particular, this means that we ignore potential signs from the twisted cyclic symmetry (see footnote 8).

Branch (4) is a prototype for several other branches, so we begin with it instead of branch (1). The solution for $\mathcal{L}$ shown in Tab. 3.1 may be represented as $\mathcal{L} = DZ$ with

$$D = \begin{array}{c} \begin{array}{cccc} i & i{+}1 & j & j{+}1 \end{array} \\ \begin{pmatrix} \alpha & 1-\alpha & 0 & 0 \\ 0 & 0 & \beta & 1-\beta \end{pmatrix} \end{array}, \tag{3.16}$$

where we display only the nonzero columns of the $2 \times n$ matrix in the indicated positions i, $i{+}1$, j and $j{+}1$. This solves the two-mass bubble on-shell conditions for all values of the parameters α and β. This branch intersects $\overline{\mathcal{A}_{n,0,1}}$ when they lie in the range $0 \leq \alpha, \beta \leq 1$, where the matrix D is non-negative. Thus we conclude that MHV amplituhedra have boundaries of type (4).

Branches (5), (6), (7), (10), and (12) can all be represented by special cases of Eq. (3.16) for α and/or β taking values 0 and/or 1, and/or with columns relabeled, so MHV amplituhedra also have boundaries of all of these types.

Branch (1) may be represented by

$$D = \begin{array}{c} \begin{matrix} \quad & i{-}1 & i & i{+}1 & i{+}2 & \quad \end{matrix} \\ \begin{pmatrix} \cdots & 0 & \alpha & 1-\alpha & 0 & \cdots \\ \cdots & \alpha_{i-1} & \alpha_i & \alpha_{i+1} & \alpha_{i+2} & \cdots \end{pmatrix} \end{array}. \tag{3.17}$$

This provides a solution to the tadpole on-shell condition $\langle \mathcal{L}\, i\, i{+}1\rangle = 0$ for all values of the parameters, and there clearly are ranges for which D is non-negative. Note that all but two of the parameters in the second row could be gauged away, but this fact is not relevant at the moment (see footnote 9). If $0 \leq \alpha \leq 1$, we could have either $\alpha_a = 0$ for $a < i+1$ and $\alpha_a > 0$ for $a > i$, or $\alpha = 0$ for $a > i$ and $\alpha_a < 0$ for $a < i+1$. We conclude that MHV amplituhedra also have boundaries of this type.

Branch (2) is the special case $\alpha = 1$ of branch (1).

Branch (3) may be represented by

$$D = \begin{array}{c} \begin{matrix} i{-}1 & i & i{+}1 \end{matrix} \\ \begin{pmatrix} 1 & 0 & \alpha \\ 0 & 1 & \beta \end{pmatrix} \end{array} \tag{3.18}$$

for arbitrary α, β, which is non-negative for $\alpha \leq 0$ and $\beta \geq 0$, so MHV amplituhedra also have boundaries of this type.

3.3.3 NMHV Lower Bounds

Branch (8) of the two-mass triangle may be represented as

$$D = \begin{array}{c} \begin{matrix} i & i{+}1 & j & j{+}1 \end{matrix} \\ \begin{pmatrix} \alpha & 1-\alpha & 0 & 0 \\ 0 & 0 & -\langle \bar{i}\, j{+}1\rangle & \langle \bar{i}\, j\rangle \end{pmatrix} \end{array} \tag{3.19}$$

for arbitrary α. For generic projected external data $\mathcal{L} \neq (j\,j{+}1)$, so criterion (3.15) shows that this configuration has a chance to lie on the boundary of an amplituhedron only if $-\langle \bar{i}\, j{+}1\rangle\langle \bar{i}\, j\rangle \geq 0$. This is not possible for MHV external data, where the ordered four-brackets are always positive, so MHV amplituhedra do not have boundaries of this type. But note that the inequality can be satisfied if there is at least one sign flip in the sequence $\langle \bar{i}\, \bullet\rangle$, between $\bullet = j$ and $\bullet = j{+}1$. This motivates us to consider k $= 1$, so let us now check that with

$$C = \begin{array}{c} \begin{array}{ccccc} i{-}1 & i & i{+}1 & j & j{+}1 \end{array} \\ \begin{pmatrix} c_{i-1} & c_i & c_{i+1} & c_j & c_{j+1} \end{pmatrix} \end{array}, \tag{3.20}$$

the pair C, D is a valid configuration. First of all, it is straightforward to check that $\mathcal{L} = D\mathcal{Z}$ still satisfies the two-mass triangle on-shell conditions. This statement is not completely trivial since these conditions now depend on $Y = C\mathcal{Z}$ because of the projection (3.2). Second, in order for C to be non-negative we need all five of the indicated c_a's to be non-negative. Moreover, in order to support generic projected external data, we need them all to be nonzero — if, say, c_i were equal to zero, then $\langle i{-}1\, i{+}1\, j\, j{+}1\rangle$ would vanish, etc. Finally, for $\binom{D}{C}$ to be non-negative we need

$$0 \leq \alpha \leq \frac{c_i}{c_i + c_{i+1}}\,. \tag{3.21}$$

This branch intersects $\overline{\mathcal{A}_{n,1,1}}$ for α in this range, so we conclude that NMHV amplituhedra have boundaries of this type.

Branch (9) is the general solution of the three-mass triangle, and is already given in Tab. 3.1 in D-matrix form as

$$D = \begin{array}{c} \begin{array}{cccc} i & i{+}1 & j & j{+}1 \end{array} \\ \begin{pmatrix} \alpha & 1-\alpha & 0 & 0 \\ 0 & 0 & \rho(\alpha) & \sigma(\alpha) \end{pmatrix} \end{array}, \tag{3.22}$$

with $\rho(\alpha)$ and $\sigma(\alpha)$ defined in Eq. (3.11). For generic projected external data this $\mathcal{L}$ can never attain the value $(i\,i{+}1)$ or $(j\,j{+}1)$. Applying criterion (3.15) for both $a = i$ and $a = j$ shows that this configuration has a chance to lie on the boundary of an amplituhedron only if $\alpha(1-\alpha) \geq 0$ and $\rho(\alpha)\sigma(\alpha) \geq 0$. This is not possible for MHV external data, so we conclude that MHV amplituhedra do not have boundaries of this type. However, the $\rho(\alpha)\sigma(\alpha) \geq 0$ inequality can be satisfied if the sequences $\langle i\,k\,k{+}1\,\bullet\rangle$ and $\langle i{+}1\,k\,k{+}1\,\bullet\rangle$ change sign between $\bullet = j$ and $\bullet = j{+}1$, as long as the sequences $\langle j\,k\,k{+}1\,\bullet\rangle$ and $\langle j{+}1\,k\,k{+}1\,\bullet\rangle$ do not flip sign here. Consider for k $= 1$ the matrix

$$C = \begin{array}{c} \begin{array}{cccccc} i & i{+}1 & j & j{+}1 & k & k{+}1 \end{array} \\ \left(\begin{array}{cccccc} \alpha c_i & (1-\alpha)c_i & c_j & c_{j+1} & c_k & c_{k+1} \end{array}\right) \end{array}. \tag{3.23}$$

Then C, D is a valid configuration because (1) $\mathcal{L} = D\mathcal{Z}$ satisfies the three-mass triangle on-shell conditions (for all values of α and the c's), and, (2) for $0 \leq \alpha \leq 1$ and all c's positive, the C-matrix is non-negative and supports generic positive external data (because it has at least k$+4 = 5$ nonzero columns), and (3) for this range of parameters $\binom{D}{C}$ is also non-negative. Since this branch intersects $\overline{\mathcal{A}_{n,1,1}}$ for a range of α, we conclude that NMHV amplituhedra have boundaries of this type.

Branch (16) is the special case $\alpha = 1$ of branch (9).

Branch (14) is the special case $j \to i+1$, $k \to j$ of branch (16).

Branch (15) is equivalent to the mirror image of branch (14), after relabeling.

Branch (11) is the special case $j = i+2$ of branch (15).

3.3.4 N^{2}MHV Lower Bounds

Branch (17) may be represented by

$$D = \begin{array}{c} \begin{array}{cccc} j & j{+}1 & k & k{+}1 \end{array} \\ \begin{pmatrix} 0 & 0 & -\langle \bar{i}\, k{+}1\rangle & \langle \bar{i}\, k\rangle \\ -\langle \bar{i}\, j{+}1\rangle & \langle \bar{i}\, j\rangle & 0 & 0 \end{pmatrix} \end{array}. \tag{3.24}$$

For generic projected external data the corresponding $\mathcal{L}$ will never attain the value $(j\, j{+}1)$ or $(k\, k{+}1)$. We can apply criterion (3.15) for both $a = j$ and $a = k$, which reveals that this configuration has a chance to lie on a boundary of an amplituhedron only if both $-\langle \bar{i}\, j{+}1\rangle\langle \bar{i}\, j\rangle \geq 0$ and $-\langle \bar{i}\, k{+}1\rangle\langle \bar{i}\, k\rangle \geq 0$. This is impossible for MHV external data, and it is also impossible in the NMHV case, where some projected four-brackets may be negative but the sequence $\langle \bar{i}\, \bullet\rangle$ may only flip sign once, whereas we need it to flip sign twice, once between $\bullet = j$ and $\bullet = j{+}1$, and again between $\bullet = k$ and $\bullet = k{+}1$. We conclude that k < 2 amplituhedra do not have boundaries of this form. Consider now pairing (3.24) with the k $= 2$ matrix

$$C = \begin{array}{c} \begin{array}{ccccccc} i{-}1 & i & i{+}1 & j & j{+}1 & k & k{+}1 \end{array} \\ \begin{pmatrix} c_{11} & c_{12} & c_{13} & c_{14} & c_{15} & 0 & 0 \\ c_{21} & c_{22} & c_{23} & 0 & 0 & c_{24} & c_{25} \end{pmatrix} \end{array}. \tag{3.25}$$

It is straightforward to check that C, D is a valid configuration for a range of values of c's, so we conclude that k $= 2$ amplituhedra have boundaries of this type.

Branch (13) may be represented by

$$D = \begin{array}{c} \begin{array}{ccc} i{-}1 & i & i{+}1 \end{array} \\ \begin{pmatrix} \langle i\, \bar{j}\rangle & -\langle i{-}1\, \bar{j}\rangle & 0 \\ 0 & -\langle i{+}1\, \bar{j}\rangle & \langle i\, \bar{j}\rangle \end{pmatrix} \end{array}, \tag{3.26}$$

which by (3.15) cannot lie on a boundary of an amplituhedron unless the sequence $\langle \bar{j} \bullet \rangle$ flips sign twice, first between $\bullet = i{-}1$ and i and again between $\bullet = i$ and $i{+}1$. Therefore, neither MHV nor NMHV amplituhedra have boundaries of this type. However it is straightforward to verify that with

$$C = \begin{array}{c} \begin{array}{cccccc} i{-}1 & i & i{+}1 & j{-}1 & j & j{+}1 \end{array} \\ \begin{pmatrix} c_{11} & c_{12} & 0 & c_{13} & c_{14} & c_{15} \\ 0 & c_{21} & c_{22} & c_{23} & c_{24} & c_{25} \end{pmatrix} \end{array} \tag{3.27}$$

the pair C, D is a valid configuration for a range of values of c's, so $\mathrm{k} = 2$ amplituhedra do have boundaries of this type.

Branches (18) and (19) of the four-mass box may be represented as

$$D = \begin{array}{c} \begin{array}{cccc} i & i{+}1 & j & j{+}1 \end{array} \\ \begin{pmatrix} \alpha & 1-\alpha & 0 & 0 \\ 0 & 0 & \beta & 1-\beta \end{pmatrix} \end{array}, \tag{3.28}$$

where α and β are fixed by requiring that $\mathcal{L}$ intersects the lines $(k\,k{+}1)$ and $(\ell\,\ell{+}1)$. The values of α and β on the two branches were written explicitly in [78]; however, the complexity of those expressions makes analytic positivity analysis difficult. We have therefore resorted to numerical testing: using the algorithm described in Sec. 5.4 of [3], we generate a random positive $n \times (\mathrm{k}+4)$ $\mathcal{Z}$-matrix and a random positive $\mathrm{k} \times n$ C-matrix. After projecting through $Y = C\mathcal{Z}$, we obtain projected external data with the correct $\mathrm{N^kMHV}$ sign-flipping properties. We have checked numerically that both four-mass box branches lie on the boundary of $\mathrm{N^kMHV}$ amplituhedra only for $\mathrm{k} \geq 2$, for many instances of randomly generated external data.

3.3.5 Emergent Positivity

The analysis of Secs. 3.3.2, 3.3.3 and 3.3.4 concludes the proof of all of the lower bounds on k shown in the fourth column of Tab. 3.1. We certainly do not claim to have written down the most general possible valid C, D configurations; the ones we display for $\mathrm{k} > 0$ have been specifically chosen to demonstrate an interesting feature we call *emergent positivity*.

In each $\mathrm{k} > 0$ case we encountered D-matrices that are only non-negative if certain sequences of projected four-brackets of the form $\langle a\, a{+}1\, b\, \bullet\rangle$ change sign k times, at certain precisely specified locations. It is straightforward to check that within the range of validity of each C, D pair we have written down, the structure of the C matrix is such that it automatically puts the required sign flips in just the right places to make the D matrix, on its own, non-negative (provided, of course, that $\binom{D}{C}$ is non-negative). It is not a priori obvious that it had to be possible to find pairs C, D satisfying this kind of emergent positivity; indeed, it is easy to find valid pairs for which it does not hold.

3.3.6 Parity and Upper Bounds

Parity relates each branch to itself or to the other branch associated with the same Landau diagram. Since parity is a symmetry of the amplituhedron [37] which relates k to $n - \mathrm{k} - 4$, the lower bounds on k that we have established for various branches imply upper bounds on k for their corresponding parity conjugates. These results are indicated in the fourth column of Tab. 3.1, where the inequalities are aligned so as to highlight the parity symmetry.

Although these k upper bounds are required by parity symmetry, they may seem rather mysterious from the analysis carried out so far. We have seen that certain branches can be boundaries of an amplituhedron only if certain sequences of four-brackets have (at least) one or two sign flips. In the next section, we explain a mechanism which gives an upper bound to the number of sign flips, or equivalently which gives the upper bounds on k that are required by parity symmetry.

3.3.7 Increasing Helicity

So far we have only established that N^kMHV amplituhedra have boundaries of certain types for specific low (or, by parity symmetry, high) values of k. It remains to show that all of the branches listed in Tab. 3.1 lie on boundaries of amplituhedra for all of the intermediate helicities. To this end we describe now an algorithm for converting a valid configuration C_0, D_0 at the initial, minimal value of k_0 (with C_0 being the empty matrix for those branches with $k_0 = 0$) into a configuration that is valid at some higher value of k.

We maintain the structure of $D \equiv D_0$ and append to C_0 a matrix C' of dimensions $(k - k_0) \times n$ in order to build a configuration for helicity k. Defining $C = \binom{C_0}{C'}$, we look for a C' such that following properties are satisfied:

1. The same on-shell conditions are satisfied.

2. In order for the configuration to support generic projected external data, the C-matrix must have $m \geq k + 4$ nonzero columns, and the rank of any $m - 4$ of those columns must be k.

3. Both C and $\binom{D}{C}$ remain non-negative.

Since the C-matrix only has n columns in total, it is manifest from property (2) that everything shuts off for $k > n - 4$, as expected.

Let us attempt to preserve the emergent positivity of D. If $k_0 = 0$ then this is trivial; the D-matrices in Sec. 3.3.2 do not depend on any brackets, so adding rows to the empty C_0 has no effect on D. For $k_0 > 0$, let A and B be two entries in D_0 that are responsible for imposing a sign flip requirement. The argument applies equally to all of the $k_0 > 0$ branches, but for the sake of definiteness consider from Eq. (3.19) the two four-bracket dependent entries $A = -\langle \bar{i}\, j{+}1\rangle$ and $B = \langle \bar{i}\, j\rangle$. Assuming that C_0 is given by Eq. (3.20) so that both A and B are positive with respect to $Y_0 = C_0\mathcal{Z}$, then $AB = -[Y_0\, \bar{i}\, j{+}1][Y_0\, \bar{i}\, j] >$

0. If we append a second row C' and define $Y' = C'\mathcal{Z}$ then we have

$$\begin{aligned} A &= -[Y_0\, Y'\, \mathcal{Z}_{i-1}\, \mathcal{Z}_i\, \mathcal{Z}_{i+1}\, \mathcal{Z}_{j+1}] = -c_j[\mathcal{Z}_j\, Y'\, \mathcal{Z}_i\, \mathcal{Z}_{i+1}\, \mathcal{Z}_{j+1}]\,, \\ B &= [Y_0\, Y'\, \mathcal{Z}_{i-1}\, \mathcal{Z}_i\, \mathcal{Z}_{i+1}\, \mathcal{Z}_j] = c_{j+1}[\mathcal{Z}_{j+1}\, Y'\, \mathcal{Z}_i\, \mathcal{Z}_{i+1}\, \mathcal{Z}_j]\,. \end{aligned} \tag{3.29}$$

Since c_j and c_{j+1} are both positive, we see that A and B still satisfy $AB > 0$, regardless of the value of Y'. By the same argument, arbitrary rows can be added to a C-matrix without affecting the on-shell conditions, so property (1) also holds trivially (and also if $k_0 = 0$).

The structure of the initial D_0 of Secs. 3.3.2, 3.3.3 and 3.3.4 are similar in that the nonzero columns of this matrix are grouped into at most two *clusters*[9]. For example, for branch (17) there are two clusters $\{j, j{+}1\}$ and $\{k, k{+}1\}$ while for branch (3) there is only a single cluster $\{i{-}1, i, i{+}1\}$. Property (3) can be preserved most easily if we add suitable columns only in a *gap* between clusters. Let us illustrate how this works in the case of branch (4) where C_0 is empty and we can start by taking either

$$\begin{pmatrix} D_0 \\ C \end{pmatrix} = \begin{array}{c} \begin{array}{cccccccccc} & i{-}1 & i & i{+}1 & i{+}2 & \cdots & j{-}1 & j & j{+}1 & j{+}2 & \\ \end{array} \\ \begin{pmatrix} \cdots & 0 & \alpha & 1-\alpha & 0 & \cdots & 0 & 0 & 0 & 0 & \cdots \\ \cdots & 0 & 0 & 0 & 0 & \cdots & 0 & \beta & 1-\beta & 0 & \cdots \\ \cdots & 0 & 0 & \vec{c}_{i+1} & \vec{c}_{i+2} & \cdots & \vec{c}_{j-1} & \vec{c}_j & 0 & 0 & \cdots \end{pmatrix} \end{array} \tag{3.30}$$

to fill in the gap between clusters $\{i, i{+}1\}$ and $\{j, j{+}1\}$, or

$$\begin{pmatrix} D_0 \\ C \end{pmatrix} = \begin{array}{c} \begin{array}{cccccccccc} & i{-}1 & i & i{+}1 & i{+}2 & \cdots & j{-}1 & j & j{+}1 & j{+}2 & \\ \end{array} \\ \begin{pmatrix} \cdots & 0 & \alpha & 1-\alpha & 0 & \cdots & 0 & 0 & 0 & 0 & \cdots \\ \cdots & 0 & 0 & 0 & 0 & \cdots & 0 & \beta & 1-\beta & 0 & \cdots \\ \cdots & \vec{c}_{i-1} & \vec{c}_i & 0 & 0 & \cdots & 0 & 0 & \vec{c}_{j+1} & \vec{c}_{j+2} & \cdots \end{pmatrix} \end{array} \tag{3.31}$$

to fill in the gap between $\{j, j{+}1\}$ and $\{i, i{+}1\}$ that "wraps around" from n back to 1. In

[9] Branch (1) appears to be an exception, but only because Eq. (3.17) as written is unnecessarily general: it is sufficient for the second row to have only three nonzero entries, either in columns $\{i{-}3, i{-}2, i{-}1\}$ or in columns $\{i{+}1, i{+}2, i{+}3\}$.

both (3.30) and (3.31) each $\vec{c}_a$ is understood to be a k-component column vector, and in both cases $\binom{D_0}{C}$ can be made non-negative as long as C is chosen to be non-negative[10]. In this manner we can trivially increment the k-validity of a given configuration until the gaps become full. This cutoff depends on the precise positions of the gaps, and is most stringent when the two clusters are maximally separated from each other, since this forces the gaps to be relatively small. In this worst case we can fit only $\lceil \frac{n}{2} \rceil$ columns into a C-matrix of one of the above two types. Keeping in mind property (2) that the C-matrix should have at least $k+4$ nonzero columns, we see that this construction can reach values of $k \leq \lceil \frac{n}{2} \rceil - 4$. In order to proceed further, we can (for example) add additional columns c_i and c_{j+1} to Eq. (3.30), or c_{i+1} and c_j to Eq. (3.31). Choosing a non-negative C then no longer trivially guarantees that $\binom{D_0}{C}$ will also be non-negative, but there are ranges of C for which this is possible to arrange, which is sufficient for our argument.

It is possible to proceed even further by adding additional, specially crafted columns in both gaps, but the argument is intricate and depends delicately on the particular structure of each individual branch (as evident from the delicate structure of k upper bounds in Tab. 3.1). In the interest of brevity we terminate our discussion of the algorithm here and note that it is straightforward to check that for all boundaries, even in the worst case the gaps are always big enough to allow the construction we have described to proceed up to and including the parity-symmetric midpoint $k = \lfloor \frac{n}{2} \rfloor - 2$; then we appeal again to parity symmetry in order to establish the existence of valid configurations for k between this midpoint and the upper bound.

This finally concludes the proof of the k-bounds shown in the fourth column of Tab. 3.1, and thereby step 1(c) from Sec. 3.1.5.

[10] If k is even this is automatic; if k is odd the two rows of D_0 should be exchanged.

3.4 The Hierarchy of One-Loop Boundaries

Step (1) of our analysis (Sec. 3.1.5) is now complete at one loop. Before moving on to step (2) we demonstrate that the boundaries classified in Sec. 3.3 can be generated by a few simple graph operations applied to the maximal codimension boundaries of MHV amplituhedra (Tab. 3.1 type (12) or, as a special case, (10)). This arrangement will prove useful in the sequel since one-loop boundaries are the basic building blocks for constructing boundary configurations at arbitrary loop order.

We call boundaries of type (2), (5)–(7), (10), (12), and (14)–(16) *low-k* boundaries since they are valid for the smallest value of k for their respective Landau diagrams. The branches (8), (11), (13) and (17) are *high-k* boundaries and are respectively the parity conjugates of (7), (10), (12) and (16). Branch (3), the parity conjugate of branch (2), is properly regarded as a high-k boundary since (2) is low-k, but it is accidentally valid for all k. Branches (1), (4), and (9) are self-conjugate under parity and are considered both low-k and high-k, as are the parity-conjugate pair (18), (19).

3.4.1 A Graphical Notation for Low-helicity Boundaries

We begin by devising a graphical notation in terms of which the operations between momentum twistor solutions are naturally phrased. These graphs are *twistor diagrams*[11] depicting various configurations of intersecting lines in $\mathbb{P}^3$. The elements of a twistor diagram, an example of which is shown in panel (a) of Fig. 3.1, are:

- The red line depicts an $\mathcal{L}$ solving some on-shell conditions, specifically:
- if $\mathcal{L}$ and a single line segment labeled i intersect at an empty node, then $\langle \mathcal{L}\, i\, i{+}1\rangle = 0$, and
- if $\mathcal{L}$ and two line segments intersect at a filled node labeled i, then $\langle \mathcal{L}\, i{-}1\, i\rangle = \langle \mathcal{L}\, i\, i{+}1\rangle = 0$.

An "empty" node is colored red, indicating the line passing through it. A "filled" node is filled in solid black, obscuring the line passing through it.

[11] Not to be confused with the twistor diagrams of [**Hodges:2005bf**].

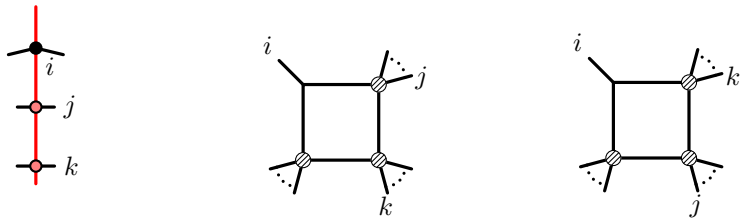

FIGURE 3.1: The twistor diagram shown in (a) depicts branch (16) of solutions to the three-mass box on-shell conditions $\langle \mathcal{L}\, i{-}1\, i\rangle = \langle \mathcal{L}\, i\, i{+}1\rangle = \langle \mathcal{L}\, j\, j{+}1\rangle = \langle \mathcal{L}\, k\, k{+}1\rangle = 0$, which is a valid boundary for k $\geq$ 1. This branch passes through the point Z_i and intersects the lines $(j\, j{+}1)$ and $(k\, k{+}1)$. As drawn, the intersection at j is an example of a non-MHV intersection, but the figure is agnostic about the relative cyclic ordering of i, j, k and is intended to represent either possibility. Therefore, the corresponding Landau diagram can be either (b) or (c) depending on whether $i < j < k$ or $i < k < j$.

In general a given $\mathcal{L}$ can pass through as many as four labeled nodes (for generic projected external data, which we always assume). If there are four, then none of them can be filled. If there are three, then at most one of them can be filled, and we choose to always draw it as either the first or last node along $\mathcal{L}$. If there are more than two, then any nodes between the first and last are called *non-MHV intersections*, which are necessarily empty. This name is appropriate because branches satisfying such on-shell constraints are not valid boundaries of MHV amplituhedra, and each non-MHV intersection in a twistor diagram increases the minimum value of k by one.

Although no such diagrams appear in this paper, the extension to higher loops is obvious: each $\mathcal{L}$ is represented by a line of a different color, and the presence of an on-shell condition of the form $\langle \mathcal{L}^{(\ell_1)}\, \mathcal{L}^{(\ell_2)}\rangle = 0$ is indicated by an empty node at the intersection of the lines $\mathcal{L}^{(\ell_1)}$ and $\mathcal{L}^{(\ell_2)}$.

To each twistor diagram it is simple to associate one or more Landau diagrams, as also shown in Fig. 3.1. If a twistor diagram has a filled node at i then an associated Landau diagram has two propagators $\langle \mathcal{L}\, i{-}1\, i\rangle$ and $\langle \mathcal{L}\, i\, i{+}1\rangle$ requiring a massless corner at i in the Landau diagram. If a twistor diagram has an empty node on the line segment marked i then an associated Landau diagram only has the single propagator $\langle \mathcal{L}\, i\, i{+}1\rangle$, requiring a massive corner in the Landau diagram. Therefore, twistor diagrams should

be thought of as graphical shorthand which both depict the low-k solution to the cut conditions and simultaneously represent one or more Landau diagrams, as explained in the caption of Fig. 3.1.

One useful feature of this graphical notation is that the nodes of a twistor diagram fully encode the total number of propagators, n_{props}, in the Landau diagram (and so also the total number of on-shell conditions): each filled node accounts for two propagators, and each empty node accounts for one propagator:

$$n_{\text{props}} = 2n_{\text{filled}} + n_{\text{empty}} \,. \tag{3.32}$$

This feature holds at higher loop order where this counting directly indicates how many propagators to associate with each loop.

Let us emphasize that a twistor diagram generally contains more information than its associated Landau diagram, as it indicates not only the set of on-shell conditions satisfied, but also specifies a particular branch of solutions thereto. The sole exception is the four-mass box, for which the above rules do not provide the twistor diagram with any way to distinguish the two branches (18), (19) of solutions. Moreover, the rules also do not provide any way to indicate that an $\mathcal{L}$ lies in a particular plane, such as $\bar{i}$. Therefore we can only meaningfully represent the low-k boundaries defined at the beginning of Sec. 3.4.

Given a twistor diagram depicting some branch, a twistor diagram corresponding to a relaxation of that branch may be obtained by deleting a non-MHV intersection of the type shown in (a) of Fig. 3.1, by replacing a filled node and its two line segments with an empty node and a single segment, or by deleting an empty node. In the associated Landau diagram, a relaxation corresponds to collapsing an internal edge of the graph. This is formalized in greater detail in Sec. 3.4.2.

3.4.2 A Graphical Recursion for Generating Low-helicity Boundaries

In Fig. 3.2 we organize twistor diagrams representing eight types of boundaries according to d and k; these are respectively the number of on-shell conditions d satisfied on

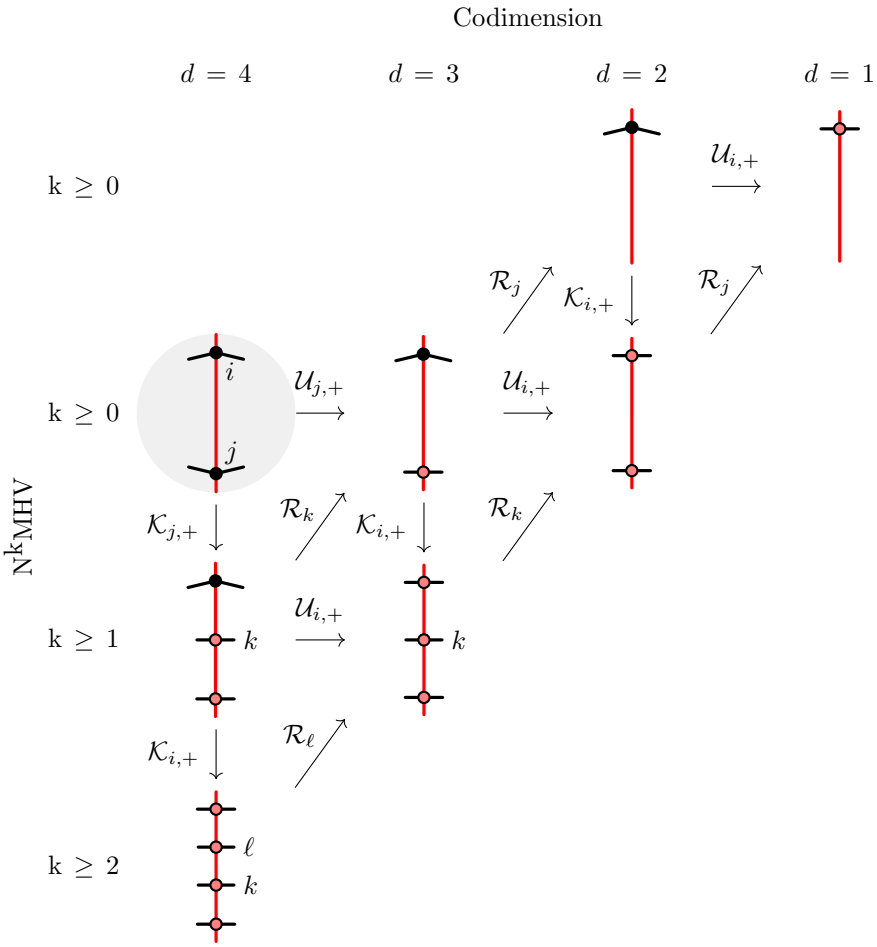

FIGURE 3.2: Twistor diagrams depicting eight types of low-k boundaries of N^kMHV amplituhedra, organized according to the minimum value of k and the codimension d (equivalently, the number of on-shell conditions satisfied). These correspond respectively to branch types (2), (1), (12), (7), (4), (16), (9) and (18)/(19). The graph operators $\mathcal{K}$, $\mathcal{R}$, and $\mathcal{U}$ are explained in the text and demonstrated in Figs. 3.3-3.5, respectively. Evidently all eight types of boundaries can be generated by acting with sequences of these operators on MHV maximal codimension boundaries of the type shown shaded in gray. There is an analogous parity-conjugated version of this hierarchy which relates all of the high-k branches to each other. The missing low-k boundary types (5), (6), (10), (11), (14) and (15) are degenerate cases which can be obtained by starting with $j = i + 1$ in the gray blob.

the boundary, and the minimum value of k for which the boundary is valid. It is evident from this data that there is a simple relation between d, k, and the number of filled (n_{filled}) and empty (n_{empty}) nodes. Specifically, we see that an N$^{\text{k}}$MHV amplituhedron can have boundaries of a type displayed in a given twistor diagram only if

$$\text{k} \geq 2n_{\text{empty}} + 3n_{\text{filled}} - d - 2 = n_{\text{empty}} + n_{\text{filled}} - 2\,, \tag{3.33}$$

where we have used Eq. (3.32) with $n_{\text{props}} = d$. In the sequel we will describe a useful map from Landau diagrams to the on-shell diagrams of [3] which manifests the relation (3.33) and provides a powerful generalization thereof to higher loop order. The amplituhedron-based approach has some advantages over that of enumerating on-shell diagrams that will also be explored in the sequel. First of all, the minimal required helicity of a multi-loop configuration can be read off from each loop line separately. Second, we immediately know the relevant solution branches for a given helicity. And finally, compared to enumerating all relevant on-shell diagrams the amplituhedron-based method is significantly more compact since it can be used to produce a minimal subset of diagrams such that all allowed diagrams are relaxations thereof, including limits where massive external legs become massless or vanish.

From the data displayed in Fig. 3.2 we see that a natural organizational principle emerges: all N$^{\text{k}}$MHV one-loop twistor diagrams can be obtained from the unique maximal codimension MHV diagram (shown shaded in gray) via sequences of simple graph operations which we explain in turn.

The first graph operation $\mathcal{K}$ increments the helicity of the diagram on which it operates. (The name $\mathcal{K}$ is a reminder that it increases k.) Its operation is demonstrated in Fig. 3.3. Specifically, $\mathcal{K}_i$ replaces a filled node at a point i along $\mathcal{L}$ by two empty nodes, one at i and a second one on a new non-MHV intersection added to the diagram. Since n_{filled} decreases by one but n_{empty} increases by two under this operation, it is clear from Eq. (3.33) that $\mathcal{K}_i$ always increases by one the minimal value of k on which the branch indicated by the twistor diagram has support. From the point of view of Landau diagrams, this operation replaces a massless node with a massive one, as illustrated in

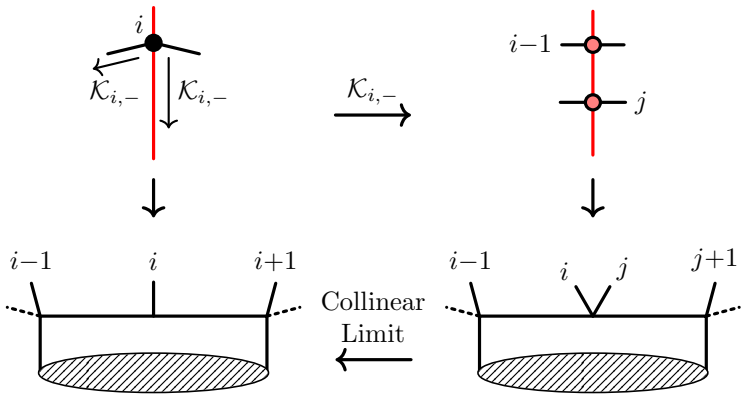

FIGURE 3.3: The graph operation $\mathcal{K}_i$ maps an N^{k}MHV twistor diagram into an N^{k+1}MHV twistor diagram as shown in the top row. On Landau diagrams, this corresponds to replacing a massless corner by a massive corner; such an operation is effectively an inverse collinear limit. The shaded region in the figures represents an arbitrary planar sub-graph. A dashed external line on a Landau diagram may be either one massless external leg so the whole corner is massive, or completely removed so the whole corner is massless.

the bottom row of Fig. 3.3, and hence it may be viewed as an "inverse" collinear limit.

The other two graph operations $\mathcal{R}$ and $\mathcal{U}$ both correspond to relaxations, as defined in Sec. 3.1.3, since they each reduce the number of on-shell conditions by one, stepping thereby one column to the right in Fig. 3.2.

The operation $\mathcal{R}_i$ simply removes (hence the name $\mathcal{R}$) an empty node i from a twistor diagram, as shown in Fig. 3.4. This corresponds to removing $\langle \mathcal{L}\, i\, i+1\rangle = 0$ from the set of on-shell conditions satisfied by $\mathcal{L}$[12].

The last operation, $\mathcal{U}$, corresponds to "un-pinning" a filled node (hence "$\mathcal{U}$"). Un-pinning means removing one constraint from a pair $\langle \mathcal{L}\, i{-}1\, i\rangle = \langle \mathcal{L}\, i\, i{+}1\rangle = 0$. The line $\mathcal{L}$, which was pinned to the point i, is then free to slide along the line segment $(i{-}1\, i)$ or $(i\, i{+}1)$ (for $\mathcal{U}_{i,-}$ or $\mathcal{U}_{i,+}$, respectively). In the twistor diagram, this is depicted by replacing the filled node at the point i with a single empty node along the line segment $(i\, i{\pm}1)$ (see Fig. 3.5). Only $\mathcal{U}_+$ appears in Fig. 3.2 because at one loop, all diagrams generated by any $\mathcal{U}_-$ operation are equivalent, up to relabeling, to some diagram generated by a $\mathcal{U}_+$. In general, however, it is necessary to track the subscript $\pm$ since both choices

[12]Note that in line with the conventions adopted in Sec. 3.4.1 we label $\mathcal{R}_i$ only with the smaller label of a pair $(i\, i{+}1)$.

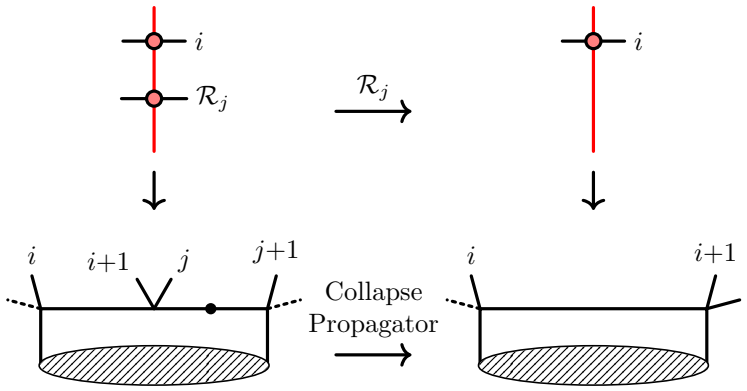

FIGURE 3.4: The graph operation $\mathcal{R}_j$ relaxes $\mathcal{L}$ by removing the condition that $\mathcal{L}$ must pass through the line $(j\,j{+}1)$; this is equivalent to removing the on-shell condition $\langle \mathcal{L}\,j\,j{+}1\rangle = 0$. On Landau diagrams, this corresponds to collapsing the propagator indicated by the filled dot in the bottom figure on the left. The shaded region in the figures represents an arbitrary planar sub-graph. A dashed external line on a Landau diagram may be either one massless external leg so the whole corner is massive, or completely removed so the whole corner is massless. It is to be understood that the graphical notation implies that $j \neq i+2$ and $i \neq j+2$; otherwise, the two empty nodes in the top left diagram would be represented by a single filled node on which the action of $\mathcal{R}$ is undefined; the appropriate graph operation in this case would instead be $\mathcal{U}$.

are equally valid relaxations and can yield inequivalent twistor and Landau diagrams. From Fig. 3.2, we read off the following identity among the operators acting on any diagram g:

$$\mathcal{U}_{j,+}g = \mathcal{R}_k\mathcal{K}_{j,+}g\,. \tag{3.34}$$

There was no reason to expect the simple graphical pattern of Fig. 3.5 to emerge among the twistor diagrams. Indeed in Sec. 3.2 we simply listed all possible sets of on-shell conditions without taking such an organizational principle into account. At higher loop order, however, the problem of enumerating all boundaries of $\mathrm{N^kMHV}$ amplituhedra benefits greatly from the fact that all valid configurations of each single loop can be iteratively generated via these simple rules, starting from the maximal codimension MHV boundaries. Stated somewhat more abstractly, these graph operations are instructions for naturally associating boundaries of different amplituhedra.

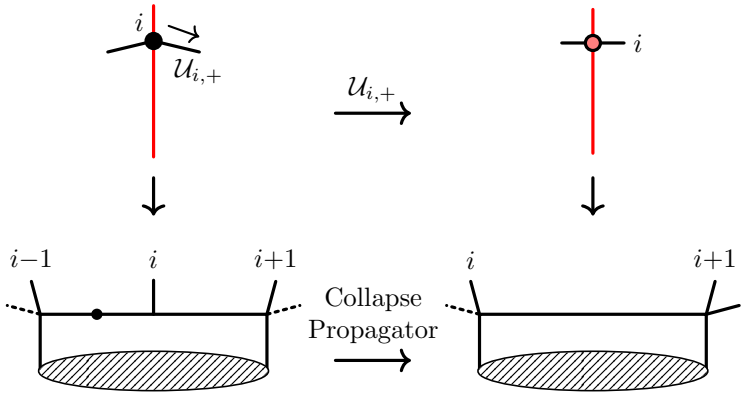

FIGURE 3.5: The graph operation $\mathcal{U}_{i,+}$ relaxes a line $\mathcal{L}$ constrained to pass through the point i, shifting it to lie only along the line $(i\,i{+}1)$. This is equivalent to removing the on-shell constraint $\langle \mathcal{L}\, i{-}1\, i\rangle = 0$. (The equally valid relaxation $\mathcal{U}_{i,-}$, not pictured here, lets the intersection point slide onto $(i{-}1\, i)$.) On Landau diagrams, this corresponds to collapsing the propagator indicated by the filled dot in the bottom figure on the left. The shaded region in the figures represents an arbitrary planar sub-graph. A dashed external line on a Landau diagram may be either one massless external leg so the whole corner is massive, or completely removed so the whole corner is massless. As explained in the caption of Fig. 3.4, the $\mathcal{U}$ operation can be thought of as a special case of the $\mathcal{R}$ operation, and we distinguish the two because only the latter can change the helicity sector k.

Before concluding this section it is worth noting (as is evident in Fig. 3.2) that relaxing a low-k boundary can never raise the minimum value of k for which that type of boundary is valid. In other words, we find that if $\mathcal{A}_{n,k,1}$ has a boundary of type B, and if B' is a relaxation of B, then $\mathcal{A}_{n,k,1}$ also has boundaries of type B'. This property does not hold in general beyond one loop; a counterexample involving two-loop MHV amplitudes appears in Fig. 4 of [17].

3.5 Solving Landau Equations in Momentum Twistor Space

As emphasized in Sec. 3.1.5, the Landau equations naturally associate to each boundary of an amplituhedron a locus in $\mathrm{Conf}_n(\mathbb{P}^3)$ on which the corresponding amplitude has a singularity. In this section we review the results of solving the Landau equations for each of the one-loop branches classified in Sec. 3.2, thereby carrying out step 2 of the algorithm summarized in Sec. 3.1.5. The results of this section were already tabulated in [16], but we revisit the analysis, choosing just two examples, in order to demonstrate the simplicity and efficiency of these calculations when carried out directly in momentum twistor space. The utility of this method is on better display in the higher-loop examples to be considered in the sequel.

As a first example, we consider the tadpole on-shell condition

$$f_1 \equiv \langle \mathcal{L}\, i\, i{+}1 \rangle = 0\,. \tag{3.35}$$

We choose any two other points Z_j, Z_k (which generically satisfy $\langle i\, i{+}1\, j\, k\rangle \neq 0$) in terms of which to parameterize

$$\mathcal{L} = (Z_i + d_1 Z_j + d_2 Z_k, Z_{i+1} + d_3 Z_j + d_4 Z_k)\,. \tag{3.36}$$

Then the on-shell condition (3.35) admits solutions when

$$d_1 d_4 - d_2 d_3 = 0\,, \tag{3.37}$$

while the four Kirchhoff conditions (3.10) are

$$\alpha_1 d_4 = -\alpha_1 d_3 = -\alpha_1 d_2 = \alpha_1 d_1 = 0\,. \tag{3.38}$$

The only nontrivial solution (that means $\alpha_1 \neq 0$; see Sec. 3.1.4) to the equations (3.37) and (3.38) is to set all four $d_A = 0$. Since this solution exists for all (generic) projected external data, it does not correspond to a branch point of an amplitude and is uninteresting to us. In other words, in this case the locus we associate to a boundary of this type is all of $\mathrm{Conf}_n(\mathbb{P}^3)$.

As a second example, consider the two on-shell conditions corresponding to the two-mass bubble

$$f_1 \equiv \langle \mathcal{L}\, i\, i{+}1\rangle = 0\,, \qquad f_2 \equiv \langle \mathcal{L}\, j\, j{+}1\rangle = 0\,. \tag{3.39}$$

In this case a convenient parameterization is

$$\mathcal{L} = (Z_i + d_1 Z_{i+1} + d_2 Z_k, Z_j + d_3 Z_{i+1} + d_4 Z_k)\,. \tag{3.40}$$

Note that an asymmetry between i and j is necessarily introduced because we should not allow more than four distinct momentum twistors to appear in the parameterization, since they would necessarily be linearly dependent, and we assume of course that Z_k is generic (meaning, as before, that $\langle i\, i{+}1\, j\, k\rangle \neq 0$). Then

$$\begin{aligned} f_1 &= -d_2\langle i\, i{+}1\, j\, k\rangle\,, \\ f_2 &= d_3\langle i\, i{+}1\, j\, j{+}1\rangle + d_4\langle i\, j\, j{+}1\, k\rangle + (d_1 d_4 - d_2 d_3)\langle i{+}1\, j\, j{+}1\, k\rangle \end{aligned} \tag{3.41}$$

and the Kirchhoff conditions are

$$\begin{pmatrix} 0 & d_4\langle i{+}1\, j\, j{+}1\, k\rangle \\ -\langle i\, i{+}1\, j\, k\rangle & -d_3\langle i{+}1\, j\, j{+}1\, k\rangle \\ 0 & \langle i\, i{+}1\, j\, j{+}1\rangle - d_2\langle i{+}1\, j\, j{+}1\, k\rangle \\ 0 & \langle i\, j\, j{+}1\, k\rangle + d_1\langle i{+}1\, j\, j{+}1\, k\rangle \end{pmatrix} \begin{pmatrix} \alpha_1 \\ \alpha_2 \end{pmatrix} = 0\,. \tag{3.42}$$

Nontrivial solutions exist only if all 2×2 minors of the 4×2 coefficient matrix vanish. Three minors are trivially zero, and the one computed from the second and third rows evaluates simply to

$$-\langle i\, i{+}1\, j\, k\rangle\langle i\, i{+}1\, j\, j{+}1\rangle = 0 \tag{3.43}$$

using the on-shell condition $f_1 = -d_2\langle i\, i{+}1\, j\, k\rangle = 0$. If this quantity vanishes, then the four remaining constraints (the two on-shell conditions $f_1 = f_2 = 0$ and the two remaining minors) can be solved for the four d_A, and then Eq. (3.42) can be solved to find the two α_J's. Since $\langle i\, i{+}1\, j\, k\rangle \neq 0$ by assumption, we conclude that the Landau equations admit nontrivial solutions only on the codimension-one locus in $\mathrm{Conf}_n(\mathbb{P}^3)$ where

$$\langle i\, i{+}1\, j\, j{+}1\rangle = 0\,. \tag{3.44}$$

These two examples demonstrate that in some cases (e.g. the tadpole example) the Landau equations admit solutions for any (projected) external data, while in other cases (e.g. the bubble example) the Landau equations admit solutions only when there is a codimension-one constraint on the external data. A common feature of these examples is that some care must be taken in choosing how to parameterize $\mathcal{L}$. In particular, one must never express $\mathcal{L}$ in terms of four momentum twistors (Z_i, Z_j, etc.) that appear in the specification of the on-shell conditions; otherwise, it can be impossible to disentangle the competing requirements that these satisfy some genericity (such as $\langle i\, i{+}1\, j\, k\rangle \neq 0$ in the above examples) while simultaneously hoping to tease out the constraints they

must satisfy in order to have a solution (such as Eq. (3.44)). For example, although one might have been tempted to preserve the symmetry between i and j, it would have been a mistake to use the four twistors Z_i, Z_{i+1}, Z_j and Z_{j+1} in Eq. (3.40).

Instead, it is safest to always pick four completely generic points $Z_a, \ldots, Z_d$ in terms of which to parameterize

$$\mathcal{L} = \begin{pmatrix} 1 & 0 & d_1 & d_2 \\ 0 & 1 & d_3 & d_4 \end{pmatrix} \begin{pmatrix} Z_a \\ Z_b \\ Z_c \\ Z_d \end{pmatrix}. \tag{3.45}$$

The disadvantage of being so careful is that intermediate steps in the calculation become much more lengthy, a problem we avoid in practice by using a computer algebra system such as Mathematica.

The results of this analysis for all one-loop branches are summarized in Tab. 3.1. Naturally these are in accord with those of [26] (as tabulated in [16]). At one loop it happens that the singularity locus is the same for each branch of solutions to a given set of on-shell conditions, but this is not generally true at higher loop order.

3.6 Singularities and Symbology

As suggested in the introduction (and explicit even in the title of this paper), one of the goals of our research program is to provide a priori derivations of the *symbol alphabets* of various amplitudes. We refer the reader to [67] for more details, pausing only to recall that the symbol alphabet of a generalized polylogarithm function F is a finite list of *symbol letters* $\{z_1, \ldots, z_r\}$ such that F has *logarithmic* branch cuts (i.e., the cover has infinitely many sheets)[13] between $z_i = 0$ and $z_i = \infty$ for each $i = 1, \ldots, r$.

To date, symbol alphabets have been determined by explicit computation only for two-loop MHV amplitudes [60]; all other results on multi-loop SYM amplitudes in the

[13] These branch cuts usually do not all live on the same sheet; the symbol alphabet provides a list of all branch cuts that can be accessed after analytically continuing F to arbitrary sheets.

literature are based on a conjectured extrapolation of these results to higher loop order. Throughout the paper we have however been careful to phrase our results in terms of branch points, rather than symbol letters, for two reasons.

First of all, amplitudes in SYM theory are expected to be expressible as generalized polylogarithm functions, with symbol letters that have a familiar structure like those of the entries in the last column of Tab. 3.1, only for sufficiently low (or, by parity conjugation, high) helicity. In contrast, the Landau equations are capable of detecting branch points of even more complicated amplitudes, such as those containing elliptic polylogarithms, which do not have traditional symbols[14].

Second, even for amplitudes which do have symbols, determining the actual symbol alphabet from the singularity loci of the amplitude may require nontrivial extrapolation. Suppose that the Landau equations reveal that some amplitude has a branch point at $z = 0$ (where, for example, z may be one of the quantities in the last column of Tab. 3.1). Then the symbol alphabet should contain a letter $f(z)$, where f in general could be an arbitrary function of z, with branch points arising in two possible ways. If $f(0) = 0$, then the amplitude will have a logarithmic branch point at $z = 0$ [23], but even if $f(0) \neq 0$, the amplitude can have an *algebraic* branch point (so the cover has finitely many sheets) at $z = 0$ if $f(z)$ has such a branch point there.

We can explore this second notion empirically since all one-loop amplitudes in SYM theory, and in particular their symbol alphabets, are well-known (following from one-loop integrated amplitudes in for example, [38, 39, 40, 41, 42, 43, 44, 45, 46]). According to our results from Tab. 3.1, we find that one-loop amplitudes only have branch points on loci of the form

- $\langle i\, i{+}1\, j\, j{+}1\rangle = 0$ or $\langle i\, \bar{j}\rangle = 0$ for $0 \leq \mathrm{k} \leq n-4$,
- $\langle i(i{-}1\, i{+}1)(j\, j{+}1)(k\, k{+}1)\rangle = 0$ for $1 \leq \mathrm{k} \leq n-5$, and
- $\Delta_{ijk\ell} = 0$ (defined in Tab. 3.1) for $2 \leq \mathrm{k} \leq n-6$,

[14] It would be interesting to understand how the "generalized symbols" of such amplitudes capture the singularity loci revealed by the Landau equations.

where i, j, k, ℓ can all range from 1 to n. Happily, the first two of these are in complete accord with the symbol letters of one-loop MHV and NMHV amplitudes, but the third reveals the foreshadowed algebraic branching since $\Delta_{ijk\ell}$ is not a symbol letter of the four-mass box integral contribution to $\mathrm{N}^{2\leq \mathrm{k}\leq n-6}$MHV amplitudes. Rather, the symbol alphabet of this amplitude consists of quantities of the form

$$f_{ij} \equiv \langle i\, i{+}1\, j\, j{+}1\rangle \quad \text{and} \quad f_{i\ell}f_{jk} \pm (f_{ik}f_{j\ell} - f_{ij}f_{k\ell}) \pm \sqrt{\Delta_{ijk\ell}}\,, \tag{3.46}$$

where the signs may be chosen independently. Since no symbol letter vanishes on the locus $\Delta_{ijk\ell} = 0$, amplitudes evidently do not have logarithmic branch points on this locus. Yet it is evident from the second expression of (3.46) that amplitudes with these letters have algebraic (in this instance, square-root- or double-sheet-type) branch points when $\Delta_{ijk\ell} = 0$.

Although we have only commented on the structure of various potential symbol entries and branch point loci here, let us emphasize that the methods of this paper can be used to determine precisely which symbol entries can appear in any given amplitude. For example, Tab. 3.1 can be used to determine values of i, j and k for which the letter $\langle i(i{-}1\, i{+}1)(j\, j{+}1)(k\, k{+}1)\rangle$ can appear, as well as in which one-loop amplitudes, indexed by n and k, such letters will appear. An example of a fine detail along these lines evident already in Tab. 3.1 is the fact that all NMHV amplitudes have branch points of two-mass easy type except for the special case $n = 6$, in accord with Eq. (2.7) of [79].

We conclude this section by remarking that the problem of deriving symbol alphabets from the Landau singularity loci may remain complicated in general, but we hope that the simple, direct correspondence we have observed for certain one-loop amplitudes (and which was also observed for the two-loop MHV amplitudes studied in [17]) will continue to hold at arbitrary loop order for sufficiently simple singularities.

3.7 Conclusion

This paper presents first steps down the path of understanding the branch cut structure of SYM amplitudes for general helicity, following the lead of [17] and using the recent "unwound" formulation of the amplituhedron from [37]. Our algorithm is conceptually simple: we first enumerate the boundaries of an amplituhedron, and from there, without resorting to integral representations, we use the Landau equations directly to determine the locations of branch points of the corresponding amplitude.

One might worry that each of these steps grows rapidly in computational complexity at higher loop order. Classifying boundaries of amplituhedra is on its own a highly nontrivial problem, aspects of which have been explored in [5, 7, 10, 13, 80]. In that light, the graphical tools presented in Sec. 3.4.2, while already useful for organizing results as in Fig. 3.2, hint at the more enticing possibility of a method to enumerate twistor diagrams corresponding to all $\mathcal{L}$-boundaries of any given $\mathcal{A}_{n,\mathrm{k},L}$. Such an algorithm would start with the maximal codimension twistor diagrams at a given loop order, and apply the operators of Sec. 3.4.2 in all ways until no further operations are possible. From these twistor diagrams come Landau diagrams, and from these come the branch points via the Landau equations. We saw in [17] and Sec. 3.5 that analyzing the Landau equations can be made very simple in momentum twistor space.

Configurations of loop momenta in (the closure of) MHV amplituhedra are represented by non-negative D-matrices. In general, non-MHV configurations must be represented by indefinite D-matrices, but we observed in Sec. 3.3.5 that even for non-MHV amplituhedra, D may always be chosen non-negative for all configurations on $\mathcal{L}$-boundaries. This 'emergent positivity' plays a crucial role by allowing the one-loop D-matrices presented in Secs. 3.3.2, 3.3.3 and 3.3.4 to be trivially recycled at higher values of helicity. One way to think about this is to say that going beyond MHV level introduces the C-matrix which "opens up" additional configuration space in which an otherwise indefinite D-matrix can become positive.

While the one-loop all-helicity results we obtain are interesting in their own right

as first instances of all-helicity statements, this collection of information is valuable because it provides the building blocks for the two-loop analysis in the sequel. There we will argue that the two-loop twistor diagrams with helicity k can be viewed as compositions of two one-loop diagrams with helicities k_1 and k_2 satisfying $k = k_1 + k_2$ or $k_1 + k_2 + 1$. We will also explore in detail the relation to on-shell diagrams, which are simply Landau diagrams with decorated nodes.

More speculatively, the ideas that higher-loop amplitudes can be constructed from lower-loop amplitudes, and that there is a close relation to on-shell diagrams, suggests the possibility that this toolbox may also be useful for finding symbols in the full, nonplanar SYM theory. For example, enumerating the on-shell conditions as we do here in the planar sector is similar in spirit to the nonplanar examples of [12] where certain integral representations were found such that individual integrals had support on only certain branches[15]. There are of course far fewer known results in the nonplanar SYM theory, though there have been some preliminary studies [82, 83, 84, 85, 86].

[15] Already in the planar case, one might interpret our algorithm as applying the Landau equations to integrands constructed in expansions around boundaries of amplituhedra, which is reminiscent of the prescriptive unitarity of [81].

Chapter 4

All-loop singularities of scattering amplitudes in massless planar theories

4.1 Landau Graphs and Singularities

We begin by reviewing the Landau equations, which encode the constraint of locality on the singularity structure of scattering amplitudes in perturbation theory via Landau graphs. We aim to connect the standard vocabulary used in relativistic field theory to that of network theory in order to streamline the rest of our discussion.

In *planar* quantum field theories, which will be the exclusive focus of this paper, we can restrict our attention to plane Landau graphs. An *L-loop m-point plane Landau graph* is a plane graph with $L+1$ faces and m distinguished vertices called *terminals* that must lie on a common face called the *unbounded face*. Henceforth we use the word "vertex" only for those that are not terminals, and the word "face" only for the L faces that are not the unbounded face.

Each edge j is assigned an arbitrary orientation and a four-component (or, more generally, a D-component) (energy-)momentum vector q_j, the analog of electric current. Reversing the orientation of an edge changes the sign of the associated q_j. At each vertex the vector sum of incoming momenta must equal the vector sum of outgoing momenta

(current conservation). This constraint is not applied at terminals, which are the locations where a circuit can be probed by connecting external sources or sinks of current. In field theory these correspond to the momenta carried by incoming or outgoing particles. If we label the terminals by $a = 1, \ldots, m$ (in cyclic order around the unbounded face) and let P_a denote the D-momentum flowing into the graph at terminal a, then energy-momentum conservation requires that $\sum_a P_a = 0$ and implies that precisely L of the q_j's are linearly independent.

Scattering amplitudes are (in general multivalued) functions of the P_a's which can be expressed as a sum over all Landau graphs, followed by a DL-dimensional integral over all components of the linearly independent q_j's. Amplitudes in different quantum field theories differ in how the various graphs are weighed (by P_a- and q_j-dependent factors) in that linear combination. These differences are indicated graphically by decorating each Landau graph (usually in many possible ways) with various embellishments, in which case they are called *Feynman diagrams*. We return to this important point later, but for now we keep our discussion as general as possible.

Our interest lies in understanding the loci in P_a-space on which amplitudes may have singularities, which are highly constrained by general physical principles. A Landau graph is said to have *Landau singularities of the first type* at values of P_a for which the *Landau equations* [26]

$$\alpha_j q_j^2 = 0 \text{ for each edge } j, \text{ and} \tag{4.1}$$

$$\sum_{\text{edges } j \in \mathcal{F}} \alpha_j q_j = 0 \text{ for each face } \mathcal{F} \tag{4.2}$$

admit nontrivial solutions for the *Feynman parameters* α_j (that means, omitting the trivial solution where all $\alpha_j = 0$). In the first line we have indicated our exclusive focus on *massless* field theories by omitting a term proportional to m_j^2 which would normally be present.

The Landau equations generally admit several branches of solutions. The *leading* Landau singularities of a graph $\mathcal{G}$ are those associated to branches having $q_j^2 = 0$ for all j (regardless of whether any of the α_j's are zero). This differs slightly from the more

conventional usage of the term "leading", which requires all of the α_j's to be nonzero. However, we feel that our usage is more natural in massless theories, where it is typical to have branches of solutions on which q_j^2 and α_j are *both* zero for certain edges j. Landau singularities associated to branches on which one or more of the q_j^2 are not zero (in which case the corresponding α_j's must necessarily vanish) can be interpreted as leading singularities of a *relaxed* Landau graph obtained from $\mathcal{G}$ by contracting the edges associated to the vanishing α_j's.

A graph is called *c-connected* if it remains connected after removal of any $c-1$ vertices. It is easy to see that the set of Landau singularities for a 1-connected graph (sometimes called a "kissing graph" in field theory) is the union of Landau singularities associated to each 2-connected component since the Landau equations completely decouple. Therefore, without loss of generality we can confine our attention to 2-connected Landau graphs.

4.2 Elementary Circuit Operations

We refer to Eq. (4.2) as the *Kirchhoff conditions* in recognition of their circuit analog where the α_j's play the role of resistances. The analog of the *on-shell conditions* (4.1) on the other hand is rather mysterious, but a very remarkable feature of massless theories is that:

The graph moves familiar from elementary electrical circuit theory preserve the solution sets of Eqs. (4.1) and (4.2), and hence, the sets of first-type Landau singularities in any massless field theory.

Let us now demonstrate this feature, beginning with the three elementary circuit moves shown in Fig. 4.1.

Series reduction (Fig. 4.1(a)) allows one to remove any vertex of degree two. Since $q_2 = q_1$ by momentum conservation, the structure of the Landau equations is trivially preserved if the two edges with Feynman parameters α_1, α_2 are replaced by a single edge carrying momentum $q' = q_1 = q_2$ and Feynman parameter $\alpha' = \alpha_1 + \alpha_2$.

Parallel reduction (Fig. 4.1(b)) allows one to collapse any bubble subgraph. It is easy to verify (see for example Appendix A.1 of [17]) that the structure of the Landau

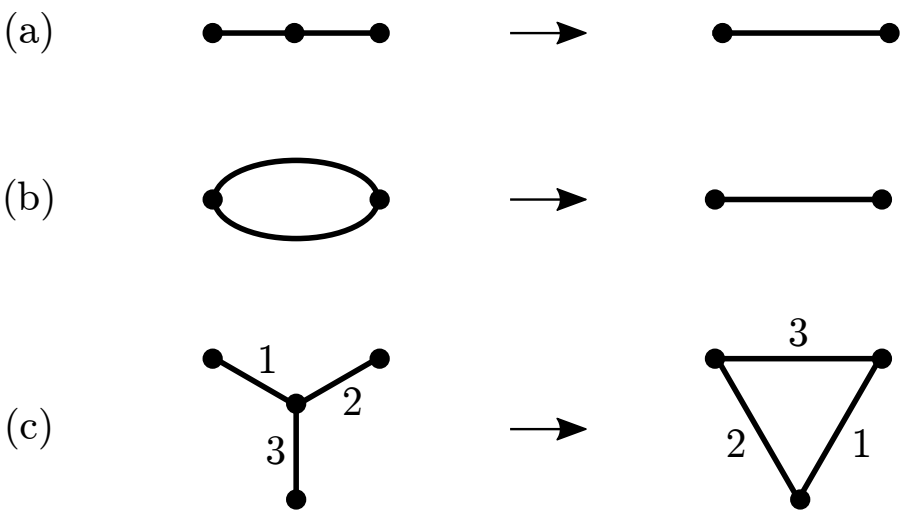

FIGURE 4.1: Elementary circuit moves that preserve solution sets of the massless Landau equations: (a) series reduction, (b) parallel reduction, and (c) Y-Δ reduction.

equations is preserved if the two edges of the bubble are replaced by a single edge carrying momentum $q' = q_1 + q_2$ and Feynman parameter $\alpha' = \alpha_1\alpha_2/(\alpha_1 + \alpha_2)$.

The Y-Δ reduction (Fig. 4.1(c)) replaces a vertex of degree three (a "Y") with a triangle subgraph (a "Δ"), or vice versa. Generically the Feynman parameters α_i of the Δ are related to those of the Y, which we call β_i, by

$$\beta_1 = \frac{\alpha_2\alpha_3}{\alpha_1 + \alpha_2 + \alpha_3}, \quad \text{and cyclic.} \tag{4.3}$$

On branches where one or more of the parameters vanish, this relation must be suitably modified. For example, if a branch of solutions for a graph containing a Y has $\beta_1 = \beta_2 = 0$ but β_3 nonzero, then the corresponding branch for the reduced graph has $\alpha_3 = 0$ but α_1, α_2 nonzero.

The invariance of the Kirchhoff conditions (4.2) under Y-Δ reduction follows straightforwardly from these Feynman parameter assignments. The invariance of the on-shell conditions (4.1) is nontrivial, and follows from the analysis in Appendix A.2 of [17] by checking that the on-shell conditions before and after the reduction are equivalent for each branch of solutions to the Landau equations. Actually [17] mentions only seven of

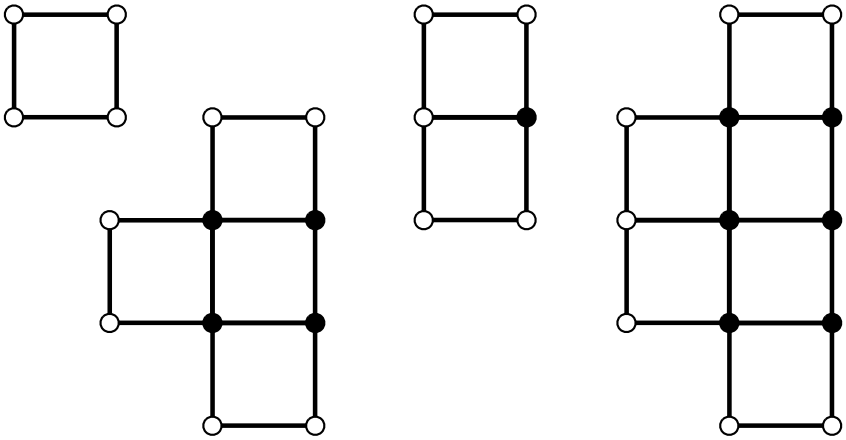

FIGURE 4.2: The four-, six-, five- and seven-terminal ziggurat graphs. The open circles are terminals and the filled circles are vertices. The pattern continues in the obvious way, but note an essential difference between ziggurat graphs with an even or odd number of terminals in that only the latter have a terminal of degree three.

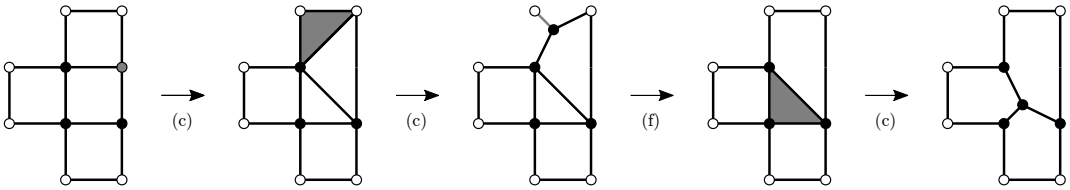

FIGURE 4.3: The six-terminal ziggurat graph can be reduced to a three loop graph by a sequence of three Y-Δ reductions and one FP assignment. In each case the vertex, edge, or face to be transformed is highlighted in gray.

the eight different types of branches. The eighth branch has $\alpha_1 = \alpha_2 = \alpha_3 = 0$, corresponding to $\beta_1 = \beta_2 = \beta_3 = 0$, but in this relatively trivial case both the Y and the Δ can effectively be collapsed to a single vertex.

The proof of the crucial theorem of [52] that we employ in the next section relies on three additional relatively simple moves that either have no analog in field theory or trivially preserve the essential content of the Landau equations. These are (d) the deletion of a "tadpole" (edges that connect a vertex or terminal to itself), (e) the deletion of a "hanging propagator" (a vertex of degree one and the edge connected to it), and (f) the contraction of an edge connected to a terminal of degree one (called "FP assignment" [87]). The last of these is strictly speaking not completely trivial at the level of the Landau equations; it just removes an otherwise uninteresting bubble singularity.

4.3 Reduction of Planar Graphs

The reduction of general graphs under the operations reviewed in the previous section is a well-studied problem in the mathematical literature. When it is declared that a certain subset of vertices are to be considered terminals (which may not be removed by series or Y-Δ reduction) the corresponding problem is called *terminal* Y-Δ *reducibility*. Aspects of terminal Y-Δ reducibility have been studied in [88, 89, 90, 91, 87, 92], including an application to Feynman diagrams in [93]. For our purpose the key result comes from the Ph.D. thesis of I. Gitler [52], who proved that any planar 2-connected graph with m terminals lying on the same face can be reduced to a graph of the kind shown in Fig. 4.2, which we call *ziggurat* graphs, or to a minor thereof. We denote the m-terminal ziggurat graph by $\mathcal{T}_m$, and note that a *minor* of a graph $\mathcal{G}$ is any graph that can be obtained from $\mathcal{G}$ by any sequence of edge contractions and/or edge deletions.

At the level of Landau equations an edge contraction corresponds, as discussed above, to a relaxation (setting the associated α_j to zero), while an edge deletion corresponds to setting the associated q_j to zero. It is clear that the Landau singularities associated to any minor of a graph $\mathcal{G}$ are a subset of those associated to $\mathcal{G}$. Consequently

we don't need to worry about explicitly enumerating all minors of $\mathcal{T}_m$; their Landau singularities are already contained in the set of singularities of $\mathcal{T}_m$ itself.

It is conventional to discuss scattering amplitudes for a fixed number n of external particles, each of which carries some momentum p_i that in massless theories satisfies $p_i^2 = 0$. The total momentum flowing into each terminal is not arbitrary, but must be a sum of one or more null vectors. The momenta carried by these individual particles are denoted graphically by attaching a total of n *external edges* to the terminals, with at least one per terminal. In this way it is clear that any Landau graph with $m \leq n$ terminals is potentially relevant to finding the Landau singularities of an n-particle amplitude. However, it is also clear that if $m < n$ then $\mathcal{T}_m$ is a minor of $\mathcal{T}_n$, so again the Landau singularities of the former are a subset of those of the latter. Therefore, to find the Landau singularities of an n-particle amplitude it suffices to find those of the n-terminal ziggurat graph $\mathcal{T}_n$ with precisely one external edge attached to each terminal. We call this the *n-particle ziggurat graph* and finally summarize:

> The first-type Landau singularities of an n-particle scattering amplitude in any massless planar field theory are a subset of those of the n-particle ziggurat graph.

While the Landau singularities of the ziggurat graph exhaust the set of singularities that may appear in any massless planar theory, we cannot rule out the possibility that in certain special theories the actual set of singularities may be smaller because of nontrivial cancellation between the contributions of different Landau graphs to a given amplitude. We return to this important point in Sec. 4.6.

Let us also emphasize that Y-Δ reduction certainly changes the number of faces of a graph, so the above statement does not hold at fixed loop order L; rather it is an all-order relation about the full set of Landau singularities of n-particle amplitudes at any finite order in perturbation theory. Since the n-particle ziggurat graph has $L = \lfloor (n-2)^2/4 \rfloor$ faces, we can however predict that a single computation at only $\lfloor (n-2)^2/4 \rfloor$-loop order suffices to expose all possible Landau singularities of any n-particle amplitude.

In fact this bound is unnecessarily high. Gitler's theorem does not imply that ziggurat graphs cannot be further reduced to graphs of lower loop order, and it is easy to see

that in general this is possible. For example, as shown in Fig. 4.3, the six-terminal graph can be reduced by a sequence of Y-Δ reductions and one FP assignment to a particularly beautiful three-loop wheel graph whose 6-particle avatar we display in Fig. 4.4. Ziggurat graphs with more than six terminals can also be further reduced, but we have not been able to prove a lower bound on the loop order that can be obtained for general n.

4.4 Landau Analysis of the Wheel

In this section we analyze the Landau equations for the graph shown in Fig. 4.4. The six external edges carry momenta $p_1, \ldots, p_6$ into the graph, subject to $\sum_i p_i = 0$ and $p_i^2 = 0$ for each i. Using momentum conservation at each vertex, the momentum q_j carried by each of the twelve edges can be expressed in terms of the six p_i and three other linearly independent momenta, which we can take to be l_r, for $r = 1, 2, 3$, assigned as shown in the figure. Initially we consider the leading Landau singularities, for which we impose the twelve on-shell conditions

$$\begin{aligned}
(l_1 - p_1)^2 = l_1^2 = (l_1 + p_2)^2 = 0\,,\\
(l_2 - p_3)^2 = l_2^2 = (l_2 + p_4)^2 = 0\,,\\
(l_3 - p_5)^2 = l_3^2 = (l_3 + p_6)^2 = 0\,,\\
(l_1 + p_2 - l_2 + p_3)^2 = 0\,,\\
(l_2 + p_4 - l_3 + p_5)^2 = 0\,,\\
(l_3 + p_6 - l_1 + p_1)^2 = 0\,.
\end{aligned} \tag{4.4}$$

So far we have not needed to commit to any particular spacetime dimension. We now fix $D = 4$, which simplifies the analysis because for generic p_i there are precisely 16 discrete solutions for the l_r's, which we denote by $l_r^*(p_i)$. To enumerate and explicitly exhibit these solutions it is technically helpful to parameterize the momenta in terms of momentum twistor variables [55], in which case the solutions can be associated with on-shell diagrams as described in [3]. Although so far the analysis is still applicable to

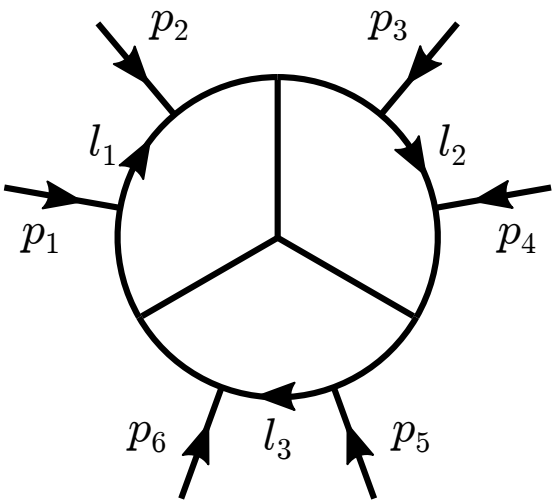

FIGURE 4.4: The three-loop six-particle wheel graph. The leading first-type Landau singularities of this graph exhaust all possible first-type Landau singularities of six-particle amplitudes in any massless planar field theory, to any finite loop order.

general massless planar theories, we note that in the special context of SYM theory, two cut solutions have MHV support, twelve NMHV, and two NNMHV.

With these solutions in hand, we next turn our attention to the Kirchhoff conditions

$$\begin{aligned}
0 =& \alpha_1(l_1 - p_1) + \alpha_2 l_1 + \alpha_3(l_1 + p_2) + \\
& \alpha_{10}(l_3 + p_6 - l_1 + p_1) + \alpha_{11}(l_1 + p_2 - l_2 + p_3)\,, \\
0 =& \alpha_4(l_2 - p_3) + \alpha_5 l_2 + \alpha_6(l_2 + p_4) + \\
& \alpha_{11}(l_1 + p_2 - l_2 + p_3) + \alpha_{12}(l_2 + p_4 - l_3 + p_5)\,, \\
0 =& \alpha_7(l_3 - p_5) + \alpha_8 l_3 + \alpha_9(l_3 + p_6) + \\
& \alpha_{12}(l_2 + p_4 - l_3 + p_5) + \alpha_{10}(l_3 + p_6 - l_1 + p_1)\,.
\end{aligned} \tag{4.5}$$

Nontrivial solutions to this 12×12 linear system exist only if the associated *Kirchhoff determinant* $K(p_i, l_r)$ vanishes. By evaluating this determinant on each of the solutions $l_r = l_r^*(p_i)$ the condition for the existence of a non-trivial solution to the Landau equations can be expressed entirely in terms of the external momenta p_i. Using variables u, v, w, y_u, y_v, y_w that are very familiar in the literature on six-particle amplitudes (their definition in terms of the p_i's can be found for example in [20]), we find that

$K(p_i, l_r^*(p_i)) = 0$ can only be satisfied if an element of the set

$$S_6 = \{u\,, v\,, w\,, 1-u\,, 1-v\,, 1-w\,, \frac{1}{u}\,, \frac{1}{v}\,, \frac{1}{w}\} \tag{4.6}$$

vanishes. We conclude that the three-loop $n = 6$ wheel graph has first-type Landau singularities on the locus

$$\mathcal{S}_6 \equiv \bigcup_{s \in S_6} \{s = 0\}\,. \tag{4.7}$$

It is straightforward, if somewhat tedious, to analyze all *subleading* Landau singularities corresponding to relaxations, as defined above. We refer the reader to [16, 17, 47] where this type of analysis has been carried out in detail in several examples. We find no additional first-type singularities beyond those that appear at leading order. Let us emphasize that this unusual feature does not occur for any of the examples in [16, 17, 47], which typically have many additional subleading singularities.

To summarize, we conclude that any six-particle amplitude in any four-dimensional massless planar field theory, at any finite loop order, can have first-type Landau singularities only on the locus $\mathcal{S}_6$ given by Eqs. (4.6) and (4.7), or a proper subset thereof.

4.5 Second-Type Singularities

The first-type Landau singularities that we have classified, which by definition are those encapsulated in the Landau equations (4.1), (4.2), do not exhaust all possible singularities of amplitudes in general quantum field theories. There also exist "second-type" singularities (see for example [58, 33]) which are sometimes called "non-Landauian" [27]. These arise in Feynman loop integrals as pinch singularities at infinite loop momentum and must be analyzed by a modified version of Eqs. (4.1), (4.2).

In the next section we turn our attention to the special case of SYM theory, which possesses a remarkable *dual conformal symmetry* [94, 95, 76] implying that there is no invariant notion of "infinity" in momentum space. As pointed out in [16], we therefore

expect that second-type singularities should be absent in any dual conformal invariant theory. Because ziggurat graphs are manifestly dual conformal invariant when $D = 4$, this would imply that the first-type Landau singularities of the ziggurat graphs should capture the entire "dual conformally invariant part" of the singularity structure of all massless planar theories in four spacetime dimensions. By this we mean, somewhat more precisely, the singularity loci that do not involve the infinity twistor.

4.6 Planar SYM Theory

In Sec. 4.3 we acknowledged that in certain special theories, the actual set of singularities of amplitudes may be strictly smaller than that of the ziggurat graphs due to cancellations. SYM theory has been shown to possess such rich mathematical structure that it would seem the most promising candidate to exhibit such cancellations. Contrary to this expectation, we now argue that:

Perturbative amplitudes in SYM theory exhibit first-type Landau singularities on *all* such loci that are possible in any massless planar field theory.

Moreover, our results suggest that this all-order statement is true separately in each helicity sector. Specifically: for any fixed n and any $0 \leq k \leq n-4$, there is a finite value of $L_{n,k}$ such that the singularity locus of the L-loop n-particle N^{k}MHV amplitude is identical to that of the n-particle ziggurat graph for all $L \geq L_{n,k}$. In order to verify this claim, it suffices to construct an n-particle on-shell diagram with N^{k}MHV support that has the same Landau singularities as the n-particle ziggurat graph; or (conjecturally) equivalently, to write down an appropriate valid configuration of lines inside the amplituhedron [4] $\mathcal{A}_{n,k,L}$ for some sufficiently high L.

To see that this is plausible, note that in general the appearance of a given singularity at some fixed k and L can be shown to imply the existence of the same singularity at lower k but higher L by performing the opposite of a parallel reduction—doubling one or more edges of the relevant Landau graph to make bubbles (see for example Fig. 2 of [47]). For example, while one-loop MHV amplitudes do not have singularities of

three-mass box type, it is known by explicit computation [60] that two-loop MHV amplitudes do. Similarly, while two-loop MHV amplitudes do not have singularities of four-mass box type, we expect that three-loop MHV and two-loop NMHV amplitudes do. (To be clear, our analysis is silent on the question of whether the symbol alphabets of these amplitudes contain square roots; see the discussion in Sec. 7 of [53].)

It is indeed simple to check that the n-particle ziggurat graph can be converted into a valid on-shell diagram with MHV support by doubling *each* internal edge to form a bubble. Moreover, in this manner it is relatively simple to write an explicit mutually positive configuration of positive lines inside the MHV amplituhedron. However, we note that while this construction is sufficient to demonstrate the claim, it is certainly overkill; we expect MHV support to be reached at much lower loop level than this argument would require, as can be checked on a case by case basis for relatively small n.

4.7 Symbol Alphabets

Let us comment on the connection of our work to symbol alphabets. In general, the presence of some letter a in the symbol of an amplitude indicates that there exists some sheet on which the analytically continued amplitude has a branch cut from $a = 0$ to $a = \infty$. The symbols of all known six-particle amplitudes in SYM theory can be expressed in terms of a nine-letter alphabet [67] which may be chosen as [69]

$$A_6 = \{u, v, w, 1-u, 1-v, 1-w, y_u, y_v, y_w\}\,, \tag{4.8}$$

where $z = \{y_u, 1/y_u\}$ are the two roots of

$$u(1-v)(1-w)(z^2+1) = \left[u^2-2uvw+(1-v-w)^2\right] z \tag{4.9}$$

and y_v and y_w are defined by cycling $u \to v \to w \to u$. It is evident from Eq. (4.9) that y_u can attain the value 0 or ∞ only if $u = 0$ or $v = 1$ or $w = 1$. We therefore see that the singularity locus encoded in the hexagon alphabet A_6 is precisely equivalent to $\mathcal{S}_6$ given

by Eqs. (4.6) and (4.7). Indeed, the hypothesis that six-particle amplitudes in SYM theory do not exhibit singularities on any other loci at any higher loop order (which we now consider to be proven), and the apparently much stronger ansatz that the nine quantities shown in Eq. (4.8) provide a symbol alphabet for all such amplitudes, lies at the heart of a bootstrap program that has made possible impressive explicit computations to high loop order (see for example [69, 96, 70, 14, 72, 73, 20]). An analogous ansatz for $n = 7$ has similarly allowed for the computation of symbols of seven-particle amplitudes [21, 22].

Unfortunately, as the y_u, y_v, y_w letters demonstrate, the connection between Landau singularity loci and symbol alphabets is somewhat indirect. It is not possible to derive A_6 from $\mathcal{S}_6$ alone as knowledge of the latter only tells us about the locus where symbol letters vanish [23] or have branch points (see Sec. 7 of [53]). In order to determine what the symbol letters actually are away from these loci it seems necessary to invoke some other kind of structure; for example, cluster algebras may have a role to play here [18, 19].

4.8 Conclusion

We leave a number of open questions for future work. What is the minimum loop order L_n to which the n-particle ziggurat graph can be reduced? Can one characterize its Landau singularities for arbitrary n, generalizing the result for $n = 6$ in Sec. 4.4? Does there exist a similar framework for classifying second-type singularities, even if only in certain theories? The graph moves reviewed in Sec. 4.2 preserve the (sets of solutions to the) Landau equations even for non-planar graphs; are there results on non-planar Y-Δ reducibility (see for example [97, 98]) that may be useful for non-planar (but still massless) theories?

In Sec. 4.4 we saw that the wheel is a rather remarkable graph. The ziggurat graphs, and those to which they can be reduced, might warrant further study for their own sake. Intriguingly they generalize those studied in [99, 100] and are particular cases of the graphs that have attracted recent interest, for example in [101, 102], in the context of

"fishnet" theories. We have only looked at their singularity loci; it would be interesting to explore the structure of their cuts, perhaps in connection with the coaction studied in [30, 103, 104, 105, 106].

In the special case of SYM theory the technology might exist to address more detailed questions. For general n and k, what is the minimum loop order $L_{n,k}$ at which the Landau singularities of the n-particle N^{k}MHV amplitude saturate? Is there a direct connection between Landau singularities, ziggurat graphs, and cluster algebras? For amplitudes of generalized polylogarithm type, now that we know (in principle) the relevant singularity loci, what are the actual symbol letters for general n, and can the symbol alphabet depend on k (even though the singularity loci do not)? How do Landau singularities manifest themselves in general amplitudes that are of more complicated (non-polylogarithmic) functional type?

Bibliography

[1] Lars Brink, John H. Schwarz, and Joel Scherk. "Supersymmetric Yang-Mills Theories". In: *Nucl. Phys.* B121 (1977), pp. 77–92. DOI: 10.1016/0550-3213(77)90328-5.

[2] Nima Arkani-Hamed et al. "The All-Loop Integrand For Scattering Amplitudes in Planar N=4 SYM". In: *JHEP* 01 (2011), p. 041. DOI: 10.1007/JHEP01(2011)041. arXiv: 1008.2958 [hep-th].

[3] Nima Arkani-Hamed et al. *Grassmannian Geometry of Scattering Amplitudes*. Cambridge University Press, 2016. ISBN: 9781107086586, 9781316572962. DOI: 10.1017/CBO9781316091548. arXiv: 1212.5605 [hep-th]. URL: http://www.cambridge.org/us/academic/subjects/physics/theoretical-physics-and-mathematical-physics/grassmannian-geometry-scattering-amplitudes?format=HB&isbn=9781107086586.

[4] Nima Arkani-Hamed and Jaroslav Trnka. "The Amplituhedron". In: *JHEP* 10 (2014), p. 030. DOI: 10.1007/JHEP10(2014)030. arXiv: 1312.2007 [hep-th].

[5] Nima Arkani-Hamed and Jaroslav Trnka. "Into the Amplituhedron". In: *JHEP* 12 (2014), p. 182. DOI: 10.1007/JHEP12(2014)182. arXiv: 1312.7878 [hep-th].

[6] Yuntao Bai and Song He. "The Amplituhedron from Momentum Twistor Diagrams". In: *JHEP* 02 (2015), p. 065. DOI: 10.1007/JHEP02(2015)065. arXiv: 1408.2459 [hep-th].

[7] Sebastian Franco et al. "Anatomy of the Amplituhedron". In: *JHEP* 03 (2015), p. 128. DOI: 10.1007/JHEP03(2015)128. arXiv: 1408.3410 [hep-th].

[8] Thomas Lam. "Amplituhedron cells and Stanley symmetric functions". In: *Commun. Math. Phys.* 343.3 (2016), pp. 1025–1037. DOI: 10.1007/s00220-016-2602-2. arXiv: 1408.5531 [math.AG].

[9] Nima Arkani-Hamed, Andrew Hodges, and Jaroslav Trnka. "Positive Amplitudes In The Amplituhedron". In: *JHEP* 08 (2015), p. 030. DOI: 10.1007/JHEP08(2015)030. arXiv: 1412.8478 [hep-th].

[10] Yuntao Bai, Song He, and Thomas Lam. "The Amplituhedron and the One-loop Grassmannian Measure". In: *JHEP* 01 (2016), p. 112. DOI: 10.1007/JHEP01(2016)112. arXiv: 1510.03553 [hep-th].

[11] Livia Ferro et al. "Towards the Amplituhedron Volume". In: *JHEP* 03 (2016), p. 014. DOI: 10.1007/JHEP03(2016)014. arXiv: 1512.04954 [hep-th].

[12] Zvi Bern et al. "Evidence for a Nonplanar Amplituhedron". In: *JHEP* 06 (2016), p. 098. DOI: 10.1007/JHEP06(2016)098. arXiv: 1512.08591 [hep-th].

[13] Daniele Galloni. "Positivity Sectors and the Amplituhedron". In: (2016). arXiv: 1601.02639 [hep-th].

[14] Lance J. Dixon et al. "Bootstrapping six-gluon scattering in planar N=4 super-Yang-Mills theory". In: *PoS* LL2014 (2014), p. 077. DOI: 10.22323/1.211.0077. arXiv: 1407.4724 [hep-th].

[15] John Golden and Marcus Spradlin. "A Cluster Bootstrap for Two-Loop MHV Amplitudes". In: *JHEP* 02 (2015), p. 002. DOI: 10.1007/JHEP02(2015)002. arXiv: 1411.3289 [hep-th].

[16] Tristan Dennen, Marcus Spradlin, and Anastasia Volovich. "Landau Singularities and Symbology: One- and Two-loop MHV Amplitudes in SYM Theory". In: *JHEP* 03 (2016), p. 069. DOI: 10.1007/JHEP03(2016)069. arXiv: 1512.07909 [hep-th].

[17] Tristan Dennen et al. "Landau Singularities from the Amplituhedron". In: *JHEP* 06 (2017), p. 152. DOI: 10.1007/JHEP06(2017)152. arXiv: 1612.02708 [hep-th].

[18] John Golden et al. "Motivic Amplitudes and Cluster Coordinates". In: *JHEP* 01 (2014), p. 091. DOI: 10.1007/JHEP01(2014)091. arXiv: 1305.1617 [hep-th].

[19] James Drummond, Jack Foster, and Ömer Gürdoğan. "Cluster Adjacency Properties of Scattering Amplitudes in $N = 4$ Supersymmetric Yang-Mills Theory". In: *Phys. Rev. Lett.* 120.16 (2018), p. 161601. DOI: 10.1103/PhysRevLett.120.161601. arXiv: 1710.10953 [hep-th].

[20] Simon Caron-Huot et al. "Bootstrapping a Five-Loop Amplitude Using Steinmann Relations". In: *Phys. Rev. Lett.* 117.24 (2016), p. 241601. DOI: 10.1103/PhysRevLett.117.241601. arXiv: 1609.00669 [hep-th].

[21] James M. Drummond, Georgios Papathanasiou, and Marcus Spradlin. "A Symbol of Uniqueness: The Cluster Bootstrap for the 3-Loop MHV Heptagon". In: *JHEP* 03 (2015), p. 072. DOI: 10.1007/JHEP03(2015)072. arXiv: 1412.3763 [hep-th].

[22] Lance J. Dixon et al. "Heptagons from the Steinmann Cluster Bootstrap". In: *JHEP* 02 (2017), p. 137. DOI: 10.1007/JHEP02(2017)137. arXiv: 1612.08976 [hep-th].

[23] Juan Maldacena, David Simmons-Duffin, and Alexander Zhiboedov. "Looking for a bulk point". In: *JHEP* 01 (2017), p. 013. DOI: 10.1007/JHEP01(2017)013. arXiv: 1509.03612 [hep-th].

[24] S. Mandelstam. "Determination of the pion - nucleon scattering amplitude from dispersion relations and unitarity. General theory". In: *Phys. Rev.* 112 (1958), pp. 1344–1360. DOI: 10.1103/PhysRev.112.1344.

[25] Stanley Mandelstam. "Analytic properties of transition amplitudes in perturbation theory". In: *Phys. Rev.* 115 (1959), pp. 1741–1751. DOI: 10.1103/PhysRev.115.1741.

[26] L. D. Landau. "On analytic properties of vertex parts in quantum field theory". In: *Nucl. Phys.* 13 (1959), pp. 181–192. DOI: 10.1016/0029-5582(59)90154-3.

[27] R. E. Cutkosky. "Singularities and discontinuities of Feynman amplitudes". In: *J. Math. Phys.* 1 (1960), pp. 429–433. DOI: 10.1063/1.1703676.

[28] Zvi Bern et al. "Fusing gauge theory tree amplitudes into loop amplitudes". In: *Nucl. Phys.* B435 (1995), pp. 59–101. DOI: 10.1016/0550-3213(94)00488-Z. arXiv: hep-ph/9409265 [hep-ph].

[29] Zvi Bern, Lance J. Dixon, and David A. Kosower. "Progress in one loop QCD computations". In: *Ann. Rev. Nucl. Part. Sci.* 46 (1996), pp. 109–148. DOI: 10.1146/annurev.nucl.46.1.109. arXiv: hep-ph/9602280 [hep-ph].

[30] Samuel Abreu et al. "From multiple unitarity cuts to the coproduct of Feynman integrals". In: *JHEP* 10 (2014), p. 125. DOI: 10.1007/JHEP10(2014)125. arXiv: 1401.3546 [hep-th].

[31] Samuel Abreu, Ruth Britto, and Hanna Grönqvist. "Cuts and coproducts of massive triangle diagrams". In: *JHEP* 07 (2015), p. 111. DOI: 10.1007/JHEP07(2015)111. arXiv: 1504.00206 [hep-th].

[32] Nima Arkani-Hamed et al. "Local Integrals for Planar Scattering Amplitudes". In: *JHEP* 06 (2012), p. 125. DOI: 10.1007/JHEP06(2012)125. arXiv: 1012.6032 [hep-th].

[33] R. J. Eden et al. *The Analytic S-Matrix*. Cambridge University Press, 1966.

[34] Freddy Cachazo, Peter Svrcek, and Edward Witten. "MHV vertices and tree amplitudes in gauge theory". In: *JHEP* 09 (2004), p. 006. DOI: 10.1088/1126-6708/2004/09/006. arXiv: hep-th/0403047 [hep-th].

[35] Ruth Britto et al. "Direct proof of tree-level recursion relation in Yang-Mills theory". In: *Phys. Rev. Lett.* 94 (2005), p. 181602. DOI: 10.1103/PhysRevLett.94.181602. arXiv: hep-th/0501052 [hep-th].

[36] Henriette Elvang and Yu-tin Huang. "Scattering Amplitudes". In: (2013). arXiv: 1308.1697 [hep-th].

[37] Nima Arkani-Hamed, Hugh Thomas, and Jaroslav Trnka. "Unwinding the Amplituhedron in Binary". In: *JHEP* 01 (2018), p. 016. DOI: 10.1007/JHEP01(2018)016. arXiv: 1704.05069 [hep-th].

[38] Gerard 't Hooft and M. J. G. Veltman. "Scalar One Loop Integrals". In: *Nucl. Phys.* B153 (1979), pp. 365–401. DOI: 10.1016/0550-3213(79)90605-9.

[39] Zvi Bern, Lance J. Dixon, and David A. Kosower. "Dimensionally regulated pentagon integrals". In: *Nucl. Phys.* B412 (1994), pp. 751–816. DOI: 10.1016/0550-3213(94)90398-0. arXiv: hep-ph/9306240 [hep-ph].

[40] Zvi Bern et al. "One loop n point gauge theory amplitudes, unitarity and collinear limits". In: *Nucl. Phys.* B425 (1994), pp. 217–260. DOI: 10.1016/0550-3213(94)90179-1. arXiv: hep-ph/9403226 [hep-ph].

[41] Zvi Bern et al. "One loop gauge theory amplitudes with an arbitrary number of external legs". In: *Workshop on Continuous Advances in QCD Minneapolis, Minnesota, February 18-20, 1994*. 1994, pp. 3–21. arXiv: hep-ph/9405248 [hep-ph]. URL: http://www-public.slac.stanford.edu/sciDoc/docMeta.aspx?slacPubNumber=SLAC-PUB-6490.

[42] Andreas Brandhuber, Bill J. Spence, and Gabriele Travaglini. "One-loop gauge theory amplitudes in N=4 super Yang-Mills from MHV vertices". In: *Nucl. Phys.* B706 (2005), pp. 150–180. DOI: 10.1016/j.nuclphysb.2004.11.023. arXiv: hep-th/0407214 [hep-th].

[43] Zvi Bern et al. "All non-maximally-helicity-violating one-loop seven-gluon amplitudes in N=4 super-yang-Mills theory". In: *Phys. Rev.* D71 (2005), p. 045006. DOI: 10.1103/PhysRevD.71.045006. arXiv: hep-th/0410224 [hep-th].

[44] Ruth Britto, Freddy Cachazo, and Bo Feng. "Generalized unitarity and one-loop amplitudes in N=4 super-Yang-Mills". In: *Nucl. Phys.* B725 (2005), pp. 275–305. DOI: 10.1016/j.nuclphysb.2005.07.014. arXiv: hep-th/0412103 [hep-th].

[45] Zvi Bern, Lance J. Dixon, and David A. Kosower. "All Next-to-maximally-helicity-violating one-loop gluon amplitudes in N=4 super-Yang-Mills theory". In: *Phys.*

Rev. D72 (2005), p. 045014. DOI: 10.1103/PhysRevD.72.045014. arXiv: hep-th/0412210 [hep-th].

[46] R. Keith Ellis and Giulia Zanderighi. "Scalar one-loop integrals for QCD". In: *JHEP* 02 (2008), p. 002. DOI: 10.1088/1126-6708/2008/02/002. arXiv: 0712.1851 [hep-ph].

[47] Igor Prlina et al. "Boundaries of Amplituhedra and NMHV Symbol Alphabets at Two Loops". In: *JHEP* 04 (2018), p. 049. DOI: 10.1007/JHEP04(2018)049. arXiv: 1712.08049 [hep-th].

[48] Jon Mathews. "Application of Linear Network Analysis to Feynman Diagrams". In: *Phys. Rev.* 113 (1959), pp. 381–381. DOI: 10.1103/PhysRev.113.381.

[49] Tai Tsun Wu. "Domains of Definition for Feynman Integrals over Real Feynman Parameters". In: *Phys. Rev.* 123 (1961), pp. 678–689. DOI: 10.1103/PhysRev.123.678.

[50] T. T. Wu. "Properties of Normal Thresholds in Perturbation Theory". In: *Phys. Rev.* 123 (1961), pp. 689–691. DOI: 10.1103/PhysRev.123.689.

[51] R. Bjorken and S. Drell. *Relativistic Quantum Fields*. McGraw-Hill, 1965.

[52] Isidoro Gitler. *Delta-wye-delta transformations: algorithms and applications*. Ph.D. Thesis, University of Waterloo, 1991.

[53] Igor Prlina et al. "All-Helicity Symbol Alphabets from Unwound Amplituhedra". In: *JHEP* 05 (2018), p. 159. DOI: 10.1007/JHEP05(2018)159. arXiv: 1711.11507 [hep-th].

[54] Igor Prlina, Marcus Spradlin, and Stefan Stanojevic. "All-loop singularities of scattering amplitudes in massless planar theories". In: *Phys. Rev. Lett.* 121.8 (2018), p. 081601. DOI: 10.1103/PhysRevLett.121.081601. arXiv: 1805.11617 [hep-th].

[55] Andrew Hodges. "Eliminating spurious poles from gauge-theoretic amplitudes". In: *JHEP* 05 (2013), p. 135. DOI: 10.1007/JHEP05(2013)135. arXiv: 0905.1473 [hep-th].

[56] S. Coleman and R. E. Norton. "Singularities in the physical region". In: *Nuovo Cim.* 38 (1965), pp. 438–442. DOI: 10.1007/BF02750472.

[57] Stephen J. Parke and T. R. Taylor. "An Amplitude for n Gluon Scattering". In: *Phys. Rev. Lett.* 56 (1986), p. 2459. DOI: 10.1103/PhysRevLett.56.2459.

[58] D. B. Fairlie et al. "Singularities of the Second Type". In: *J. Math. Phys.* 3 (1962), p. 594. DOI: 10.1063/1.1724262.

[59] D. B. Fairlie et al. "Physical sheet properties of second type singularities". In: *Phys. Lett.* 3 (1962), p. 55. DOI: 10.1016/0031-9163(62)90200-7.

[60] S. Caron-Huot. "Superconformal symmetry and two-loop amplitudes in planar N=4 super Yang-Mills". In: *JHEP* 12 (2011), p. 066. DOI: 10.1007/JHEP12(2011)066. arXiv: 1105.5606 [hep-th].

[61] Jacob L. Bourjaily and Jaroslav Trnka. "Local Integrand Representations of All Two-Loop Amplitudes in Planar SYM". In: *JHEP* 08 (2015), p. 119. DOI: 10.1007/JHEP08(2015)119. arXiv: 1505.05886 [hep-th].

[62] Tristan Dennen. "Unpublished Notes".

[63] Zvi Bern, Lance J. Dixon, and Vladimir A. Smirnov. "Iteration of planar amplitudes in maximally supersymmetric Yang-Mills theory at three loops and beyond". In: *Phys. Rev.* D72 (2005), p. 085001. DOI: 10.1103/PhysRevD.72.085001. arXiv: hep-th/0505205 [hep-th].

[64] Arthur E. Lipstein and Lionel Mason. "From d logs to dilogs the super Yang-Mills MHV amplitude revisited". In: *JHEP* 01 (2014), p. 169. DOI: 10.1007/JHEP01(2014)169. arXiv: 1307.1443 [hep-th].

[65] K Chen. "Iterated path integrals". In: *Bull. Amer. Math. Soc.* 83 (1977), pp. 831–879. DOI: 10.1090/S0002-9904-1977-14320-6. eprint: 1008.2958.

[66] A. B. Goncharov. "A simple construction of Grassmannian polylogarithms". In: *arXiv:0908.2238v2 [math.AG]* (2009).

[67] Alexander B. Goncharov et al. "Classical Polylogarithms for Amplitudes and Wilson Loops". In: *Phys. Rev. Lett.* 105 (2010), p. 151605. DOI: 10.1103/PhysRevLett.105.151605. arXiv: 1006.5703 [hep-th].

[68] Davide Gaiotto et al. "Pulling the straps of polygons". In: *JHEP* 12 (2011), p. 011. DOI: 10.1007/JHEP12(2011)011. arXiv: 1102.0062 [hep-th].

[69] Lance J. Dixon, James M. Drummond, and Johannes M. Henn. "Bootstrapping the three-loop hexagon". In: *JHEP* 11 (2011), p. 023. DOI: 10.1007/JHEP11(2011)023. arXiv: 1108.4461 [hep-th].

[70] Lance J. Dixon et al. "Hexagon functions and the three-loop remainder function". In: *JHEP* 12 (2013), p. 049. DOI: 10.1007/JHEP12(2013)049. arXiv: 1308.2276 [hep-th].

[71] Lance J. Dixon et al. "The four-loop remainder function and multi-Regge behavior at NNLLA in planar N = 4 super-Yang-Mills theory". In: *JHEP* 06 (2014), p. 116. DOI: 10.1007/JHEP06(2014)116. arXiv: 1402.3300 [hep-th].

[72] Lance J. Dixon and Matt von Hippel. "Bootstrapping an NMHV amplitude through three loops". In: *JHEP* 10 (2014), p. 065. DOI: 10.1007/JHEP10(2014)065. arXiv: 1408.1505 [hep-th].

[73] Lance J. Dixon, Matt von Hippel, and Andrew J. McLeod. "The four-loop six-gluon NMHV ratio function". In: *JHEP* 01 (2016), p. 053. DOI: 10.1007/JHEP01(2016)053. arXiv: 1509.08127 [hep-th].

[74] V. P. Nair. "A Current Algebra for Some Gauge Theory Amplitudes". In: *Phys. Lett. B* 214 (1988), p. 215. DOI: 10.1016/0370-2693(88)91471-2.

[75] L. F. Alday, D. Gaiotto, and J. Maldacena. "Thermodynamic Bubble Ansatz". In: *JHEP* 32 (1962), p. 1109. DOI: 10.1007/JHEP09(2011)032.

[76] J. M. Drummond et al. "Dual superconformal symmetry of scattering amplitudes in N=4 super-Yang-Mills theory". In: *Nucl. Phys. B* 317 (2010), p. 828. DOI: 10.1016/j.nuclphysb.2009.11.022.

[77] G. F. Sterman and M. E. Tejeda-Yeomans. "Multiloop amplitudes and resummation". In: *Phys. Lett. B* 48 (2003), p. 552. DOI: 10.1016/S0370-2693(02)03100-3.

[78] J. L. Bourjaily, S. Caron-Huot, and J. Trnka. "Dual-Conformal Regularization of Infrared Loop Divergences and the Chiral Box Expansion". In: *JHEP* 1 (2015), p. 1501. DOI: 10.1007/JHEP01(2015)001.

[79] D. A. Kosower, R. Roiban, and C. Vergu. "The Six-Point NMHV amplitude in Maximally Supersymmetric Yang-Mills Theory". In: *Phys. Rev. D* 83 (2011). DOI: 10.1103/PhysRevD.83.065018.

[80] S. N. Karp, L. K. Williams, and Y. X. Zhang. "Decompositions of amplituhedra". In: *arXiv:1708.09525 [math.CO]* (2017).

[81] J. L. Bourjaily, E. Hermann, and J. Trnka. "Prescriptive Unitarity". In: *JHEP* 59 (2017), p. 1706. DOI: 10.1007/JHEP06(2017)059. arXiv: 1704.05460 [hep-th].

[82] N. Arkani-Hamed et al. "Singularity Structure of Maximally Supersymmetric Scattering Amplitudes". In: *Phys. Rev. Lett.* 26 (2014), p. 113. DOI: 10.1103/PhysRevLett.113.261603. arXiv: 1410.0354 [hep-th].

[83] Z. Bern et al. "Logarithmic Singularities and Maximally Supersymmetric Amplitudes". In: *JHEP* 202 (2015), p. 1506. DOI: 10.1007/JHEP06(2015)202. arXiv: 1412.8584 [hep-th].

[84] Z. Bern et al. "Dual Conformal Symmetry, Integration-by-Parts Reduction, Differential Equations and the Nonplanar Sector". In: *Phys. Rev. D.* 9 (2017), p. 96. DOI: doi:10.1103/PhysRevD.96.096017. arXiv: 1709.06055 [hep-th].

[85] S. Franco et al. "Non-Planar On-Shell Diagrams". In: *JHEP* 199 (2015), p. 1506. DOI: doi:10.1007/JHEP06(2015)199. arXiv: 1502.02034 [hep-th].

[86] J. L. Bourjaily et al. "Stratifying On-Shell Cluster Varieties: the Geometry of Non-Planar On-Shell Diagrams". In: *JHEP* 3 (2015), p. 1610. DOI: 10.1007/JHEP10(2016)003. arXiv: 1607.01781 [hep-th].

[87] I. Gitler and F. Sagols. "On terminal delta-wye reducibility of planar graphs". In: *Networks* 57 (2011), p. 174.

[88] I. Gitler and F. Sagols. “The use of wye-delta transformations in network simplification”. In: *Oper. Res.* 8 (1960), p. 311.

[89] T. A. Feo and J. S. Provan. “Delta-wye transformations and the efficient reduction of two-terminal planar graphs”. In: *Oper. Res.* 41 (1993), p. 572.

[90] Y. C. Verdière, I. Gitler, and D. Vertigan. “Réseaux électriques planaires II”. In: *Comment. Math. Helv.* 71 (1996), p. 144.

[91] D. Archdaecon et al. “Four-terminal reducibility and projective-planar wye-delta-wye-reducible graphs”. In: *J. Graph Theory* 33 (2000), p. 83.

[92] L. Demasi and B. Mohar. “Four terminal planar Delta-Wye reducibility via rooted K 2, 4 minors”. In: *Proceedings of the Twenty-Sixth Annual ACM-SIAM Symposium on Discrete Algorithms* (2015), p. 1728.

[93] A. T. Suzuki. “Correpondence between the one-loop three-point vertex and the Y- and Δ- electric resistor networks”. In: *Can. J. Phys.* 92 (2014), p. 131.

[94] J. M. Drummond et al. “Magic identities for conformal four-point integrals”. In: *JHEP* 64 (2007), p. 701.

[95] L. F. Alday and J. M. Maldacena. “Gluon scattering amplitudes at strong coupling”. In: *JHEP* 64 (2007), p. 706.

[96] L. J. Dixon, J. M. Drummond, and Henn. “Analytic result for the two-loop six-point NMHV amplitude in N=4 super Yang-Mills theory”. In: *JHEP* 24 (2012), p. 1201.

[97] D. K. Wagner. “Delta–wye reduction of almost-planar graphs”. In: *Discrete Appl. Math.* 158 (2015), p. 180.

[98] I. Gitler and G. Sandoval-Angeles. “Delta-Wye Transformations and the Efficient Reduction of Almost-Planar Graphs”. In: *ENDM* 129 (2017), p. 62.

[99] J. L. Bourjaily et al. “Elliptic Double-Box Integrals: Massless Scattering Amplitudes beyond Polylogarithms”. In: *Phys. Rev. Lett.* 12 (2018), p. 120.

[100] J. L. Bourjaily et al. "Traintracks Through Calabi-Yaus: Amplitudes Beyond Elliptic Polylogarithms". In: *arXiv:1805.09326* (2018).

[101] D. Chicherin et al. "Yangian Symmetry for Bi-Scalar Loop Amplitudes". In: *JHEP* 3 (2018), p. 1805.

[102] B. Basso and L. J. Dixon. "Gluing Ladder Feynman Diagrams into Fishnets". In: *Phys. Rev. Lett.* 7 (2017), p. 119.

[103] S. Abreu et al. "Cuts from residues: the one-loop case". In: *JHEP* 114 (2017), p. 1706.

[104] S. Abreu et al. "Algebraic Structure of Cut Feynman Integrals and the Diagrammatic Coaction". In: *Phys. Rev. Lett.* 5 (2017), p. 119.

[105] S. Abreu et al. "Diagrammatic Hopf algebra of cut Feynman integrals: the one-loop case". In: *JHEP* 90 (2017), p. 1712.

[106] S. Abreu et al. "The diagrammatic coaction and the algebraic structure of cut Feynman integrals". In: *PoS RADCOR* 2 (2018), p. 20017.